THERMAL AND PHOTOSTABILITY STUDIES OF TRIPROLIDINE HYDROCHLORIDE AND ITS MIXTURES WITH CYCLODEXTRIN AND GLUCOSE

A thesis submitted in fulfilment of the requirements for the degree of

MASTER OF SCIENCE

OF

RHODES UNIVERSITY

BY

VUYELWA JACQUELINE NDLEBE

AUGUST 2003

Abstract

Triprolidine hydrochloride ($C_{19}H_{22}N_2.HCl.H_2O$) (TPH) is a well-known antihistamine drug. It melts between 118 ^oC and 122 ^oC and the amount of water present is 4.5 mass percent. TPH is reported as being photosensitive and must be stored in sealed, light-tight containers**.** The thermal stabilities of TPH and of 1:1 molar and 1:1 mass ratio physical mixtures of TPH with beta-cyclodextrin (BCD) and with glucose have been examined using DSC, TG and TG-FTIR, complemented by X-ray powder diffraction (XRD) and infrared spectroscopic (IR) studies. Thermal studies of the solid TPH/BCD mixtures indicated that interaction between the components occurs and it is possible that the TPH molecule may be least partially accommodated in the cavity of the BCD host molecule. XRD results support this indication of inclusion. The results for mixtures of TPH/glucose also suggest that there is interaction between the two components. The results of molecular modelling suggest that TPH is most likely to be accommodated in the BCD cavity as a neutral triprolidine molecule with the toluene portion of the molecule entering first. There is also an indication that the Z-isomer should be accommodated slightly more readily than the E-isomer.

Photostability studies were done by irradiating thin layers of solid samples of TPH and its mixtures for various times at 40°C using an Atlas Sun test CPS lamp operating at 550 W h m^{-2}. An analytical method using HPLC was developed and validated to determine the amounts of any photodegradants. DSC, TG, FTIR, XRD and IR were also used examine the irradiated samples. XRD results showed that changes in the TPH crystal structure occurred during irradiation and that these changes increased with the time of irradiation. Irradiation for 20 hours with UV or exposure to sunlight showed the presence of degradants.

The results obtained illustrate the general stability of TPH, especially in the solid state. Although the potential for isomerization to the pharmaceutically inactive Z-isomer exists, this transformation would require extreme light conditions. The study has also shown TPH to be compatible with both glucose and BCD, which are potential excipients both in solid and liquid dosage forms. The presents of these excipients in dosage forms will thus not adversely affect the stability and the therapeutic efficacy of TPH.

ACKNOWLEDGEMENTS

I would like to thank Prof M.E. Brown for his supervision in this project, his encouragement and patience and for helping to get funding from DAAD and NRF to enable me to proceed with my studies.

Also my co-supervisor Prof B.D. Glass for her support and teaching me to be independent.

The technical staff Mr A. Sonemann and Mr J. Fourie for helping me with the hot-stage microscopy.
Edith Beukes for helping with HPLC-MS and HPLC-Diode array. Emmanuel Lamprecht for helping with DSC, TG, XRD and TG-FTIR and Kevin Lobb for helping with molecular modelling.

To my parents Nomathamsanqa and Vuyisile Ndlebe and brothers Mzingisi, Lunga, my cousin brother Bulelani and my sisters Nomahlubi, Siphosethu and the late Bulelwa and rest of my family, thank you all and may the Lord Bless you.

My Friends Kauna Ndakunda, Moses Rotich, Kimutai Cheruiyot, Babalwa Melane, Weziwe Maqanda, Pastor Debbie Sloane, Duduzile Molefe, Robert Thsikudo, Nkululeko Gojela, Tendai Mashingaidze, Amos Mpofu and Jonathan Johnson, thank you for your support.

Dedicated

to

my parents

Mr and Mrs Ndlebe

TABLE OF CONTENTS

LIST OF ABBREVIATIONS

BCD - betayclodextrin

CD - cyclodextrin

TA - thermal analysis

DSC - differential scanning calorimetry

DTG - derivative thermogravimetry

FTIR - Fourier transform infrared

GCD - gamma cyclodextrin

HSM - hot-stage microscopy

HPLC - high performance liquid chromatography

IR - infrared spectroscopy

LC - liquid chromatography-mass spectroscopy

MS - mass spectroscopy

NMR - nuclear magnetic resonance

UV/Vis - ultraviolet visible

TLC - thin layer chromatography

TG - thermogravimetry

TPH - triprolidine hydrochloride

XRPD -X-ray powder diffraction

LIST OF FIGURES

LIST OF TABLES

1. INTRODUCTION

1.1. Triprolidine hydrochloride (TPH)

Triprolidine hydrochloride, $C_{19}H_{22}N_2HCl.H_2O$, (TPH) **1** is a white, crystalline powder, odourless or almost odourless [1] and bitter in taste [2]. The melting point is between 118 ^oC and 122 ^oC and the amount of water present is 4.5 mass percent [2]. TPH is reported as being photosensitive and must be stored in sealed, light-tight containers [3]**.**

TPH is soluble at room temperature (25 ^oC in water 316 mg/ml), 95 % ethanol (316 mg/ml), 0.1 M HCl (319 mg/ml), n-octanol (75 mg/ml), chloroform (48 mg/ml), propylene glycol (273 mg/ml) and insoluble in diethyl ether (<1 mg/ml) [4]. The drug substance is required to contain not less than 98.0 and not more than 101 % of $C_{19}H_{22}N_2$.HCl, which is calculated on an anhydrous basis [3]. Triprolidine can exist as both the Z- and E-isomer (see Figure 1.1) because of the exocyclic double bond, but only the E-isomer [5], {(E)-2-[3-(pyrrolidinyl)-1-*p*-tolypropenyl] pyridine mono-hydrochloride; molecular mass 332.88 g mol^{-1} [6]} is pharmaceutically active.

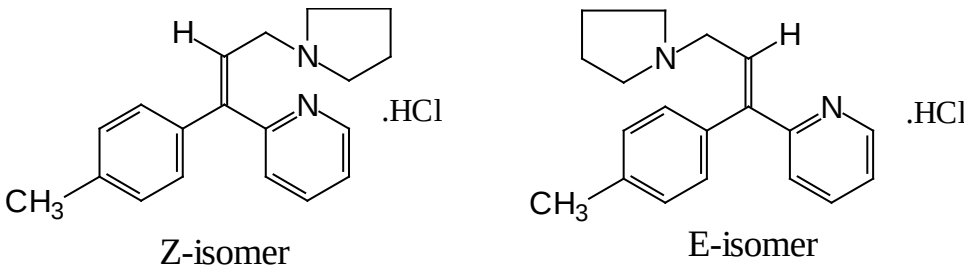

Figure 1.1 Molecular structures of the Z- and E-isomers of triprolidine hydrochloride (TPH) **1** $C_{19}H_{22}$.HCl. [7]

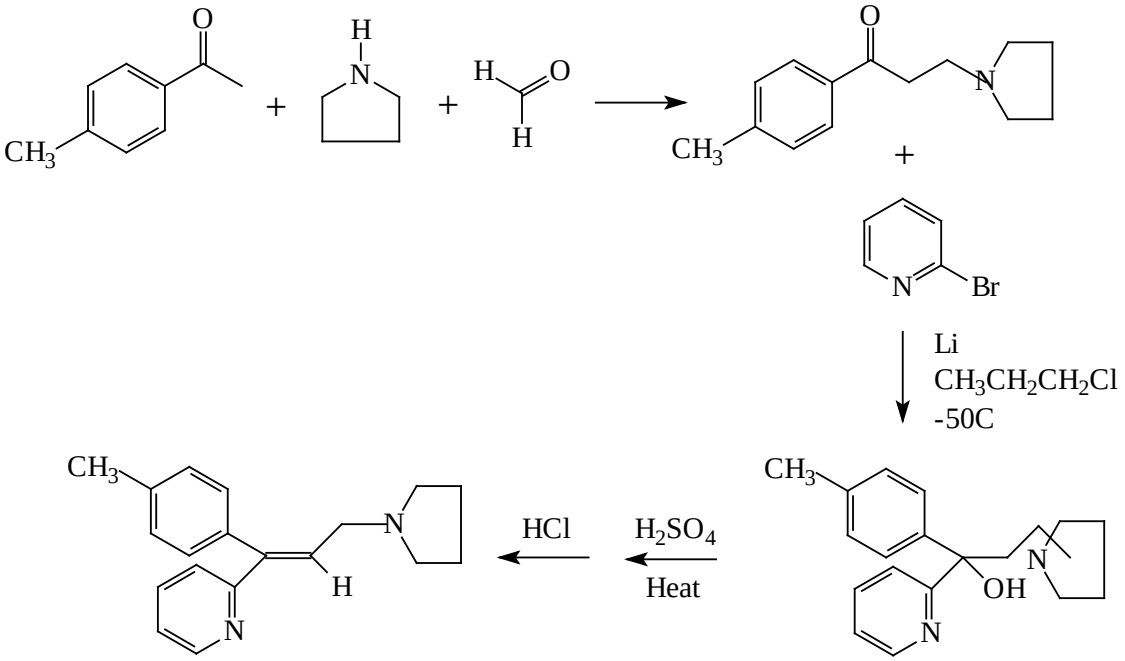

Figure 1.2 Synthesis of TPH [4]

The synthesis of TPH is outlined in Figure 1.2 [4]. The 4-methyl-ω-pyrrolidinopropiophenone formed in the first step was prepared by the Mannich reaction of 4-methylacetophenone and pyrrolidine. Under suitable dehydration conditions, the carbinol yields the desired product in the E-conformation.

1.2. Pharmaceutical uses and action of triprolidine hydrochloride

Triprolidine hydrochloride is a propylamine antihistamine commonly used as an over-the counter drug and is available in both liquid and solid dosage forms. TPH is marketed under the trade name, Actidil® [8], and relieves the symptoms of hay fever by blocking the effect of histamine, which causes swelling, itching, watery eyes, dizziness, dry mouth and other allergies [9,10].

In the propylamine derivatives, which are unsaturated compounds, the co-planar aromatic double bond system has been suggested to be an important factor for antihistamine activity. Those compounds possessing a pyrrolidino group, as the side-chain tertiary amine, are the more active members in the group [11]

Mepyramine **2** and chloropheniramine **3** are compounds related to TPH that are also used as H_1 antagonists in pharmacological studies [12]. During the last 25 years there has been great interest [13] in the antihistamine properties of substituted 1,1-diaryl-4-aminoprop-1-ene (e.g. triprolidine) and 1,2-diaryl-4-amino-but-2-enes. Isomers of triprolidine and pyrrobutamine have been prepared [12] and their geometrical configurations established by proton NMR spectroscopy. The differences in the reactivity of the isomers have been ascribed to the interactions possible when the α-pyridyl and aminomethyl groups are *trans* to each other, or when the p-tolyl and amino methyl groups are *cis* to each other.

Some studies have been reported [6] on the synthesis of geometrical isomers related to triprolidine and the effect of structure upon antihistamininic activity. The work was validated using UV and proton NMR and showed that the isomeric purity of tested E-Z isomers was greater than 99.5 %, as assessed by the HPLC method developed for these isomers. The E-configuration of triprolidine itself was found to be the most active antihistamine compound amongst the range of isomeric compounds tested.

Triprolidine hydrochloride is available in tablets containing 2.5 mg and in an elixir containing 1 mg in 4 ml [9]. The usual oral adult daily dose is up to 10 mg/day. Children aged 6 to 12 years take 1.25 mg every 4 to 6 hours. This drug is not recommended for pregnant or breast-feeding women or infants. The maximum effect usually occurs in about 3½ to 4 hours and the duration is about 12 hours [14]. The toxicity was estimated as an acute lethal dose in man of between 25 and 250 mg/kg [14]. Spectrophotometric methods have been developed [10] for the analysis of tablets containing pseudoephedrine **4,** triprolidine, and dextromethorphan **5**.

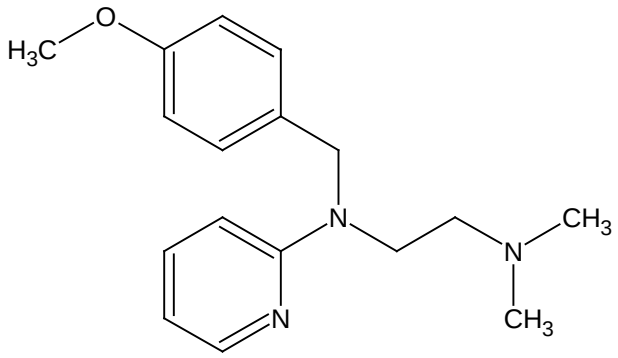

mepyramine **2**

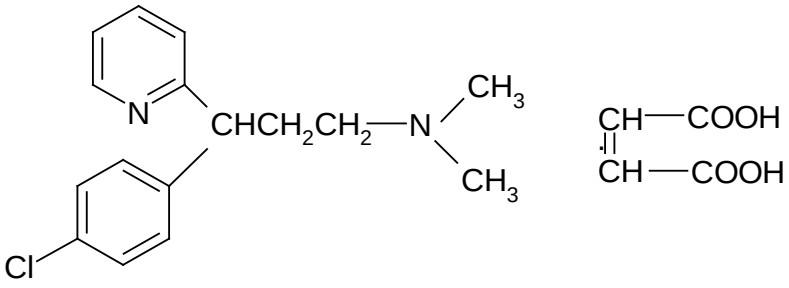

3

chloropheniramine **3**

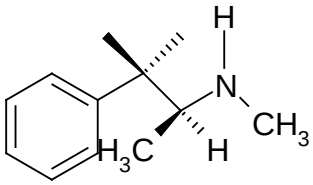

4

pseudoephedrine **4**

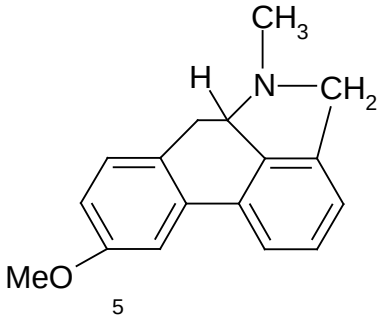

5

dextromethorphan **5**

Figure 1.3 Structures of mepyramine **2**, chloropheniramine **3**, pseudoephedrine **4** and dextromethorphan **5**.

1.3. Cyclodextrins as excipients

Cyclodextrins (CDs) are cyclic oligosaccharides, consisting of ∀-1.4-linked D-glucopyranose units. The most common of these naturally occurring ring-shaped molecules are the ∀- (ACD), ∃- (BCD) and (- (GCD) cyclodextrins which have six, seven, (β-CD) or eight glucopyranose units respectively [15] (see Figure 1.4). The cyclodextrin molecules have a central cavity that is hydrophobic, while the exterior is hydrophilic and are thus capable of accommodating various kinds of guest molecules (drugs) in this cavity forming inclusion complexes. The internal diameter of the cavity increases from ACD (0.5 nm) and BCD (0.6 nm) to γ- cyclodextrin (0.8 nm) (See Figure 1.5) [16]. These three cyclodextrins also differ in their solubility (see Table 1.1) and β-cyclodextrin is the least soluble.

Table 1.1 Properties of the natural cyclodextrins (CDs) **[**14**]**

Cyclodextrins	ACD	BCD	GCD
Molecular mass/g mol^{-1}	972	1135	1297
Glucose units	6	7	8
Water solubility/ 25 ^{o}C (%w/v)	14.5	1.85	23.2
Cavity diameter/nm	0.47 – 0.53	0.60 – 0.65	0.75 – 0.83
Total diameter/nm	1.46	1.54	1.75
Water content	6 – 7	11 – 12	17

The topology of the beta-cyclodextrin ring and the molecular structure are shown in Figure 1.4.

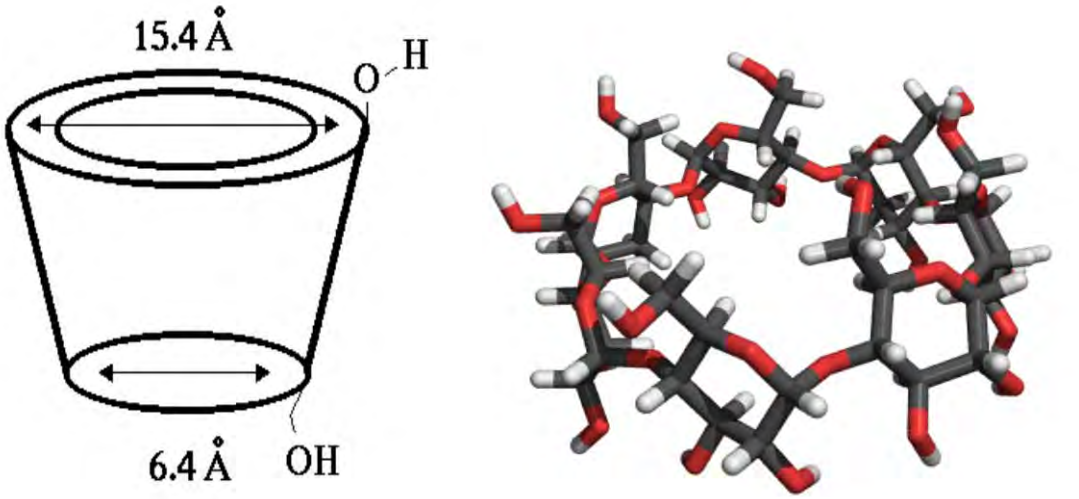

Figure 1.4 The topology and molecular structure of BCD [15, 16].

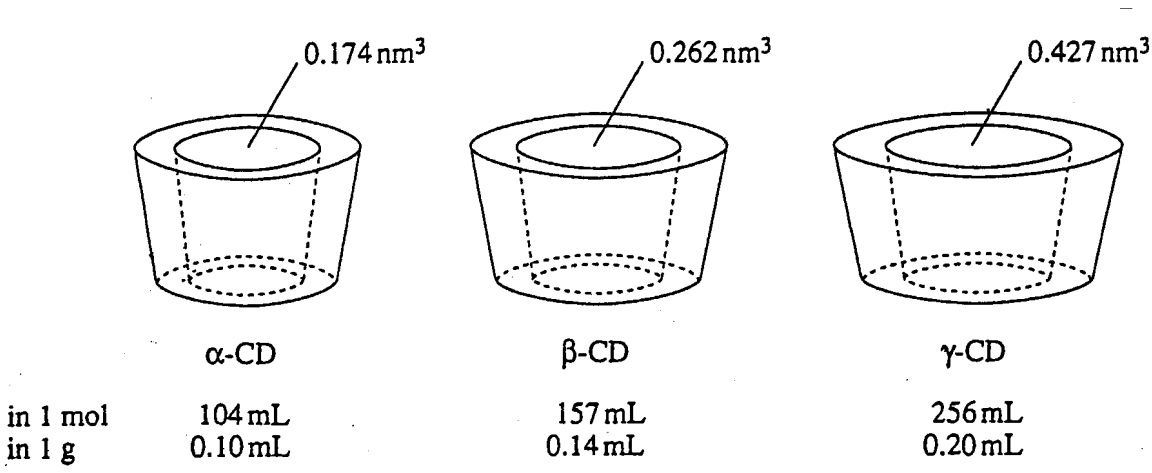

Figure 1.5 Volumes of the cavities of α- β- and γ-CDs [17].

The process of inclusion of a guest molecule in the cyclodextrin cavity is illustrated in Figure 1.6. The size, shape and polarity of the potential guest molecule are all important in determining whether inclusion will occur. Partial inclusion is possible, as is inclusion of different parts of a large, complex molecule by several cyclodextrin units.

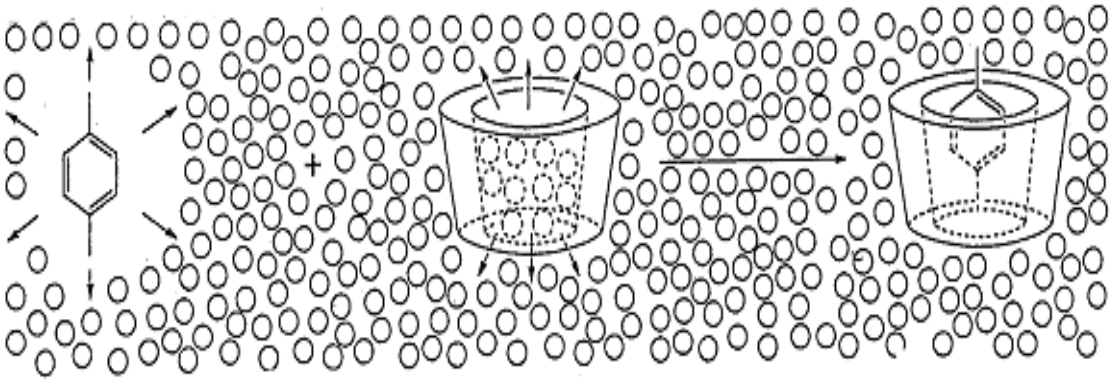

Figure 1.6 Schematic illustration of inclusion of *p*-xylene in BCD. (The small circles represent water molecules.) [17].

Formation of an inclusion complex in aqueous solution involves the following steps [18]:

(1) The water from the CD cavity has to escape. In this process, hydrogen bonds and van der Waals interactions have to be overcome, giving effectively gaseous water molecules.

(2) The conformational energy of the CD molecule decreases as the cavity relaxes.

(3) The guest molecule then has to shed its hydrate shell, thus also effectively becoming the equivalent of a gaseous molecule.

(4) The guest molecule enters the empty CD cavity and the complex is the stabilized by van der Waals interactions and sometimes by hydrogen bonding.

(5) The water molecules that were displaced from the CD cavity become part of the aqueous surroundings, interacting with any exposed part of the guest molecule or with the outer surface of the CD ring.

Cyclodextrins have become important pharmaceutical excipients because they have been shown to enhance the dissolution rate of poorly soluble drugs. They can also increase the stability of compounds that tends to sublime, e.g. clofibrate **6** and isosorbide **7** [19]. When reactive groups of a guest molecule are accommodated within the cyclodextrin cavity, the chemical stability of the guest can then be enhanced by prevention of intermolecular reactions. Inclusion may also influence intramolecular processes. Bioavailability is often enhanced and side-effects may be decreased [20].

Some excipients actually promote degradation of the drug while serving some other function in the formulation. An ideal excipient should retard degradation, by

preventing interactions between functional groups on the same molecule, by screening the drug from environmental components such as water vapour and sunlight, and protecting the drug from processing stresses such as grinding, sterilizing, etc. If the affinity for water of the excipient is stronger than that of the drug, the presence of the excipient can stabilize the drug against hydrolysis [19].

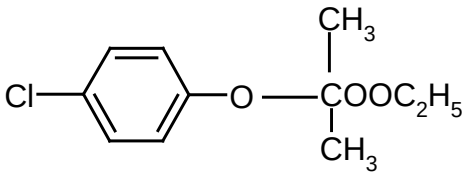

clofibrate **6**

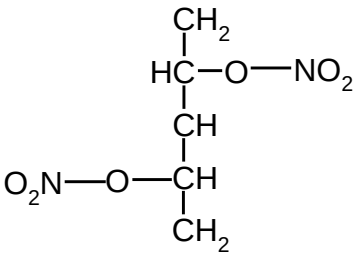

isosorbide **7**

Figure 1.7 Structures of clofibrate **6** and isosorbide **7**

1.4. The stability of TPH in liquid dosage form

Many factors have been found to affect the stability of TPH in liquid dosage form. These include pH, UV-light, water and some excipients [4, 20]. UV-light has a pH-dependent effect on the stability of TPH. At pH 2 the degradation rate was slower than at pH 8 and in pure water TPH was unstable [20]. As mentioned above, TPH is only active as the E-isomer. If the E-isomer is exposed to UV-light it converts to the Z-isomer [4]. Some excipients, such as sorbitol, mannitol and glycerin, have been found to stabilise TPH, while others, like propylene glycol and sodium saccharine, have no effect on its stability. Glucose as an excipient increases the degradation of TPH [20]. After two years at 37 ^{o}C, the syrup dosage form of TPH had not decomposed more than 10%. This formulation has to be kept in a light-tight container because exposure to light causes it to discolour. BCD was found to have a small

positive effect on the stability of aqueous solutions of TPH but had no effect in the presence of sucrose. It was suggested that any substance that may enhance the water structure would improve the stability of TPH in water e.g beta-cyclodextrin [20].

1.5. The impact of stereoisomers

In the early 1960's, the teratogenicity associated with the (R)-form of the drug thalidomide highlighted the importance of chiral compounds in pharmaceuticals. The presence of the pure (S)-form of thalidomide would not have solved the problem, however, due to racemisation from the (S)- to (R)-form in the blood stream. Development of chiral drugs is increasing directed by the FDA which insists on pure enantiomers to reduce side effects [21]. Use of the more active isomer may be advantageous in terms of wastage in manufacture and extension of the patent for the pharmaceutical industry. For the patient, the dose may in many cases be halved and the possibility of the occurrence of side-effects from the unwanted isomeric form is removed. The FDA has divided pairs of enantiomers into three categories:

1) Both enantiomers have similar activities (e. g. ibuprofen **8** , promethazine **9**)
2) One enantiomer is pharmacologically active while the other is inactive (e. g. terbutaline **10**) and
3) Each enantiomer has a completely different activity (e .g. propranolol **11**) [22]

The importance of stereoisomers in pharmacokinetics and toxicology is well established [23]. More that a quarter of drugs in clinical use are chiral, although many are marketed as racemates. Some drugs are marketed as mixtures of geometric isomers. Although triprolidine hydrochloride is not marketed as a racemate, the United States Pharmacopoeia specifies a limit of not greater than 2 % of the Z-isomer [24].

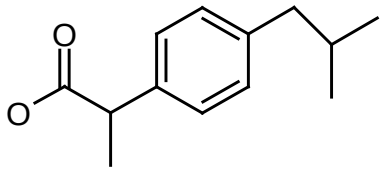

ibuprofen **8**

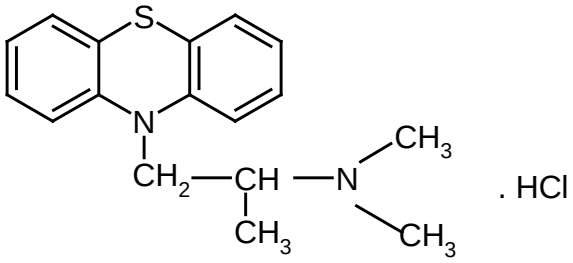

promethazine **9**

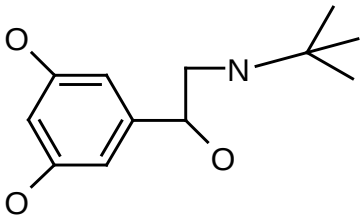

terbutaline **10**

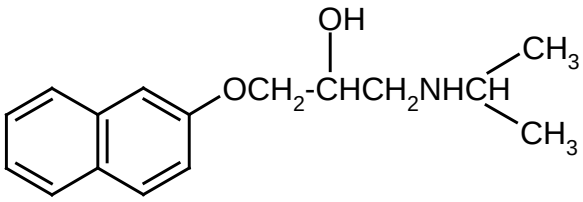

propranolol **11**

Figure 1.8 Structures of ibuprofen **8**, promethazine **9**, terbutaline **10** and propranolol **11.**

1.6. Solid-state stability

In general, very much less is known about the solid-state reactions of pharmaceuticals than is known about their reactions in aqueous solution. During formulation, the processing effects and/or interactions with excipients, can result in solid-state reactions

(including dehydration, desolvation, cyclization, oxidation and hydrolysis) taking place in the drug substances, which may accelerate degradation. Excipients that are present in formulated products may not be directly involved in the degradation, but may add components, e.g. water, which may take part in solid-state reactions.

Both temperature and humidity play very important parts in the solid-state hydrolysis of water-soluble drugs. The process may involve reaction with water vapour or the formation of an adsorbed moisture layer [25].

2. THE THERMAL AND PHOTOSTABILITY OF DRUGS

2.1. Thermal analysis of pharmaceuticals

The applications of thermal analysis in the study of pharmaceuticals are vast and enable many aspects of thermal behaviour, such as polymorphism, melting, glass transitions, sublimation, dehydration, decomposition, oxidation and hydrolysis to be examined in quantitative detail using routine techniques such as thermogravimetry (TG) and differential scanning calorimetry (DSC) [26].

Thermogravimetry (TG), coupled with evolved gas analysis by Fourier transform infrared spectroscopy (FTIR), permits the detection of the release of gases (trapped solvent or products of thermal decomposition) from a compound during the heating programme. The recently developed modulated temperature techniques show great promise for the separation of reversible and irreversible processes, and micro-thermal analysis, using a modified atomic force microscope, has great potential for examining solid drug formulations.

2.2. Thermal studies of pure drugs

There have been numerous studies of the thermal behaviour of drugs and drug formulations [27]. In this section, only a few examples of studies with some relevance to the behaviour of TPH, particularly acid chlorides and their hydrates, are described.

There has been some previous work on the thermal stability of TPH. The DSC curve for TPH [28] exhibited a sharp (melting) endotherm at 121-122 ^{o}C but there was no indication of polymorphism or of a glass transition. Analytical Profiles [4] records that TPH melts at 115-122 ^{o}C in a sealed capillary tube.

Kitaoka and Ohya [29] used DTA and TG to study the dehydration behaviour of nafagrel hydrochloride **12** which is a thromboxane A_2 synthetase inhibitor. The drug exists as a hemihydrate and a monohydrate. The influence of water vapour was studied using quasi-sealed and completely sealed systems. In an open system, the

DTA curve of the hemihydrate showed an endotherm with peak at 80.7 ^{o}C, accompanied by a 2.9 % loss of mass on the TG curve, corresponding to loss of ½ mole of water of crystallization per mole of drug, while the DTA curve of the monohydrate showed an endotherm with peak at 84.9 ^{o}C with a 5.7 loss of mass on the TG curve, corresponding to loss of 1 mole of water of crystallization per mole of drug. In a quasi-sealed system, the TG-DTA results for the hemihydrate showed that the temperature of the dehydration increased, with a 2.8 % loss of mass on the TG curve. For the monohydrate, the dehydration was divided into two endothermic stages with peaks at 127.4 ^{o}C and 145.9 ^{o}C. Dehydration of the hydrate thus occurs via the intermediate formation of the hemihydrate. The enthalpy change for dehydration of the hemihydrate was greater than that of the corresponding stage in the dehydration of the monohydrate [29].

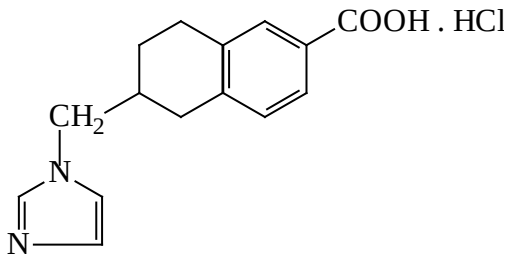

Figure 2.1 Structure of nafagrel hydrochloride **12** (6-(1-imidazolylmethyl)-5,6,7,8-tetrahydro-naphthalene-2-carboxylic acid hydrochloride) also known as DP-1904.

2.3 Thermal studies of some drug/cyclodextrin mixtures

A major part of this study is concerned with binary mixtures of TPH with β-cyclodextrin (BCD) and with ternary mixtures of TPH with BCD and glucose. There have many been studies of the thermal behaviour of BCD and other cyclodextrins [15,30].

Thermal analysis alone cannot prove the occurrence of inclusion of a drug molecule in the cavity of a cyclodextrin molecule. It is quite possible that any inclusion indicated (usually by changes in the appearance, or complete disappearance, of the melting

endotherm of the drug in the presence of a CD) may have resulted from the heating programme. If the thermal behaviour of the drug is, however, unchanged in the presence of the CD, this is a good indication that significant inclusion has not occurred. A variety of non-thermal techniques have been used to detect or prove inclusion. Particularly valuable are X-ray diffraction and spectroscopic studies, of which some examples are given below.

Bayomi and his group [31] studied solid state mixtures of nifedipine **13** with CDs (α-, β- and γ-cyclodextrin), using DSC. The DSC curves of pure nifedipine showed a sharp melting endotherm at 175.1 ^{o}C with an enthalpy of fusion of 78.6 ± 2.2 J g^{-1}, while the curves for the CDs showed no endotherms in this temperature region. The DSC curves for physical mixtures of nifedipine and the CDs showed superimposition of the features of the CD curve and the melting of the drug. Some broadening of the nifedipine melting endotherm and shifting of the onset temperature could indicate slight interaction between the nifedipine and CDs in the solid state.

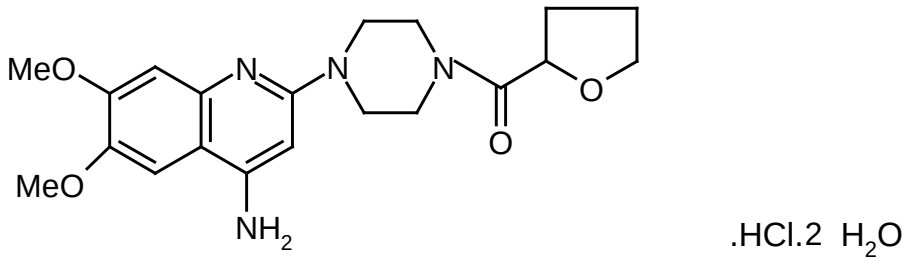

Figure 2.2 Structure of nifedipine **13**.

Li and his group [32] studied the interaction of procaine hydrochloride **14** (See Figure 2.3) with BCD in solution, using UV/visible and fluorescence spectroscopy. Pure procaine hydrochloride absorbs at 231 and 290 nm, while BCD does not absorb in this region. The absorption at 231 nm is due to the NH_2- group and at 290 nm to the benzene ring. The absorption peaks in a mixture of procaine hydrochloride and BCD shifted to 241 and 307 nm, increasing $\Delta\lambda_{max}$ values by 10 and 17 nm, respectively. These shifts suggest that the procaine hydrochloride could have been accommodated in the BCD cavity. The diameter of the BCD cavity is about 0.68 nm, while the diameter of the benzene ring in procaine is about 0.67 ~ 0.68 nm, thus allowing a close fit to occur and suggesting that partial inclusion occurs from this side of the molecule.

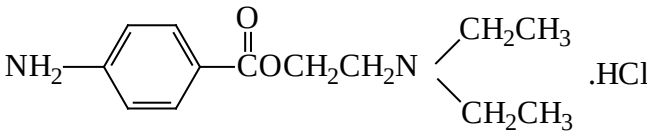

Figure 2.3 Structure of procaine hydrochloride **14** [32]

Ficarra *et al.* [33] investigated the inclusion of a variety of flavonoids (hesperitin, heperidin, naringerin and naringin) by BCD in the solid state and in aqueous solution, using proton NMR and FTIR spectroscopy. The FTIR spectrum of a physical mixture of hesperitin **15** (See Figure 2.4) and BCD showed disappearance of the OH- phenol bands at 1200 cm^{-1} and 1350 cm^{-1}, the methoxy band at 1250 cm^{-1} and the aromatic bands at 1581 cm^{-1} and 1500 cm^{-1}, indicating that partial inclusion had taken place. The ^{1}H NMR spectra of the flavonoids dissolved in deuterium oxide showed variations in the chemical shifts in the presence of BCD confirming that some interaction had occurred between the drug and the cyclodextrin.

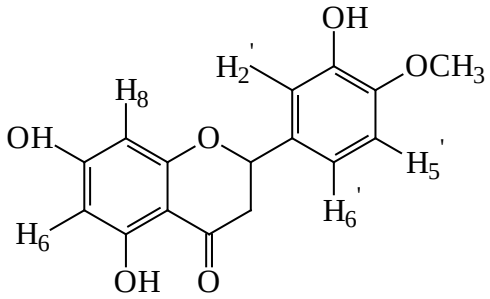

Figure 2.4 Structure of hesperitin **15** [33].

X-ray diffraction studies give the most satisfactory evidence of inclusion in the solid state. There are many examples of powder diffraction studies of drug/cyclodextrin mixtures where the appearance of new diffraction peaks, shows a change in crystalline structure and hence indicates that inclusion has occurred.

2.4 Photostability studies of pure drugs

When a compound is subjected to irradiation with light of a sufficiently short wavelength and adequate intensity, photoisomerisation may occur on its own or in addition to other photodegradation processes. Photostability studies are simpler and

more reproducible in solution than in the solid state. The participation of the solvent in the photo-processes makes results obtained in solution difficult to extrapolate to the solid state [34].

The E-Z isomerisation (see Figure 2.5) of the anti-ulcer agent, 2'-carboxymethoxy-4, 4- bis (3 -methyl-2-butenyloxy) chalcone (CBC) **16** during photoirradiation has been reported [31]. HPLC, HPLC-MS and ^{1}H-NMR were used to confirm the presence of the Z-isomer.

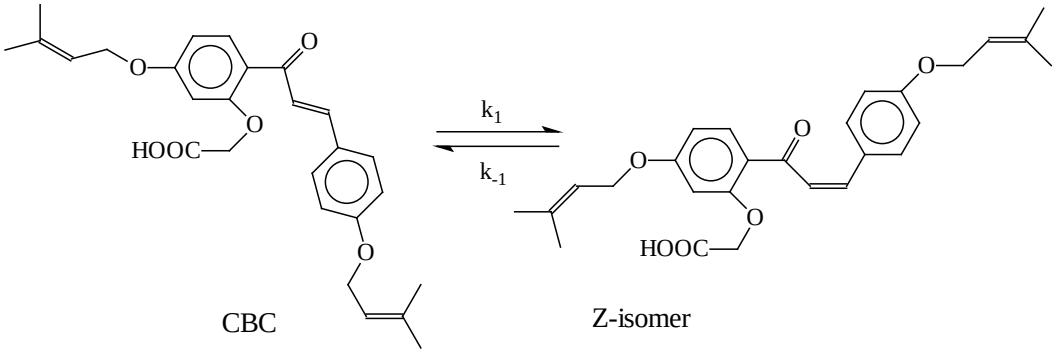

Figure 2.5 The E-Z isomerisation of 2'-carboxymethoxy-4, 4-bis (3-methyl-2-butenyloxy) chalcone (CBC) **16** brought about by photoirradiation [34].

Li wan Po and Irwin [35] reported that irradiation of the tricyclic neuroleptic drugs, flupenthixol **17**, clopenthixol **18** and chlorprothixene **19** (see Figure 2.6) induced rapid to cis – trans isomerization.

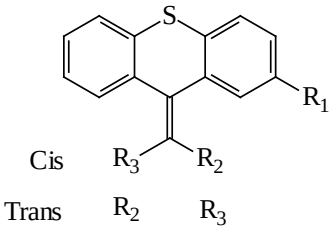

Cis R_3 R_2

Trans R_2 R_3

Flupenthixol	$R_1 = CF_3$	$R_2 = CH_2CH_2$—N N—CH_2CH_2OH	$R_3 = H$
Clopenthixol	$R_1 = Cl$	$R_2 = CH_2CH_2$—N N—CH_2CH_2OH	$R_3 = H$
Chlorprothixene	$R_1 = Cl$	$R_2 = CH_2CH_2N(CH_3)_2$	$R_3 = H$

Figure 2.6 The chemical structures of the tricyclic neuroleptic drugs, flupenthixol **17**, clopenthixol **18** and chlorprothixene **19** [35].

The presence of the substituent at position-2 (see Figure 2.6) results in the existence of geometrical isomers about the exocyclic olefin. An HPLC method was used to study the cis-trans isomerisation. Samples protected from light showed no degradation and the HPLC trace showed only a peak due to the cis-isomer. On exposure to the light source (which was rated at 3.4 times the intensity of sunlight), with exclusion of oxygen, isomerisation occurred and peaks in the ratio of (1:1) were observed. HPLC results for samples irradiated without exclusion of air showed that some decomposition had occurred but that cis – trans isomerisation was still the major process.

2.5. Photostability studies of drug/cyclodextrin mixtures

The difficulties, described above, of relating the photo-processes in solution to those in the solid state, apply even more in the presence of excipients in general and cyclodextrins in particular. Any information on the possible formation and resulting structure of inclusion complexes can, however, be useful in explaining any protective, or other, effect of the cyclodextrin on the photostability of the drug.

Tadanobu and his group [34] investigated the photostability of aqueous solutions of mixtures of 2'-carboxymethoxy-4, 4-bis (3 - methyl-2- butenyloxy) chalcone (CBC) **16** with cyclodextrins. 1:1 and 1:2 molar ratio (drug: CD) mixtures showed different photoreactivities. The E-Z photoisomerisation of CBC was decelerated in the 1:1 mixtures and accelerated in the 1:2 mixtures. These results were interpreted as indicating the formation of different inclusion complexes with the corresponding molar ratios (see Figure 2.5).

Degradation of tetracycline hydrochloride (TC.HCl) **20** (Figure 2.7) occurs [36] on exposure to light, high temperature and humidity. The photostability of TC.HCl was increased by complexing it with hydroxypropyl-β-cyclodextrin (HPBCD) in the mole ratio of 2:1 (drug:CD). DSC results confirmed that there was at least partial inclusion of TC.HCl in the HPBCD cavity in the solid state. The DSC curve for the TC.HCl/HPBCD complex did not show the exotherm at 235 ^{o}C found for TC.HCl alone and a new endotherm appeared. Tablets containing TC.HCl and HPBCD were exposed to light for up to 3 months. Colour changes and homogeneity were examined

and the TC.HCl remaining and its photodegradation products were determined by HPLC methods [36].

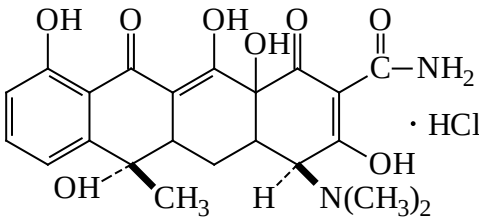

Figure 2.7 The molecular structure of tetracycline hydrochloride, TC.HCl **20** [36].

Hiramaya and his group [37] investigated the effect of dimethyl-β-cyclodextrin (DMBCD) on the photoisomerization of the thromboxane synthetase inhibitor, (*E*)-4-(1-imidazoylmethyl) cinnamic acid (IMC) **21**. IMC photoisomerizes direct to its *Z*-isomer. BCD and DMBCD were found to decelerate the photoisomerization and the quantum yield was significantly decreased by complex formation with BCD. UV-spectroscopy, circular dichroism and NMR indicated that the IMC is included in an axial mode in the cavity of DMBCD and that the suppressing effect of the BCDs on the photoisomerization of IMC arises mainly from steric effects.

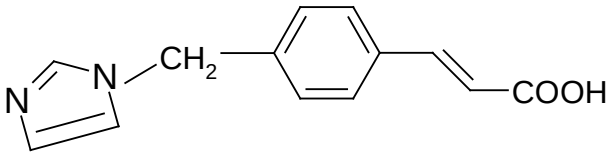

Figure 2.8 The molecular structure of (*E*)-4-(1-imidazoylmethyl) cinnamic acid (IMC) **21** [37].

Lutka [38] studied the effect of beta-cyclodextrin and its derivatives on the photostability and solubility of promethazine **22** (see Figure 2.9) in the solid state and in solution. In the solid state the mixtures were evaluated using FTIR, ^{13}C-NMR and DSC methods. The presence of cyclodextrin decreased the solubility of promethazine, but in acidic solution the CD increased the photostability of promethazine.

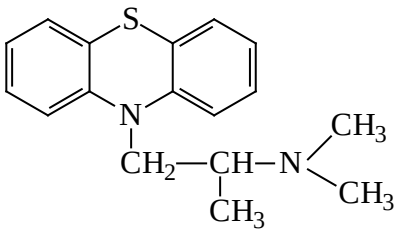

Figure 2.9 The molecular structure of promethazine **22** [38].

Mielcarek and Daczkowska [39] studied the photochemical decomposition of isradipine (IS) **23** (see Figure 2.10) and its complexation with methyl-beta-cyclodextrin. HPLC and UV-spectrophotometry were used to assessed the photodegradation of IS. Inclusion of IS within the methyl-beta-cyclodextrin cavity increased the photostability of IS by a factor of two.

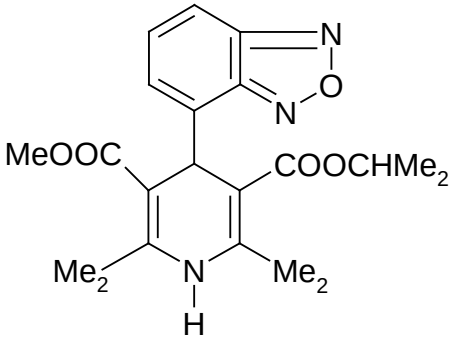

Figure 2.10 The molecular structure of isradipine, IS **23** [39].

3. PROJECT PROPOSAL

This study was initiated in response to a request from a South African pharmaceutical manufacturer to investigate the stability of triprolidine in liquid dosage form. Triprolidine as the hydrochloride salt was formulated with glucose as an excipient in a paediatric mixture. The potential of this drug to undergo photoisomerisation to the inactive Z-isomer (as described above) has resulted in strict pharmacopoeial limits and, in general, there is an increasing involvement by regulatory authorities in the usage of chiral drug molecules. For these reasons, the effects of light and heat on the drug and on drug/glucose mixtures both in the solid state and in aqueous solution required investigation. Because of the ability of cyclodextrins to improve both the solubility and stability of drug molecules, as well as reports on the photostabilization of drug molecules as a result of interaction with cyclodextrins, the study includes mixtures of the drug with beta-cyclodextrin (BCD).

The project: commences with the characterization of the TPH to ensure its identity and purity, using the following techniques:

- Ultraviolet-visible spectrophotometry (UV-vis)
- Mass spectrometry (MS)
- Infrared (IR) and ^{1}H NMR spectroscopy
- X-ray powder diffraction (XRD)
- Thin-layer chromatography (TLC)
- High performance liquid chromatography (HPLC)

The solid-sate thermal studies involve an extensive investigation of the thermal behaviour of TPH using the following techniques:

- Differential scanning calorimetry (DSC)
- Thermogravimetry (TG) and TG-FTIR
- Hot-stage microscopy

The abovementioned techniques are used to evaluate the thermal behaviour of the physical mixtures of TPH with both glucose and BCD, in order to determine the extent of interaction and to predict potential incompatibilities. XRD and FTIR studies are used to further investigate the interactions.

The photostability studies of TPH and the physical mixtures, both in the solid-state and in aqueous solution, are conducted according to the conditions specified by the International Committee on Harmonization (ICH) for UV and visible light exposure. The solid-state samples after irradiation are analyzed using DSC, TG, XRD and FTIR, while the studies of TPH in the solution are quantitated using a validated HPLC method capable of detecting both the E- and Z-isomers.

The aim of this research was thus to study both the thermal and photostabilities of triprolidine hydrochloride (TPH) in the solid state, and also the photostability in aqueous solution for comparison with the solid-state results. The effects on stability of forming physical mixtures of TPH with beta-cyclodextrin (BCD) and with glucose were also examined.

4. EXPERIMENTAL

4.1. Materials

Samples of triprolidine hydrochloride (TPH), glucose and β-cyclodextrin (BCD) were supplied by Aspen Pharmacare Laboratories in Port Elizabeth (South Africa) and their molecular masses and water contents are listed in Table 4.1

Table 4.1 Molecular masses and water contents of materials

Compound	Molar mass/g mol^{-1}	Water content % w/w
Triprolidine hydrochloride (TPH)	332.85	4.5
∃-Cyclodextrin (BCD)	1135	14.9*
Glucose (anhydrous)	180.16	-

* The water content of BCD was determined by Karl Fischer titration (Mettler DL 18 Karl Fischer, Mettler-Toledo, Switzerland)

Physical mixtures were prepared in the stoichiometric ratios listed below by weighing the appropriate amounts of TPH, BCD and glucose (which had been stored in desiccators over P_2O_5). The individual components were simply blended until thoroughly mixed and stored away from light in sealed containers in a desiccator.

1:1 mass ratio TPH/β-cyclodextrin (equivalent to a 3.41:1.00 mole ratio)
1:1 mass ratio TPH/glucose (equivalent to a 0.54:1.00 mole ratio)
1:1 mass ratio glucose/β-cyclodextrin (equivalent to a 6.30:1.00 mole ratio)

1:1 mole ratio TPH/β-cyclodextrin (equivalent to a 0.29:1.00 mass ratio)
1:1 mole ratio TPH/glucose (equivalent to a 1.85:1.00 mass ratio)
1:1 mole ratio glucose/β-cyclodextrin (equivalent to a 0.16:1.00 mass ratio)

4.2 Thermal studies on TPH and mixtures with glucose and/or BCD

The techniques used in the thermal studies were:

(a) Differential scanning calorimetry (DSC),

(b) Thermogravimetry coupled to Fourier-transform infrared spectroscopy (TG-FTIR)

(c) Hot-stage microscopy (HSM)

4.2.1 Differential scanning calorimetry (DSC)

A Perkin-Elmer Series 7 differential scanning calorimeter was used. The melting of pure indium metal was used for calibration. Samples (6-9 mg) were accurately weighed using a Sartorius MC5 electronic microbalance into sample pans. These were either (i) aluminium pans, (ii) sealed aluminium pans, or (iii) stainless-steel high pressure pans with gold gaskets. Unless otherwise stated, samples were heated at 10 ^{o}C min^{-1} under a nitrogen purge over the 50-250 ^{o}C temperature range.

4.2.2 Thermogravimetry (TG) coupled with Fourier-transform infrared spectroscopy

Thermogravimetry was carried out on a Perkin-Elmer Series 7 TG, which was calibrated in standard fashion using magnetic materials. Samples, in an open platinum pan, were heated in flowing nitrogen at 10 ^{o}C min^{-1} over the 50-350 ^{o}C temperature range. The TG could be connected to a Perkin-Elmer Spectrum 2000 FTIR via a heated interface (Perkin-Elmer). The purge gas, containing the volatile decomposition products, was passed through a heated gas cell for analysis.

4.2.3 Hot-stage microscopy (HSM)

A Leitz Ortholux microscope and hot-stage was used for hot-stage microscopy. The changes in structures and colours of samples could be observed during heating and subsequent cooling. Digital images were obtained through an eyepiece adaptor using a Nikon digital camera (Model E 995).

4.3. Photostability testing

4.3.1. Solid-state studies

Solid samples of TPH and its mixtures with BCD and glucose were irradiated using an Atlas Sun test CPS+ lamp at 550W h/m^2 at 40 ^oC according to ICH specifications. Samples were placed in thin layers in petri-dishes and covered with polyethylene film. "Dark control" samples were treated similarly but covered with aluminium foil.

The thermal behaviour of samples after irradiation was compared with the behaviour of the original material (see Section 11). The X-ray powder diffraction patterns and infrared absorption spectra of the irradiated samples were also compared with those of the original material (see Section 11).

4.3.2. Studies in aqueous solution

1 mg of triprolidine hydrochloride was dissolved in 100 ml of 50/50 % by volume mixture of ethanol (95 %) and water to give a concentration of 0.01 mg/ml. 5 ml portions of solution were sealed in clear ampoules prior to irradiation and dark control ampoules were prepared and treated similarly.

Solutions of the 1:1 mass ratio mixtures for irradiation were prepared in a similar way to give concentrations of 0.01 mg/ml of TPH, i.e. 0.02 mg/ml of mixture.

The main analytical technique used to monitor the effects of irradiation was high performance liquid chromatography (HPLC) and the amount of drug present was quantified by the measurement of peak height. In order to determine the purity of the peak attributed to TPH. HPLC was performed using a photodiode array detector and also a UV detector.

4.4 Characterization of materials

In addition to the thermal analysis techniques described above, the following analytical techniques were used to characterize the TPH samples in terms of their identity and purity used in this study:

Ultraviolet-visible spectrophotometry

Mass spectroscopy

Infrared spectroscopy

X-ray powder diffraction

Thin-layer chromatography

High performance liquid chromatography (HPLC)

^{1}H NMR spectroscopy.

Detailed backgrounds to these well-established techniques are not given, but the types of instruments and any specific experimental details are recorded in the following sections.

4.4.1 Ultraviolet-visible spectrophotometry

The UV spectrum (CARY 500 Scan UV/Vis-Nir Spectrophotometer) of triprolidine hydrochloride (1 mg of TPH dissolved in 100 ml of 0.1 M HCl) (Figure 4.1) [4] shows absorption maxima at 232 nm and 290 nm due to the conjugated double bonds in the molecule, which are consistent with those of literature findings [4,11]. The spectrum was also recorded in distilled methanol and these results are shown in Table 4.1 together with the literature findings [4]. Spectrophotometric methods have been developed [40] for the analysis of tablets containing pseudoephedrine **4**, triprolidine **1** and dextromethorphan **5**.

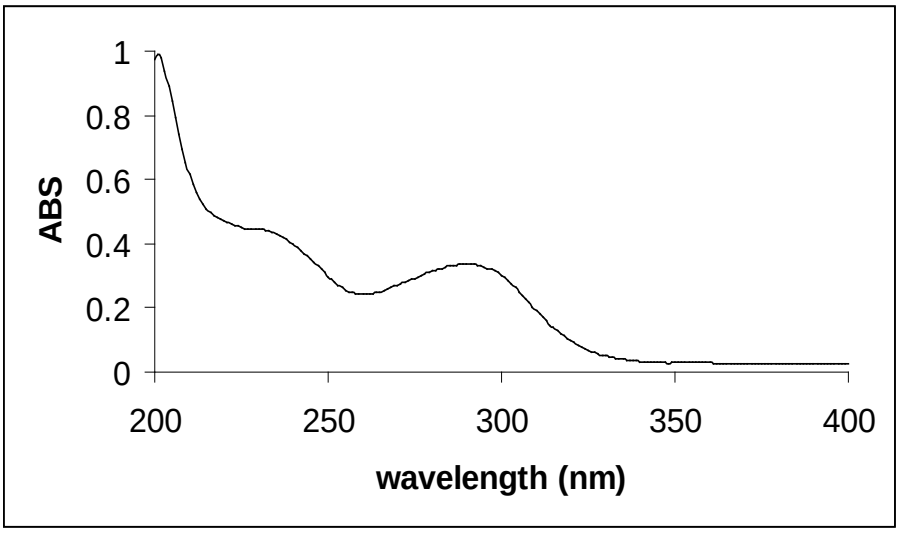

Figure 4.1 The UV spectrum of triprolidine hydrochloride in 0.1 M HCl.

Table 4.1 UV absorption maxima of TPH solutions [4,11]

Solvent l	Literature /nm	Experimental /nm
0.1 M HCl	232	231
	290	289
Distilled methanol	233	232
	282	281

4.4.2 Mass spectroscopy

The mass spectrum (Finnigan LCQ system equipped with atmospheric pressure chemical ionisation, APCI) of TPH is shown in Figure 4.2 and the proposed structures of the major fragments including the base peak at m/e 208 are consistent with literature findings as shown in Figure 4.3. The sample was prepared by dissolving 1 mg of triprolidine hydrochloride in a 100 ml of ethanol.

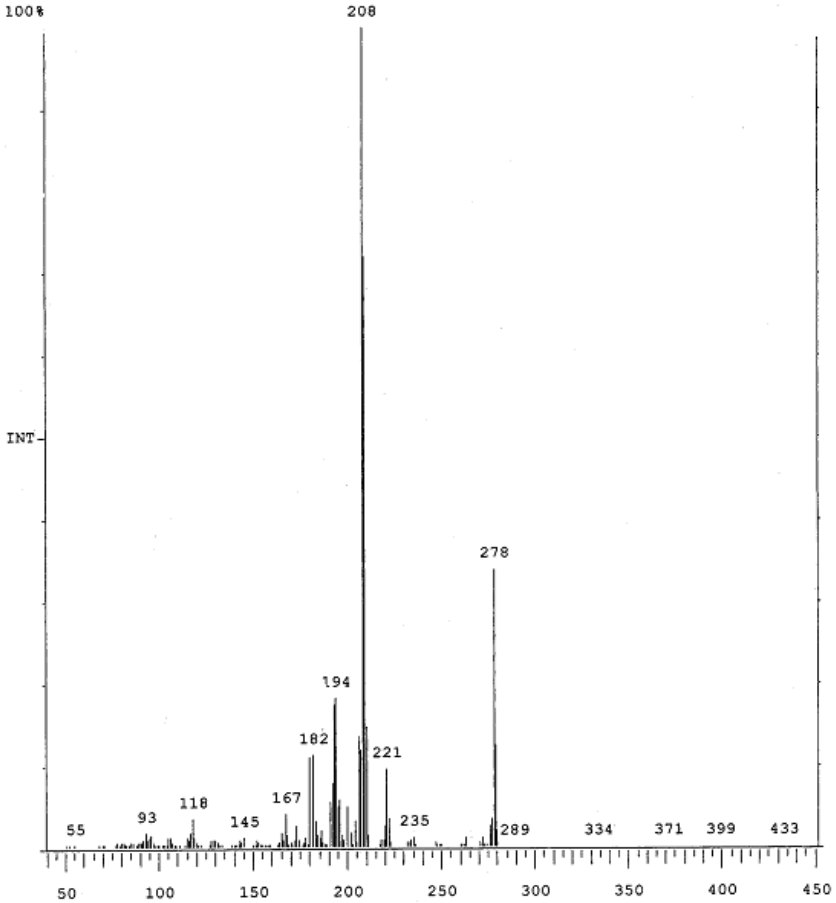

Figure 4.2 The mass spectrum of triprolidine hydrochloride

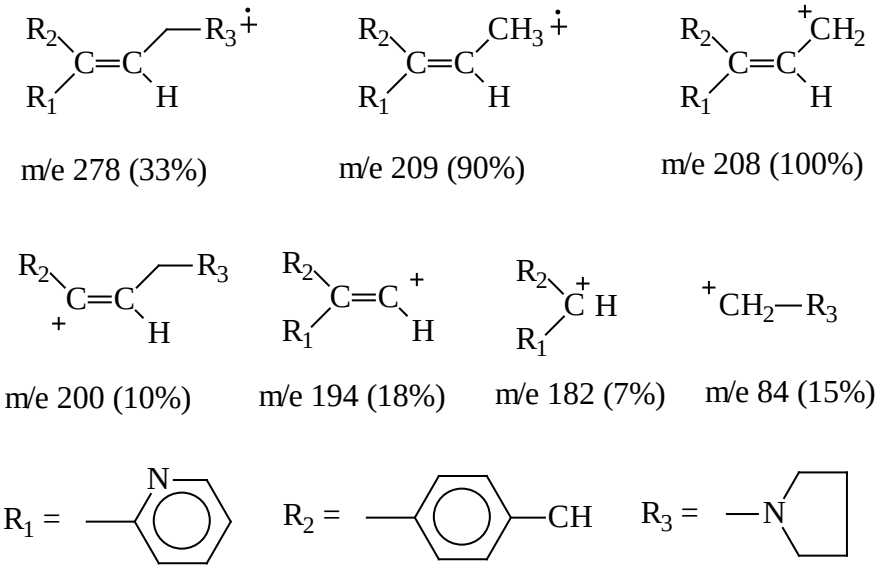

Figure 4.3 The major fragments of TPH observed in the mass spectrum [4].

4.4.3 Infrared spectroscopy

A Perkin-Elmer Spectrum 2000 FTIR spectrometer was used to record the infrared absorption spectrum of TPH (in KBr disk) over the range 4000 and 400 cm^{-1} (see Figure 4.3). The absorption bands are compared with literature values [2,4] in Table 4.2. and are consistent.

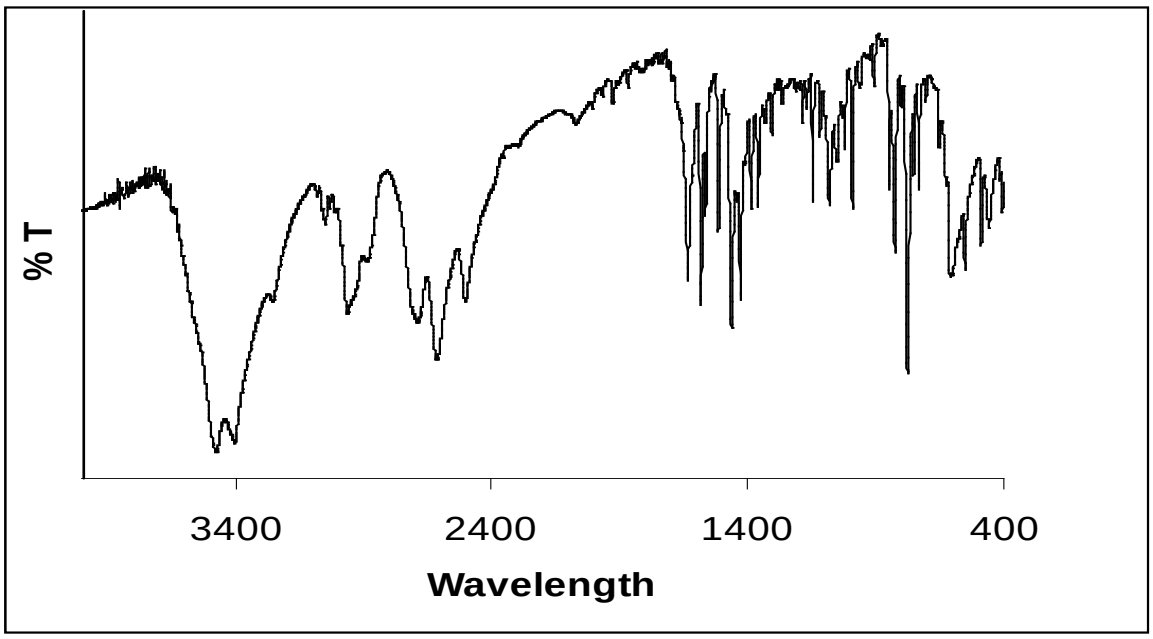

Figure 4.4 Infrared spectrum of TPH.

Table 4. 2 Infrared absorption bands of TPH

Literature cm^{-1} [4]	Experimental cm^{-1}	Assignment
3480	3477	OH stretch (hydrate)
2958	2959	CH stretch (- CH_3)
2960	2961	NH^+ stretch
1630	1631	C=C stretch
1582	1582	C=stretch (aromatic)
1562	1563	C=C stretch (pyridine)
1462	1462	-CH_3 asym. bend
1386	1386	-CH_3 sym. bend
1358	1359	C-N stretch (tert. amine)
846	847	=C-H rock
824	825	Para subst. benzene
776	775	1-subst.pyridine

4.4.4 X-ray powder diffraction

X-Ray powder diffraction patterns were measured using a Rigaku Denki Max III diffractometer fitted with a horizontal goniometer, graphite monochromator and scintillation detector. Na-filtered cu-K∀ radiation was generated at a voltage of 40 kV and a current of 20 mA. A fixed time step scanning method was employed. Step-scans were recorded for all samples for 2θ from 5 to 60°.

A powder pattern was simulated using data taken from the *Cambridge Structural Database* [40]. The results are compared with the experimental pattern in Figure 4.5.

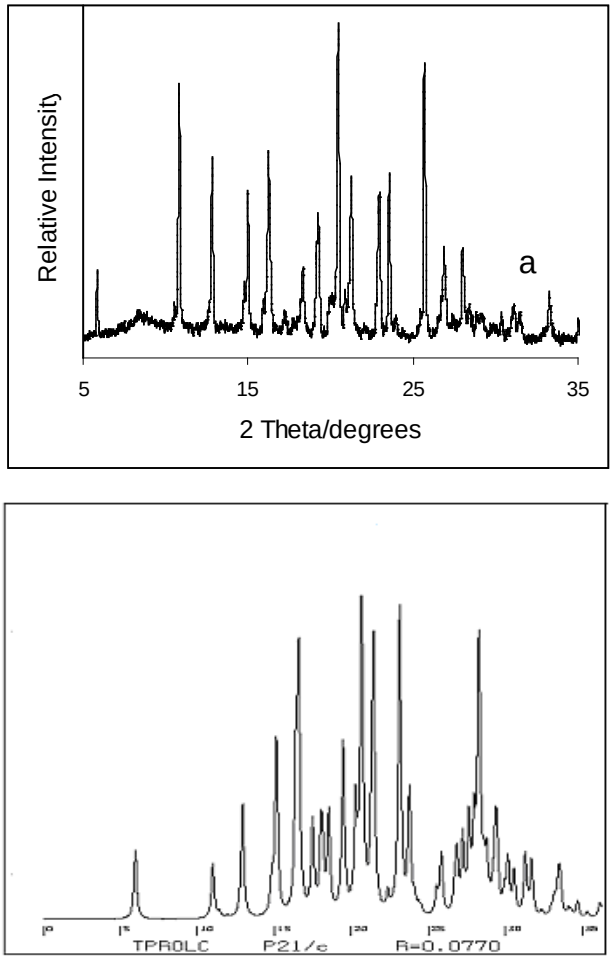

Figure 4.5 X-ray powder diffraction patterns of TPH: (a) experimental pattern and (b) pattern simulated from the single-crystal structure of TPH [40].

4.4.5 Nuclear magnetic resonance spectroscopy

The ^{1}H-NMR spectra of TPH in D_2O and in deuterated-DMSO as solvents, were recorded on a Bruker DR X 400 MHZ spectrometer and the results were compared with the reported spectrum [4] recorded on a Varian X L100, 100 MHz NMR spectrometer in deuterated DMSO as a solvent with tetramethylsilane as an internal standard. The spectrum is illustrated in Figure 4.6 and the interpretation given in Table 4.3 and Figure 4.7. Consistency between the literature and experimental findings confirms the identity of the triprolidine sample material.

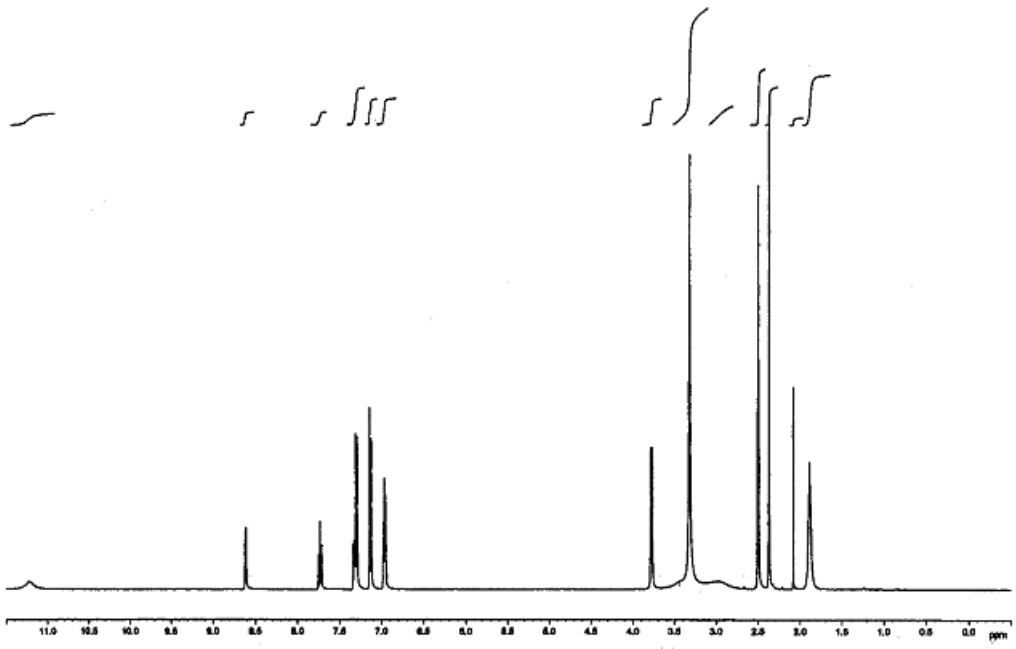

Figure 4.6 NMR spectrum of TPH

Table 4.3 NMR results for TPH

Chemical shift (ppm) Literature	Chemical shift (ppm) Experimental	No of protons	Multiplicity	Assignment
11.5	11.4	1	1	j
8.63	8.83	1	multiplet	a
7.74	7.74	1	6	b
7.34	7.32	1	multiplet	c
7.00	7.00	1	multiplet	d
7.12 – 7.38	7.12 – 7.38	4	4	benzene ring
6.95	6.94	1	3	e
3.78	7.80	2	2	f
3.49	3.49	2	1(broad)	h
2.94	2.94	2	1(broad)	h
2.37	2.37	3	1	i
1.88	1.89	4	multiplet	g

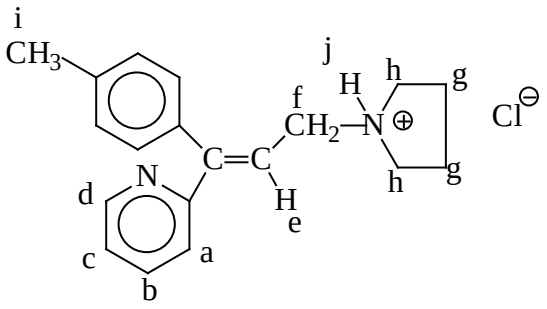

Figure 4.7 Structure of TPH

4.4.6 Thin-layer chromatography

Thin-layer chromatography (TLC) was used to separate reactants and degradation products and also to test the purity of the compounds used. Glass plates were coated with silica-gel F. The first mobile phase consisted of chloroform: diethylamine (95%: 5%) and 0.5 mg of TPH was dissolved in 10 mL chloroform and then spotted onto the plate. The R_f value was calculated as $R_f = 2.05/5 = 0.41$. An alternative mobile phase of chloroform: methanol: ammonia (89 %: 10 %: 1 %) was also used. 0.5 mg of TPH was dissolved in 10 mL of methanol and the solution was spotted on a plate. Again only a single spot was observed and the R_f value was similar: $R_f = 2.04/5 = 0.40$. These results confirm the purity of the triprolidine samples used.

5. THE THERMAL BEHAVIOUR OF TRIPROLIDINE HYDROCHLORIDE

5.1. DSC and TG results for TPH

DSC and TG (including TG-FTIR see section 5.2), were used, as described in Section 4, to examine the thermal behaviour of samples of TPH (as supplied, after storage in a dessicator over P_2O_5 at room temperature for 15 days, and dried TPH after re-exposure to water vapour at room temperature for 1 day). Unless otherwise specified, samples were heated in nitrogen at 10 ^oC min^{-1} in unsealed aluminium pans or stainless-steel pressure pans (as specified), for DSC, and in an open platinum pan for TG.

The DSC curves for TPH (as supplied) in a sealed pressure pan and in an uncrimped aluminium pan are shown in Figure 5.1. TPH shows a sharp melting endotherm at 122-123 ^oC which corresponds to the literature value [2], and a broad exotherm between 195 and 240 ^oC. The endotherm is broadened and more complex in the aluminium pan and a variety of processes may be taking place, e.g. sublimation, decomposition and melting. It is also possible that the HCl from the TPH might be reacting with the aluminium pan.

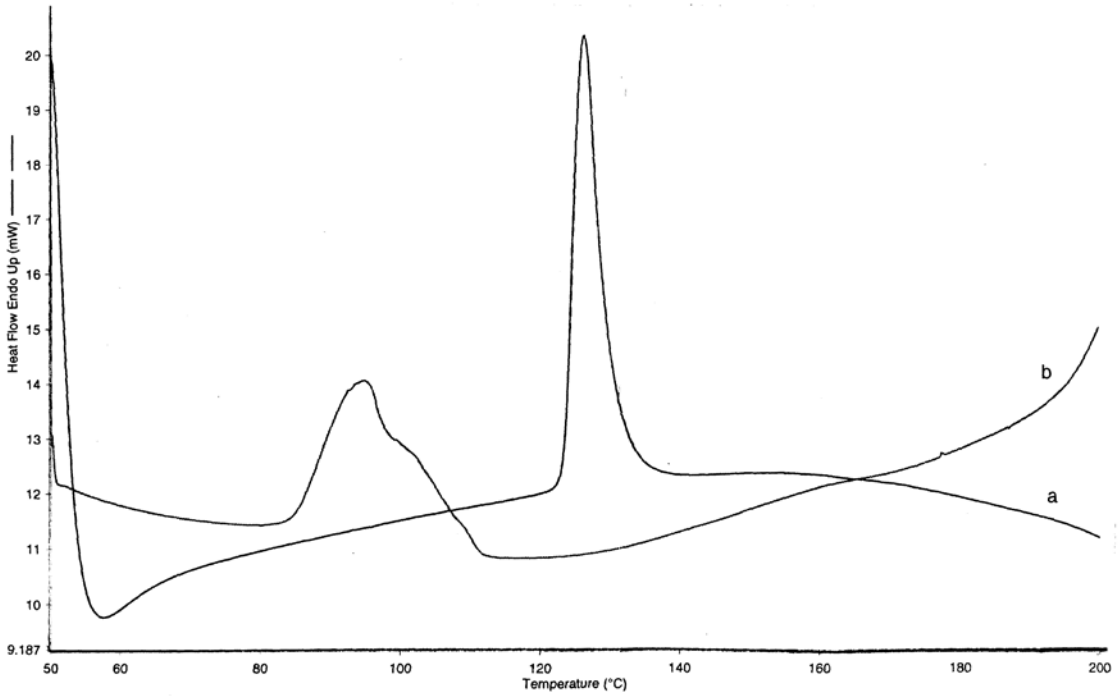

Figure 5.1 DSC curves for TPH heated at 10 ^{o}C min^{-1} in flowing nitrogen, using (a) a sealed pressure pan and (b) an uncrimped aluminium pan.

Figure 5.2 shows the DSC curves for TPH (a) as supplied, and (b) after drying and (c) after being exposed to water for 1 day, heated at 10 ^{o}C min^{-1} in flowing nitrogen, in sealed pressure pans. Curve (a) shows a sharp endotherm at 123.6 ^{o}C, ΔH = 117 J g^{-1} and a broad exotherm with onset 202 ^{o}C, ΔH = -88 J g^{-1}. The dried TPH shows a broader endotherm at 120 ^{o}C, ΔH = 113 J g^{-1}, while curve (c) for the sample stored over water shows also a broad endotherm 121 ^{o}C, ΔH = 95 J g^{-1}. The changes in the thermal behaviour caused by the drying treatment and re-exposure to water are thus slight.

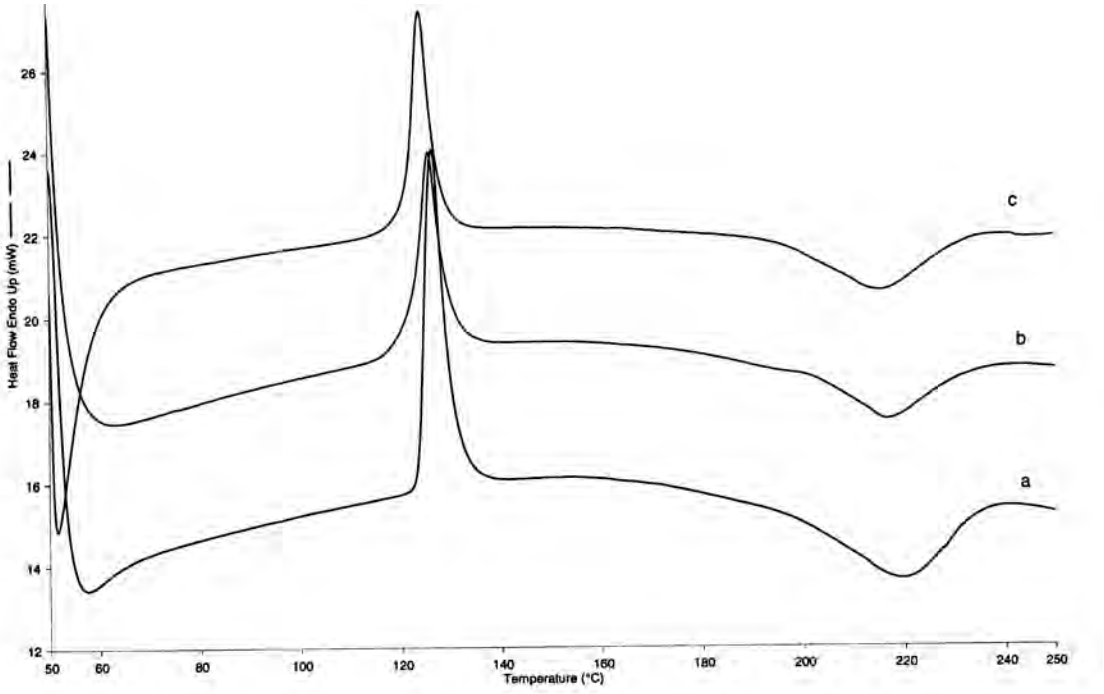

Figure 5.2 DSC curves for TPH (a) as supplied, (b) after drying and (c) after dried TPH was re-exposed to water vapour for 1 day (heated at 10 ^{o}C min^{-1} in flowing nitrogen, using sealed pressure pans).

A sample of dried TPH was heated at 10 ^{o}C min^{-1} in a sealed pressure pan in the DSC to 125 ^{o}C and then cooled at 10 ^{o}C min^{-1}. On reheating (see Figure 5.3), no endotherm was observed, which shows that the transition is not readily reversible and may be accompanied by decomposition.

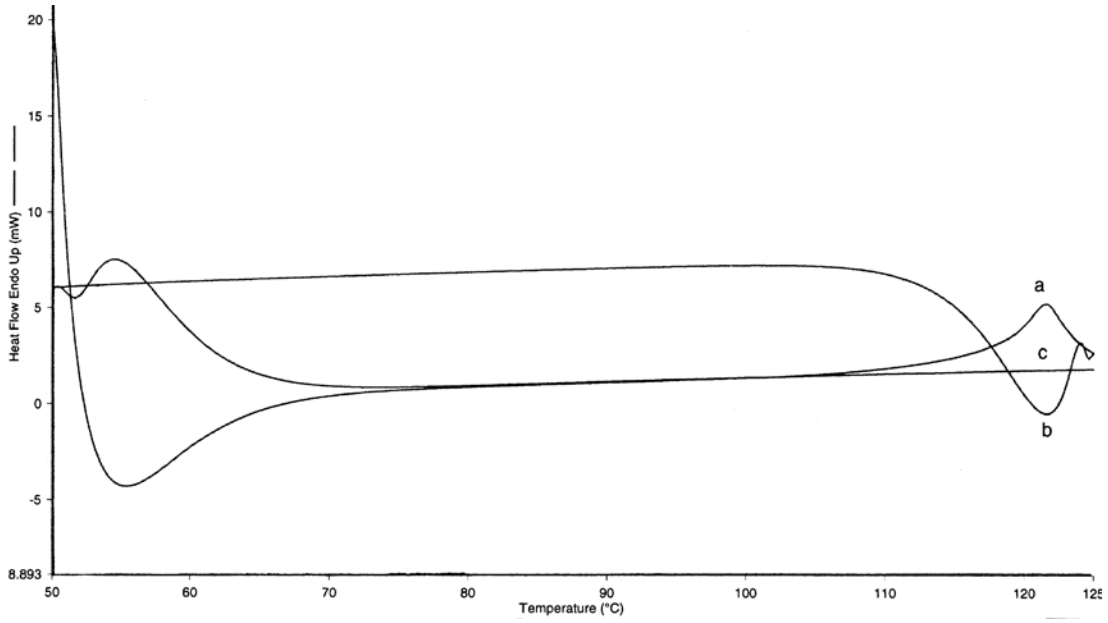

Figure 5.3 DSC curves for dried TPH (a) heated at 10 ^{o}C min $^{-1}$ in flowing nitrogen using a sealed pressure pan, followed by cooling (b) at 10 ^{o}C min $^{-1}$ and reheating (c) at 10 ^{o}C min $^{-1}$.

The TG curves for the original TPH, dried TPH and for TPH re-exposed to water vapour are shown in Figure 5.4. The TG curves show multi-step loss of components. For the original TPH, there is an initial mass-loss between 50 and 100 ^{o}C of 4.9 %. For the dried TPH, the mass-loss is decreased to 3.4 %. For the original $C_{19}H_{22}N_2.HCl.H_2O$ (molar mass = 332.5 g mol^{-1}) loss of water corresponds to a 5.4 % mass-loss. Loss of HCl corresponds to an 11.0 % mass-loss. The TPH samples re-exposed to water showed a mass-loss between 50-100 ^{o}C of 4.4 % indicating, that TPH had adsorbed water during the storage.

The major mass-loss to a residue of about 20 % of the original mass of dried TPH by 400 ^{o}C occurs in two overlapping stages. The onset of the first stage of the major mass-loss occurs soon after the melting endotherm on the corresponding DSC curve (Figure 5.2). The mass-loss may be a combination of evaporation and decomposition of the liquid.

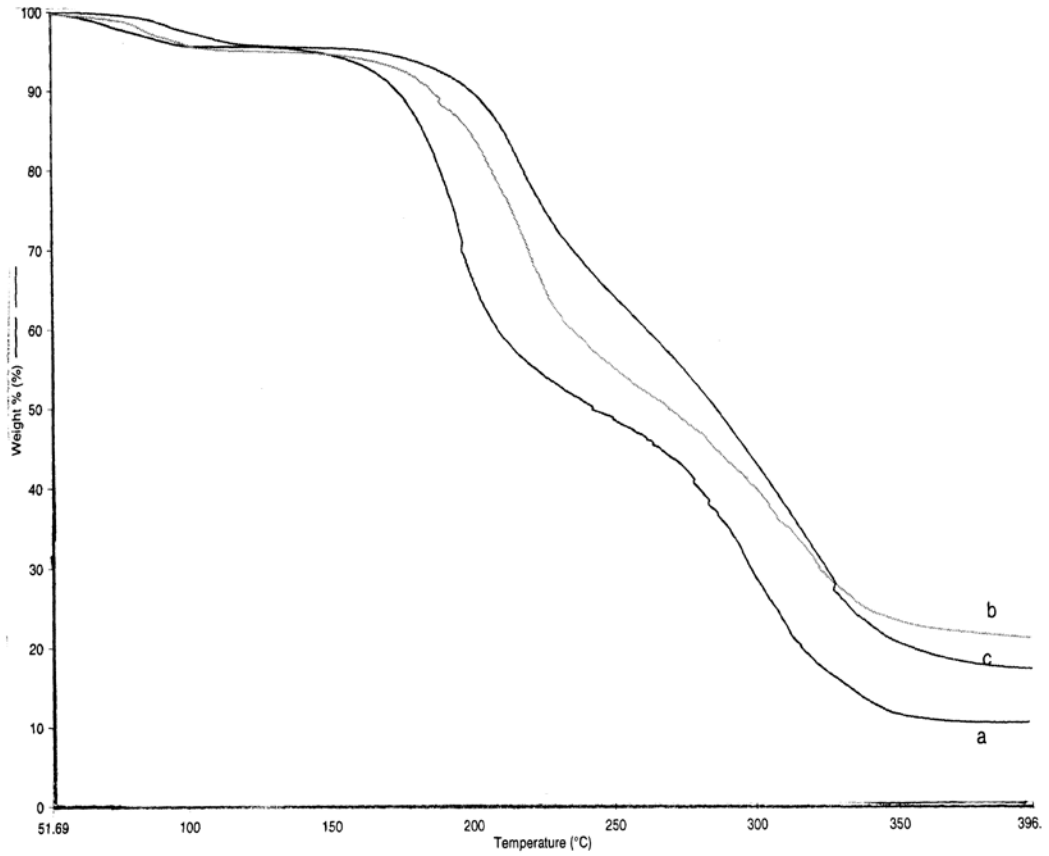

Figure 5.4 TG curves for various samples of TPH (a) original, (b) dried and (c) re-exposed to water, heated at 10 ^{o}C min $^{-1}$ in flowing nitrogen in an open platinum pan.

5.2. TG-FTIR results for TPH

TG–FTIR was used to detect any gases evolved by TPH on heating in nitrogen. The stacked FTIR plots, over the spectral region between 4000 and 400 cm^{-1}, for the original TPH and dried TPH are similar (Figure 5.5). Evolution of HCl is expected to result in strong absorbances at just above and just below 3000 cm^{-1} (see Figure 5.6 [41]).

For the original TPH, formation of HCl gas is shown in the stack plot (Figure 5.5 (a)) between 10 and 30 minutes, which, at a heating rate of 10 ^{o}C min^{-1} from a starting temperature of 50 ^{o}C, corresponds to release between 150 and 350 ^{o}C, which is the temperature range of the overall mass loss in the TG curve (Figure 5.4).

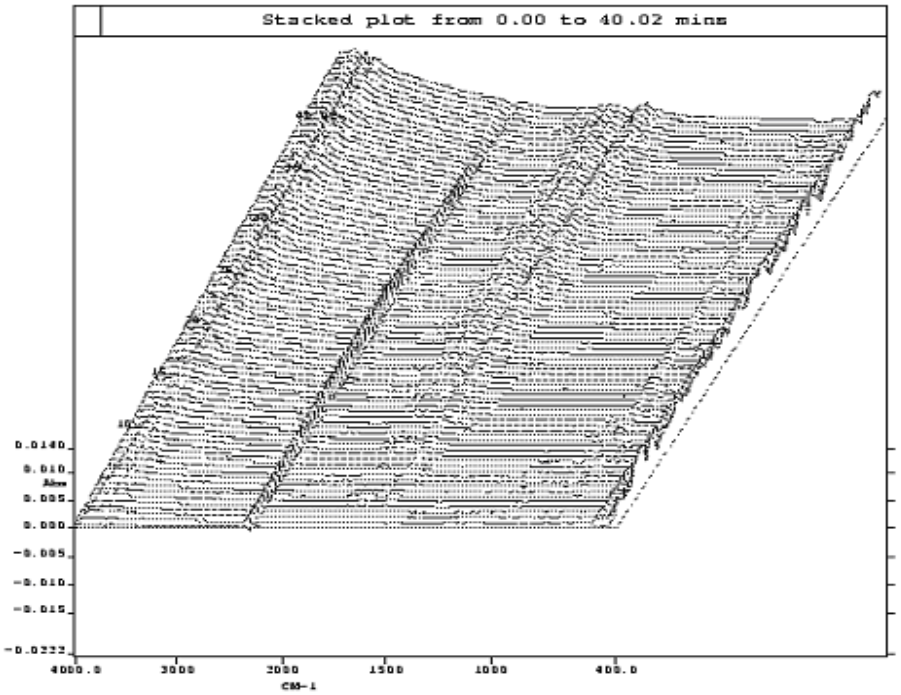

Figure 5.5 (a) Stacked FTIR plot recorded during the TG runs (see Figure 5.4) on the original TPH, heated at 10 ^{o}C min^{-1} in flowing nitrogen from 50 to 400 ^{o}C.

For the dried TPH, formation of HCl gas is shown in the stack plot (figure 5.5 (b) over a decreased interval between 17 and 21 minutes, that is between 220 and 260 ^{o}C, which corresponds to the second stage of mass-loss in the TG curve, (Figure 5.4).

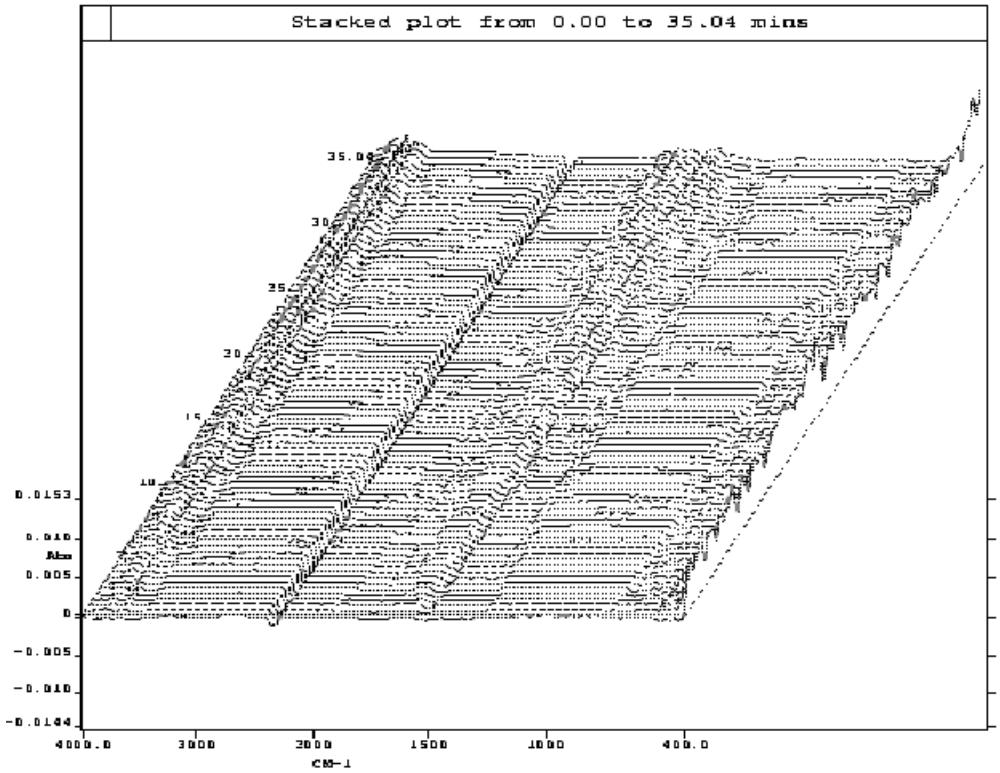

Figure 5.5 (b) Stacked FTIR plot recorded during the TG runs (see Figure 5.4) on the dried TPH heated at 10 ^{o}C min^{-1} in flowing nitrogen from 50 to 400 ^{o}C.

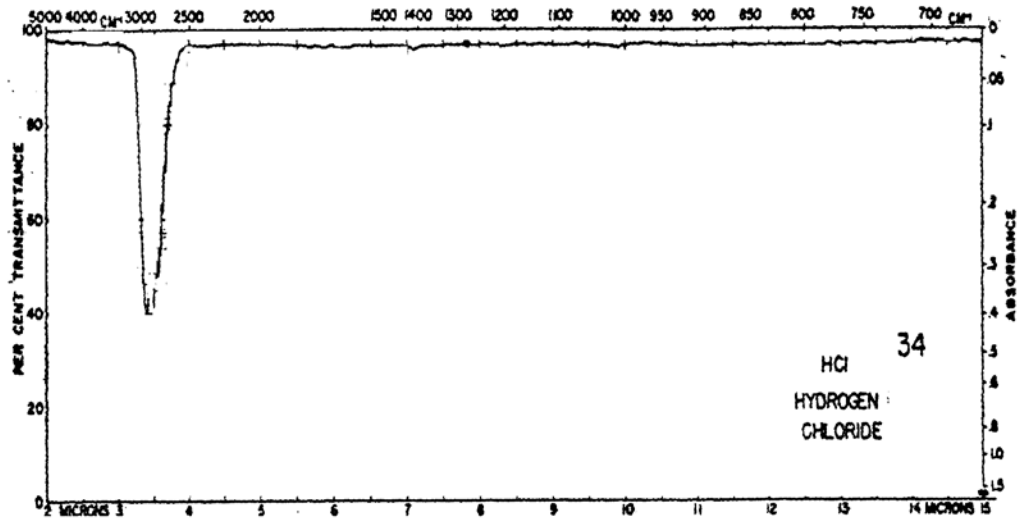

Figure 5.6 The infrared spectrum of HCl [41]

5.3 Hot-stage microscopy (HSM) of TPH

To supplement the DSC results (Figure 5.1) hot-stage microscopy of a small portion of pure TPH was performed, using polarized light and the equipment described in Section 4. A typical sequence of pictures taken at the temperatures indicated is shown in Figure 5.7. TPH is a white crystalline powder (a) which starts to melt at 82-84 ^{o}C, (b) and there is formation of a dark ring of liquid at about 88 ^{o}C (c). The thickness of the liquid layer grows as the crystalline core melts or dissolves (d and e). Neighbouring droplets coalesce (f and g) and the sample is totally liquid by 122 ^{o}C (h). Picture (c) indicates evolution of some trapped gas through the liquid surface.

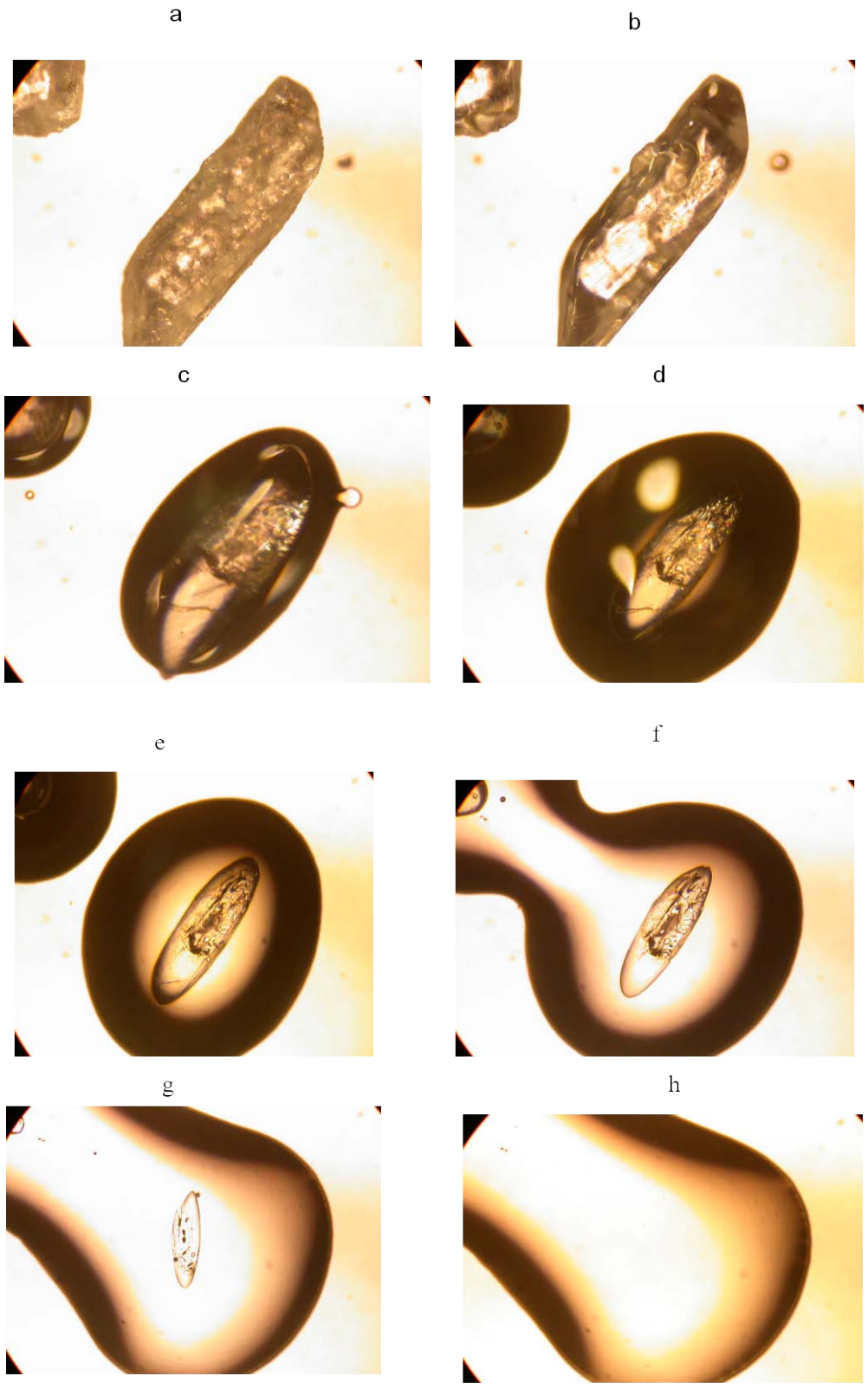

Figure 5.7 Photomicrographs of crystals of TPH taken on a hot-stage microscope at: (a) 25 ^{o}C, (b) 84 ^{o}C, (c) 91 ^{o}C, (d) 103 ^{o}C, (e) 109 ^{o}C, (f) 116 ^{o}C, (g) 119 ^{o}C and (h) 122 ^{o}C

6. THE THERMAL BEHAVIOUR OF β-CYCLODEXTRIN (BCD) AND O F GLUCOSE

6.1. The thermal behaviour of β-cyclodextrin (BCD)

The DSC curves of samples of the original BCD, BCD that had been stored in a dessicator over P_2O_5 for 15 days, and of dried BCD re-exposed to water vapour for 1 day are shown in Figure 6.1.

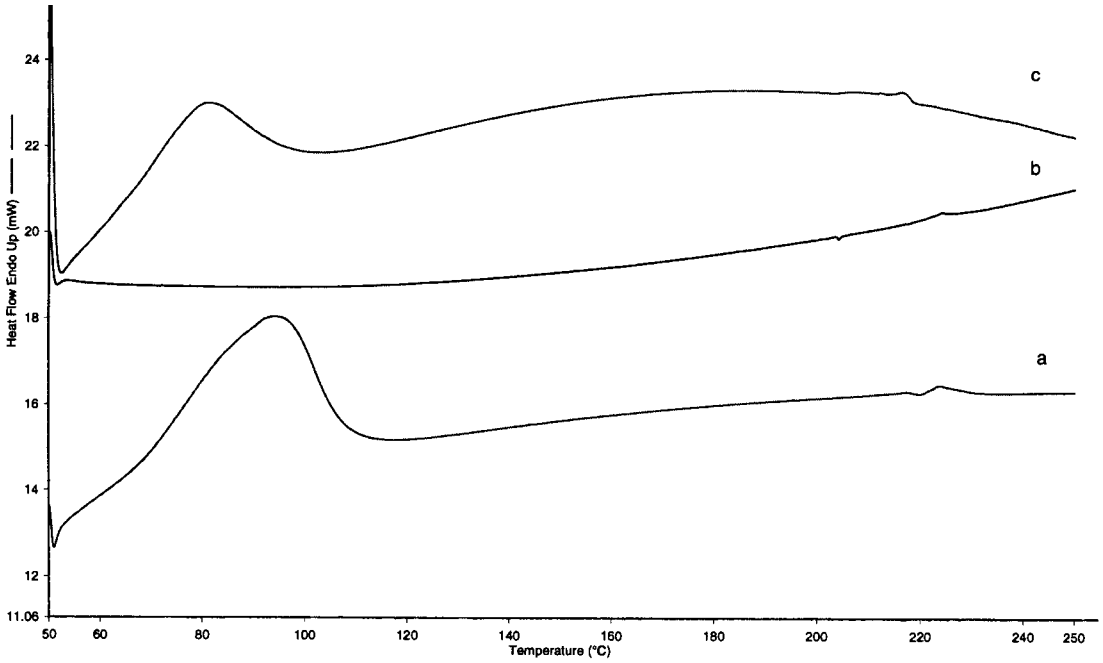

Figure 6.1 DSC curves for (a) the original BCD, (b) the dried BCD and (c) dried BCD re-exposed to water vapour for 1 day, heated at 10 ^{o}C min^{-1} in flowing nitrogen using uncrimped aluminium pans.

The DSC curve for the original BCD (a) shows a broad dehydration endotherm between 65 and 110 ^{o}C with ΔH = 279 J g^{-1}, and a small exotherm at 220 ^{o}C with ΔH = 2.16 J g^{-1}. The curve for the dried BCD (b) shows no dehydration endotherm, which indicates that the water has been removed after storage over P_2O_5. The small exotherm still exists at about 220 ^{o}C in the dried BCD, while for dried BCD re-exposed to water vapour there is a broad endotherm between 55 and 100 ^{o}C and the small exotherm is still observed (Figure 6.1).

The removal of water from BCD during storage over P_2O_5 and re-adsorption of water is confirmed by the TG curves for the original, dried and re-exposed samples, shown in Figure 6.2. The TG curves for all of these samples show a single-step mass-loss. The original BCD contains 12.5 % water and the dried BCD re-exposed to water vapour shows 10 % of water. Degradation of BCD occurs above 300 ^{o}C for the three samples. The small exotherm in the DSC curve at about 220 ^{o}C is not accompanied by a mass-loss in the TG curve.

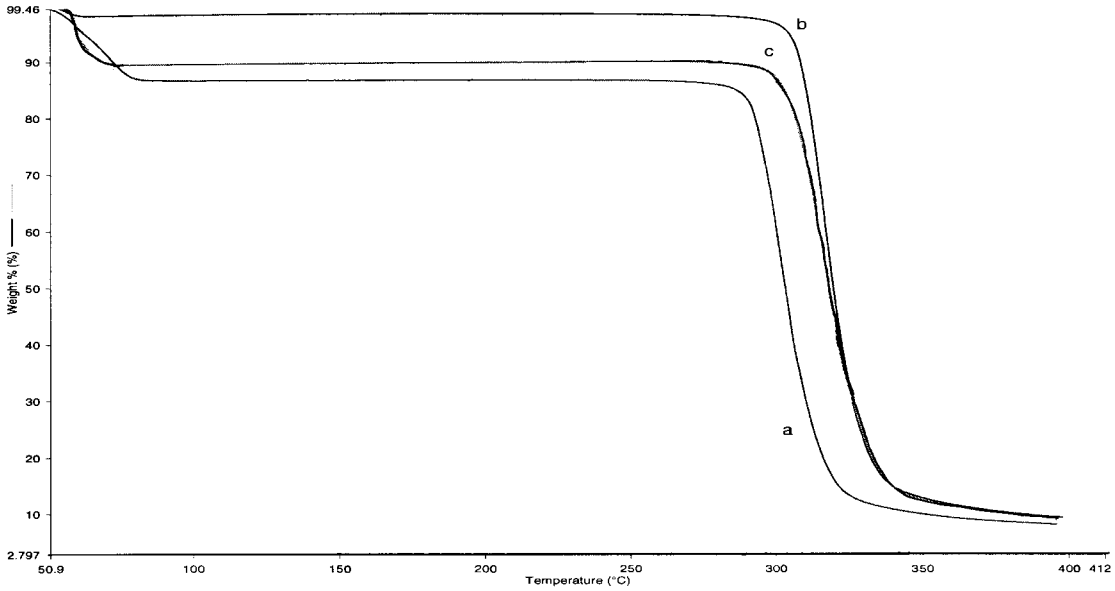

Figure 6.2 TG curves for (a) the original BCD, (b) the dried BCD and (c) dried BCD re-exposed to water vapour for 1 day, heated at 10 ^{o}C min^{-1} in flowing nitrogen in open platinum pans.

6.2 Hot-stage microscopy (HSM) of BCD

The HSM photomicrographs of BCD powder are shown in Figure 6.3. At room temperature the white powder shows small crystalline particles (a). At about 70 ^{o}C (b) the samples shows some movement which is probably caused by the loss of water from the BCD crystallites. Melting starts at 245 ^{o}C (c to g) and is accompanied by charring. At 280 ^{o}C (h) a black residue remains.

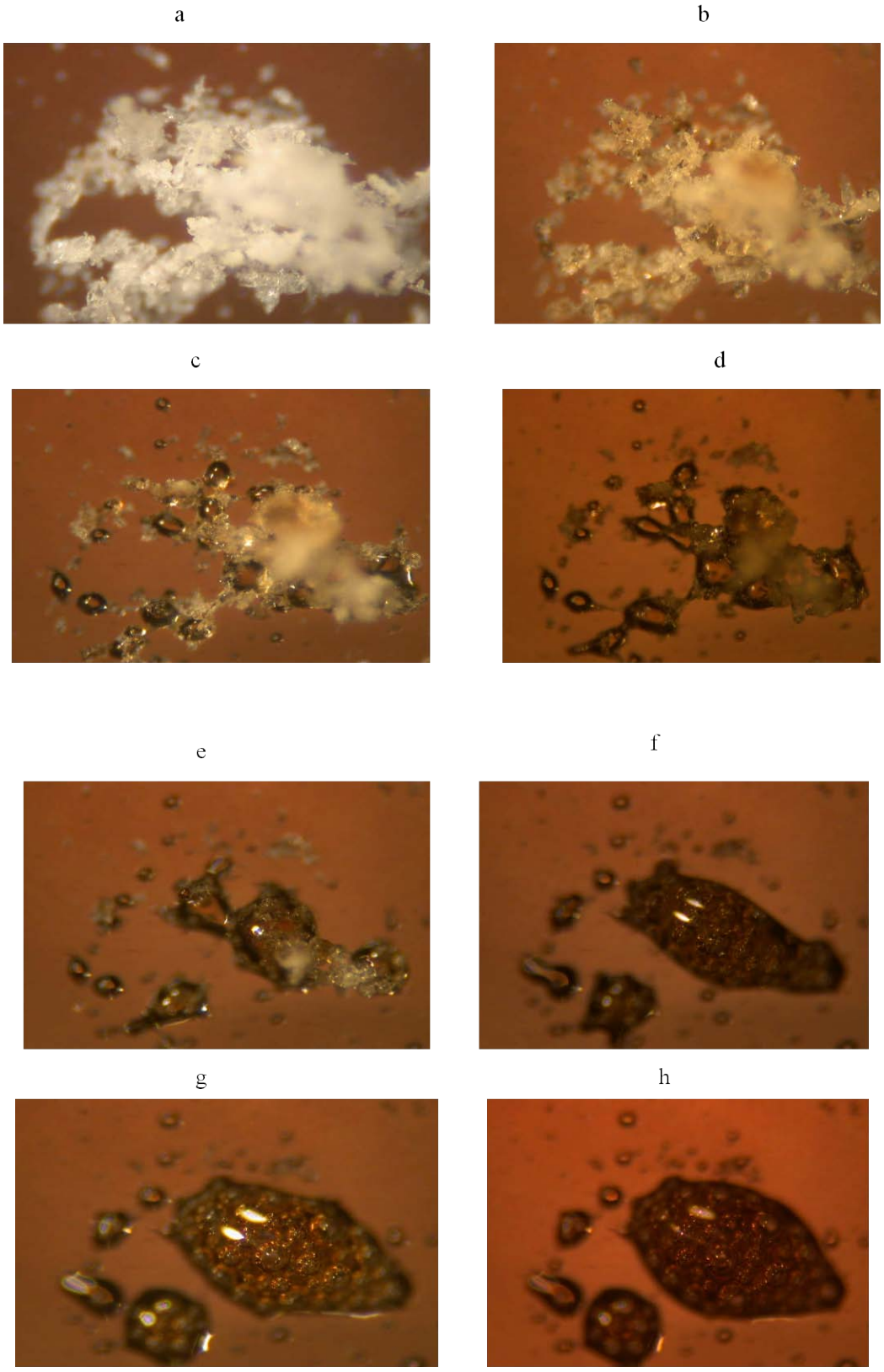

Figure 6.3 Photomicrographs of BCD powder taken during hot-stage microscopy at: (a) 25 ^{o}C, (b) 70 ^{o}C, (c) 245 ^{o}C, (d) 253 ^{o}C, (e) 259 ^{o}C, (f) 261 ^{o}C, (g) 269 ^{o}C and (h) 280 ^{o}C.

6.3. The thermal behaviour of glucose

The DSC curve for the original sample (a) of glucose (Figure 6.4) shows a sharp endotherm (melting) with onset 158 ^{o}C and ΔH = 190 J g^{-1}, which correspond with the literature values [2]. The curve for dried glucose shows a broader endotherm with onset temperature 156 ^{o}C, ΔH = 191 J g^{-1}, while curve (c) shows that glucose adsorbs water during exposure to water vapour. There is a broad dehydration endotherm between 50 and 100 ^{o}C with a peak at about 85 ^{o}C and a total ΔH = 209 J g^{-1}. A further broad endotherm follows with onset temperature 157 ^{o}C and ΔH = 109 J g^{-1}. The effect of prior dehydration on the behaviour of glucose in sealed pressure pans is slight.

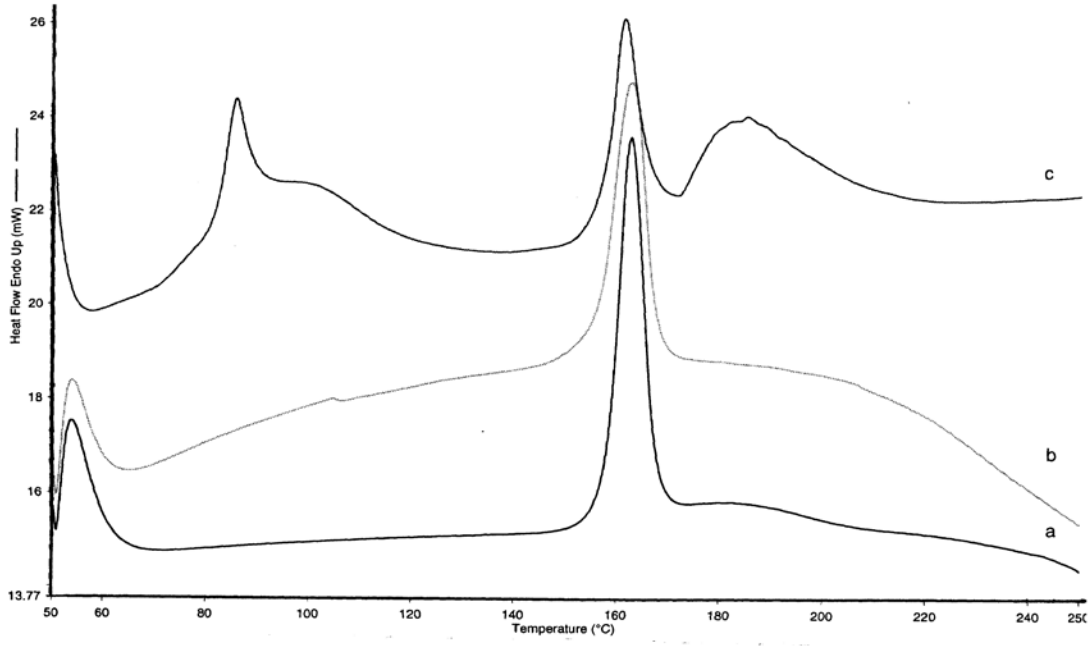

Figure 6.4 DSC curves for glucose (a) the original, (b) dried and (c) dried glucose exposed to water vapour for 1 day, heated at 10 ^{o}C min^{-1} in flowing nitrogen, using sealed pressure pans.

The TG curves (Figure 6.5) of the original and dried samples of glucose show however, that the drying process has decreased the thermal stability of the glucose, with the onset temperature of decomposition being lowered from about 170 to 110 ^{o}C when the samples are heated in open pans. The results are summarized in Table 6.1.

The results characterizing the thermal behaviour of the individual compounds are summarized in Table 6.1 for later comparison with the thermal behaviour of mixtures

Table 6.1 Summary of the thermal behaviour of pure compounds

Sample	Molar mass / g mol^{-1}	Onset temperature of DSC endotherms /EC	ΔH / J g^{-1}	ΔH / kJ mol^{-1}	Initial mass – loss (50 to 110EC)
TPH	332.5	122	117	38.9	4.9
TPH (dried)		119	113	37.6	3.9
BCD	1135	64	279	317	10
BCD (dried)		-			-
Glucose	180	158	190	34.4	-
Glucose (dried)		156	191	34.0	-

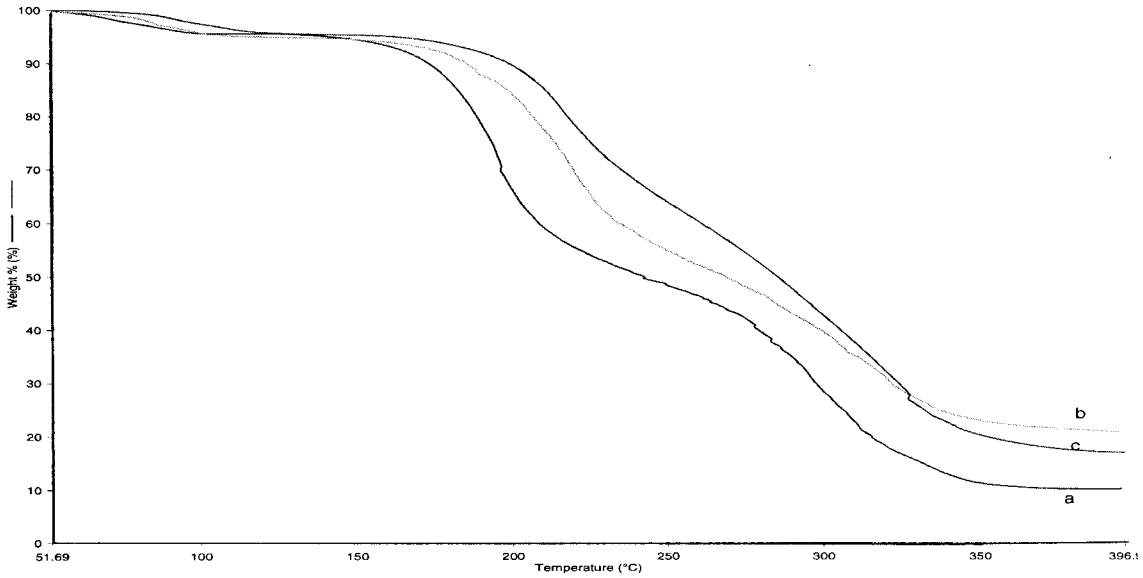

Figure 6.5 TG curves of glucose (a) the original, (b) dried and (c) dried glucose re-exposed to water vapour for 1 day, heated at 10 ^{o}C min^{-1} in open platinum pans.

6.4. Hot-stage microscopy of glucose

Photomicrographs of glucose are shown in Figure 6.6 with their related temperatures. The white crystals photographed at room temperature are shown in (a). Melting starts at 147 ^{o}C (b) and is complete at 156 ^{o}C (d to h). These results support the thermal behaviour shown in the DSC curves in Figure 6. 4.

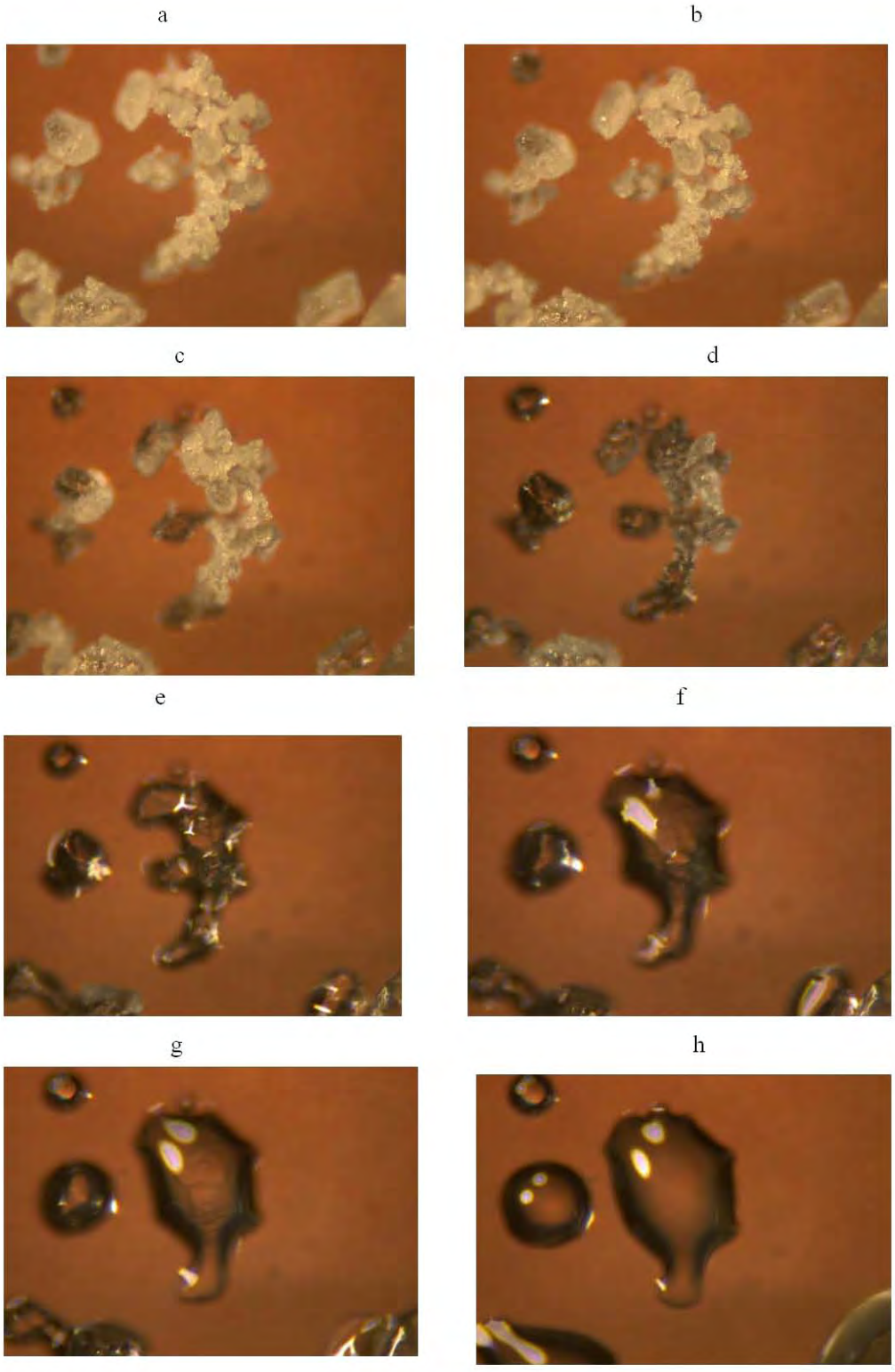

Figure 6.6 Photomicrographs of crystals of glucose taken during hot-stage microscopy at: (a) 25 ^{o}C, (b) 50 ^{o}C, (c) 145 ^{o}C, (d) 149 ^{o}C, (e) 251 ^{o}C, (f) 153 ^{o}C, (g) 154 ^{o}C and (h) 156 ^{o}C.

6.5 The thermal behaviour of mixtures of glucose and BCD

The DSC curves for physical mixtures of glucose and BCD (1:1 mass ratio (1.0 : 0.16 mole ratio) physical mixture of glucose and BCD and a 1:1 mole ratio physical mixture of glucose and BCD), heated at 10 ^{o}C min^{-1} using uncrimped aluminium pans, are shown in Figure 6.7. The curves for the mixtures (c) and (d) show the features of the pure samples, although the glucose melting endotherm shows slight broadening. The lack of significant changes in the thermal behaviour on mixing indicates little if any interaction between glucose and BCD. There is no indication of inclusion of the glucose by BCD in the solid state. These results are supported by XRD in Section 9 and IR in Section 10. Molecular modelling in Section 14 suggests that glucose could be included in the BCD cavity. The results for glucose/BCD mixtures are summarized in Table 6.2.

Table 6.2 Summary of the thermal behaviour of physical mixtures of BCD and glucose.

Sample	Onset temperature of BCD dehydration / EC	Onset temperature of melting of glucose / EC	Expected ΔH value / kJ mol^{-1}	Observed ΔH value / kJ (mol BCD)$^{-1}$	Observed ΔH value / kJ (mol glucose)$^{-1}$
BCD	64		317		
glucose		159	34		
1:1 mass ratio BCD and glucose	52	155		219	39
1:1 molar ratio BCD and glucose	60	154		263	31

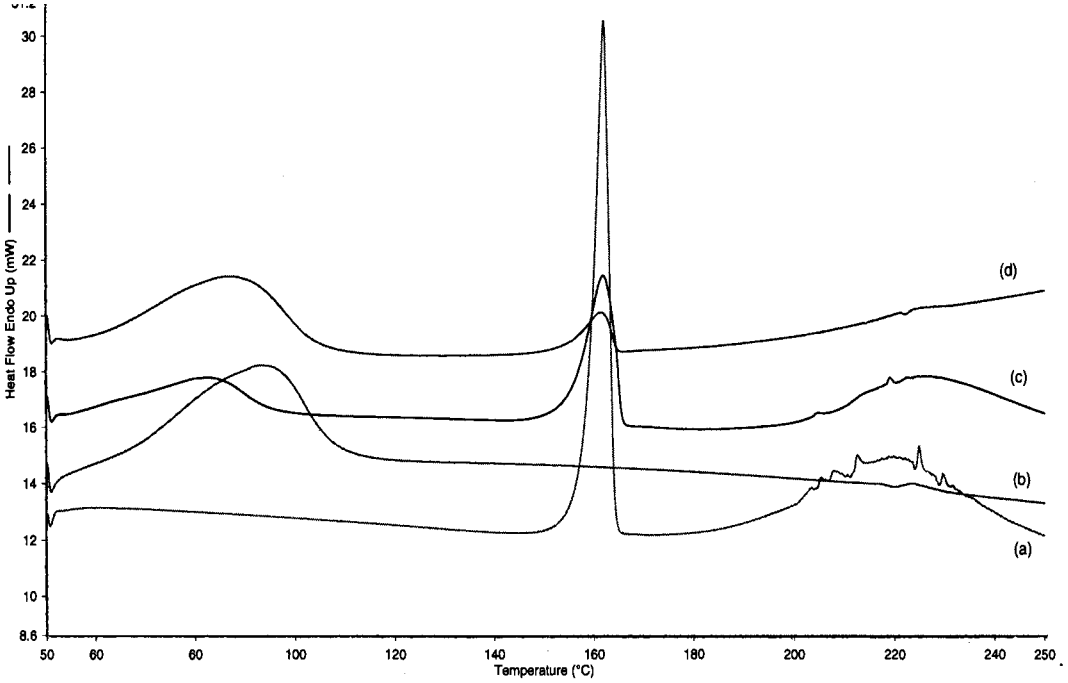

Figure 6.7 DSC curves for (a) glucose, (b) BCD, (c) a 1:1 mass ratio (1.0 : 0.16 mole ratio) physical mixture of glucose and BCD and (d) a 1:1 mole ratio physical mixture of glucose and BCD (heated at 10 ^{o}C min^{-1} in flowing nitrogen, using uncrimped aluminium pans).

6.6 Hot-stage microscopy of physical mixtures of glucose and BCD

The photomicrographs of a 1:1 mass ratio (1.0 : 0.16 mole ratio) physical mixture of glucose and BCD are shown in Figure 6.9. A similar set for a 1:1 molar ratio physical mixture are shown in Figure 6.10. At room temperature it was not possible to identify particles of the individual constituents (both white powder) even though there is a higher molar proportion of BCD in Figure 6.10. On heating some of the particles of glucose started melting at d, while at g the glucose has melted completely and the particles of BCD completely at h.

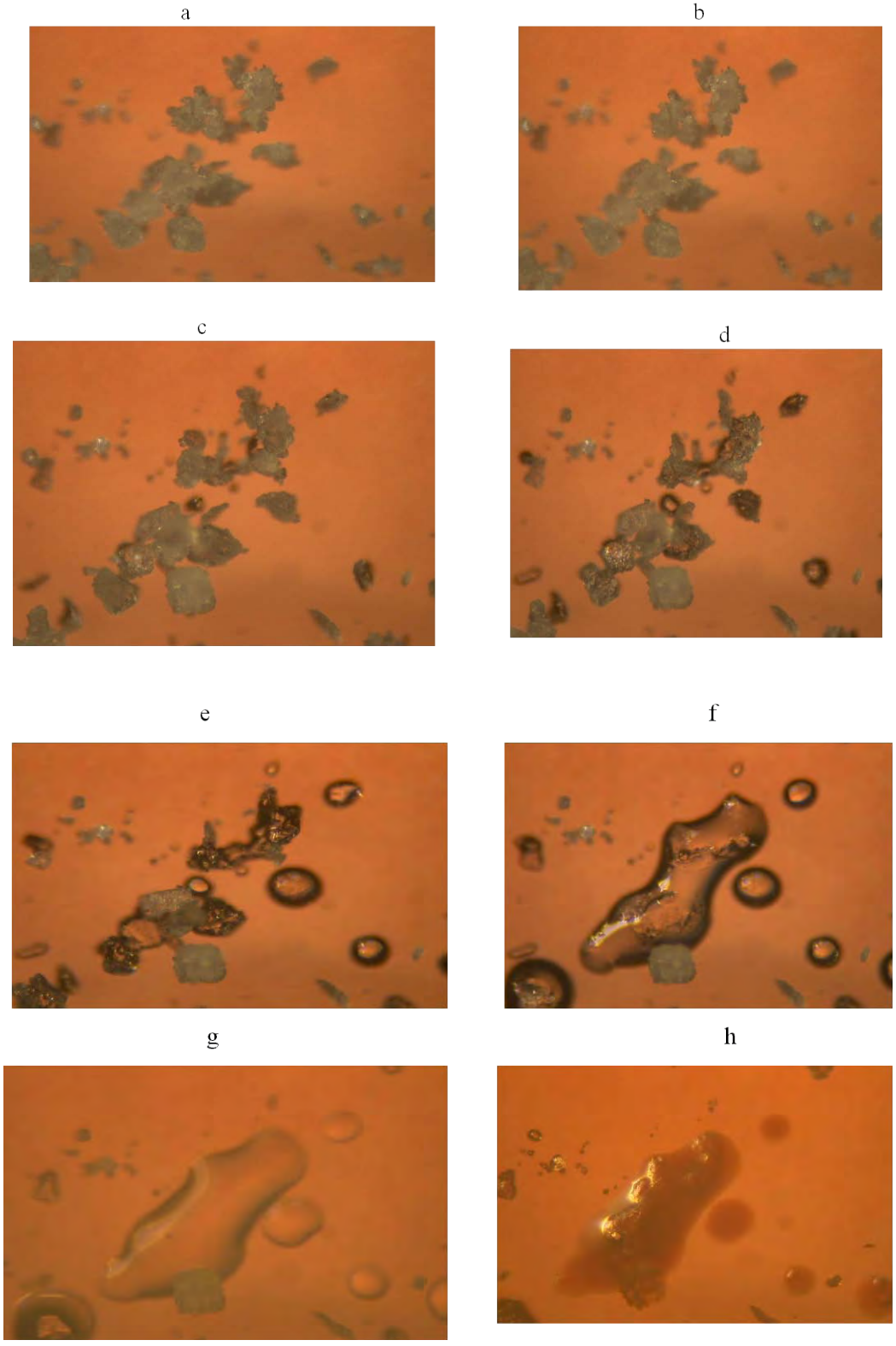

Figure 6.9 Photomicrographs of crystals of a 1:1 mass physical mixture of glucose and BCD taken during hot-stage microscopy at: (a) 25 ^{o}C, (b) 47 ^{o}C, (c) 140 ^{o}C, (d) 141 ^{o}C, (e) 151 ^{o}C, (f) 154 ^{o}C, (g) 156 ^{o}C and (h) 279 ^{o}C.

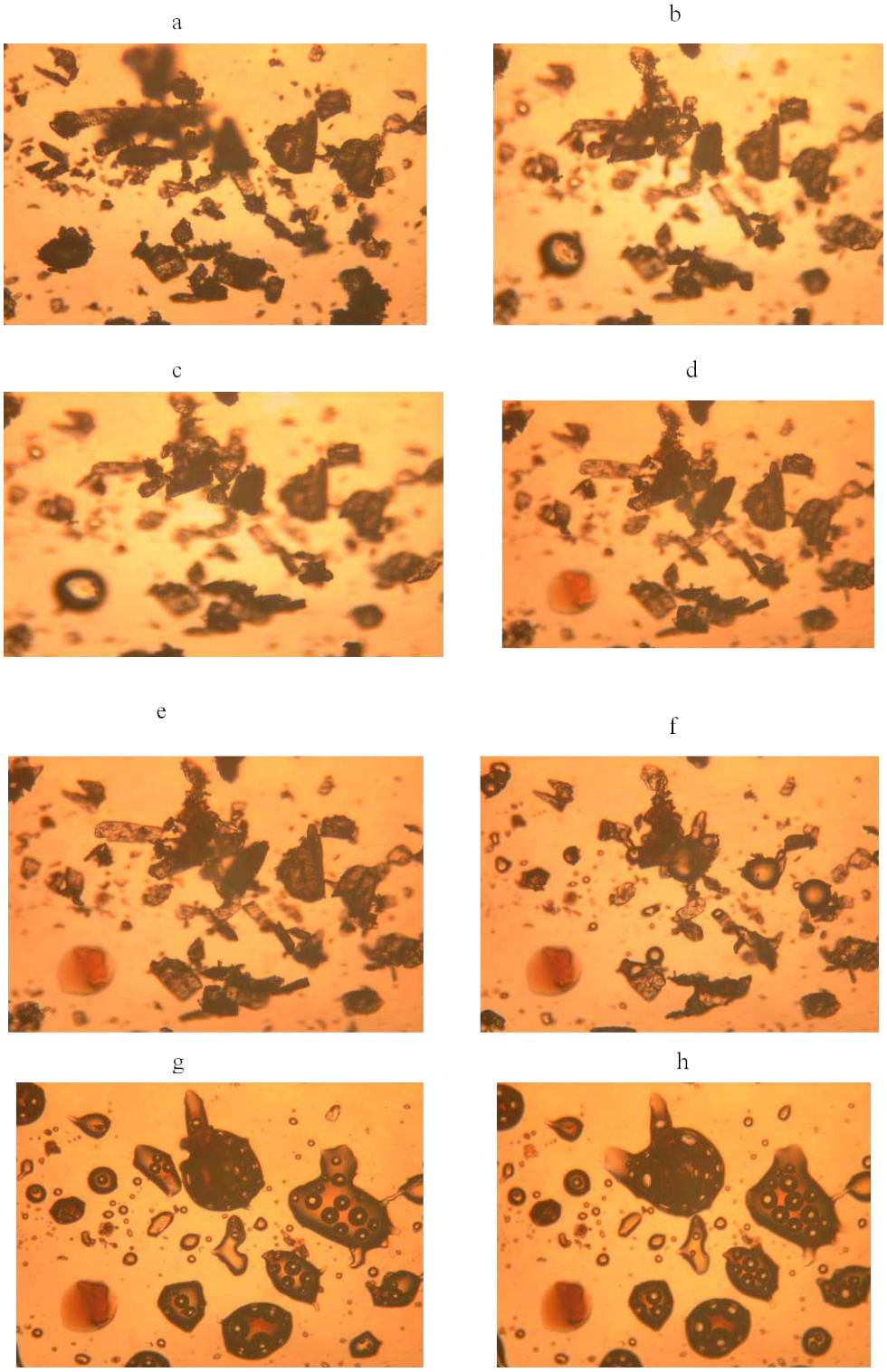

Figure 6.10 Photomicrographs of crystals of a 1:1 mole ratio physical mixture of glucose and BCD taken during hot-stage microscopy at: (a) 25 ^{o}C, (b) 151 ^{o}C, (c) 155 ^{o}C, (d) 261 ^{o}C, (e) 263 ^{o}C, (f) 267 ^{o}C, (g) 276 ^{o}C and (h) 283 ^{o}C.

7. THE THERMAL BEHAVIOUR OF MIXTURES OF TRIPROLIDNE HYDROCHLORIDE (TPH) AND β-CYCLODEXTRIN (BCD)

7.1. DSC and TG studies

Physical mixtures of TPH and BCD in 1:1 molar ratio and 1:1 mass ratio (equivalent to 3.4:1.0 molar ratio) were prepared as described in Section 4. DSC and TG were used to compare the thermal behaviour of these mixtures with that of the individual compounds.

The DSC curves of 1:1 mass ratio and 1:1 molar ratio physical mixtures of TPH and BCD are shown in Figure 7.1, together with the DSC curves for pure TPH and BCD. The endotherm associated with the melting of TPH disappears almost completely in the DSC curves of the mixtures. The dehydration endotherm of BCD is also decreased significantly in the DSC curve of the mixtures. The exotherm at above 200 ^{o}C associated with TPH appears at slightly higher temperatures in the DSC curves for the mixtures.

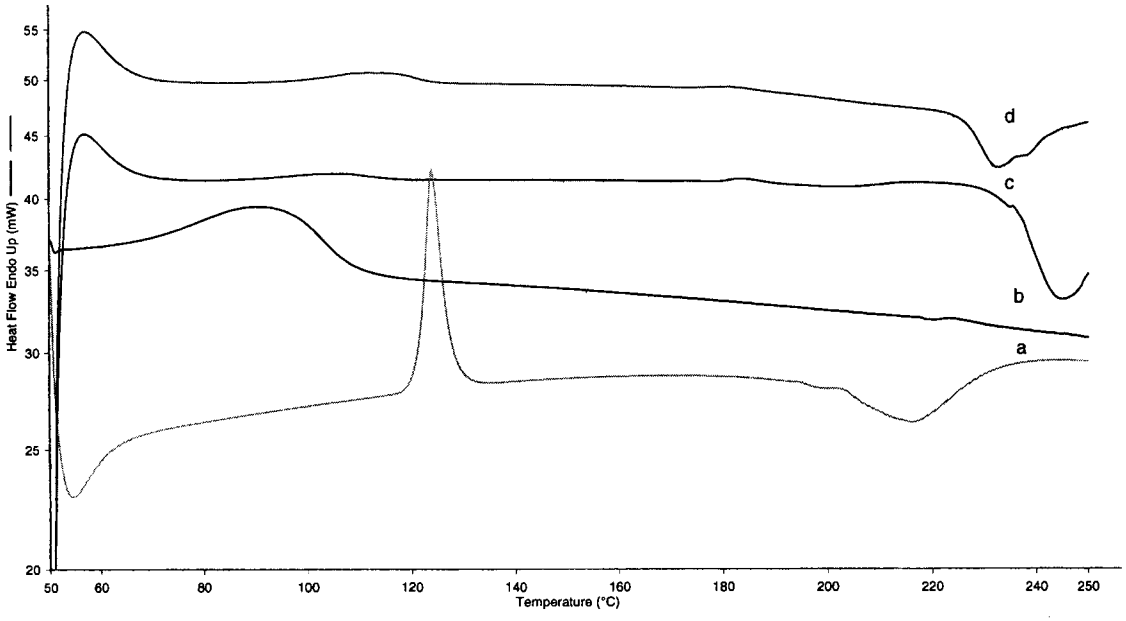

Figure 7.1 DSC curves for (a) TPH (b) BCD (in an aluminium pan) (c) a 1:1 mass ratio (equivalent to a 3.4:1.0 molar ratio) physical mixture of TPH and BCD and (d) a 1:1 molar ratio physical mixture of TPH and BCD (in sealed pressure pans, heated at 10 ^{o}C min^{-1} in flowing nitrogen).

The lack of a distinct fusion endotherm for TPH in the DSC curves for both of the physical mixtures suggests that mixing in this proportion has resulted in drug inclusion in this CD or that the drug has been converted to an amorphous form by heating in the presence of BCD, similarly to that observed in a study on nifedipine and randomly methylated-∃-cyclodextrin [42, 43] suggested that since the physical mixture is an intimate blend of crystalline drug and cyclodextrin matrix, upon heating the drug molecules are either monomolecularly dispersed onto the surface of the cyclodextrin or included into the cyclodextrin cavity. Inclusion complexation has been cited as the main reason for the unusual thermal behaviour of the heated physical mixtures [44,45] The possibility of inclusion is supported by X-ray powder diffraction in Section 9 and molecular modelling in Section 14.

The TG curves of the 1:1 mass and 1:1 molar ratio physical mixtures of TPH and BCD are compared to those of pure TPH and BCD in Figure 7.2. The 1:1 mass ratio physical mixture of TPH and BCD shows an initial-mass loss of 8.2 %, while for the 1:1 molar ratio mixture the mass-loss is 10.1 %, as expected for the higher content of BCD. Two further stages of mass-loss are seen in the TG curves for both of the mixtures. These would correspond to the decomposition of the BCD followed by decomposition of the TPH at higher temperatures.

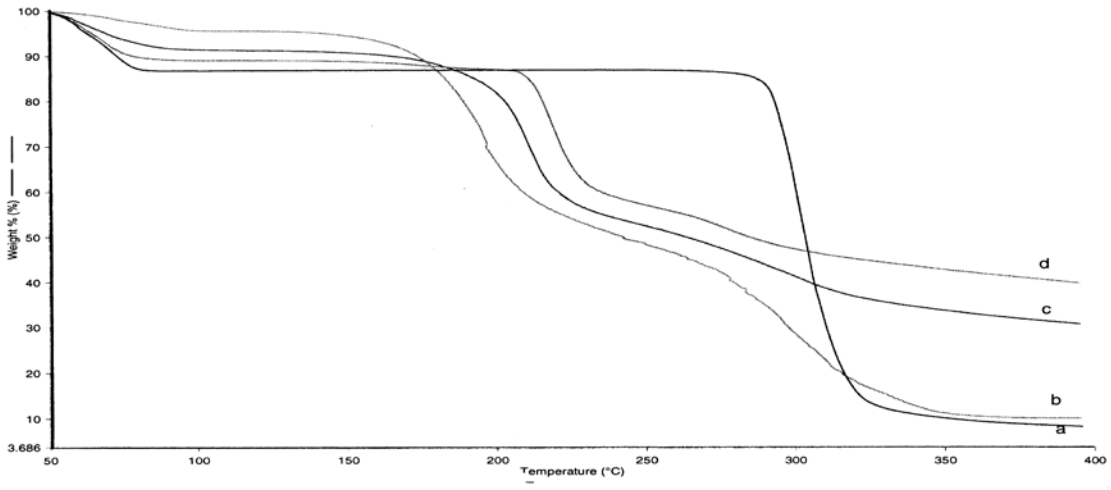

Figure 7.2 TG curves for (a) TPH, (b) BCD, (c) a 1:1 mass ratio (equivalent to a 3.4:1.0 molar ratio) physical mixture of TPH and BCD and (d) a 1:1 mole ratio physical mixture of TPH and BCD, (heated at 10 ^{o}C min^{-1} in flowing nitrogen using platinum pans).

The thermal behaviour of samples of TPH and BCD and its mixtures that had been dried over P_2O_5, was examined using TG and DSC. The DSC curves in (Figure 7.3) show the expected absence of the endotherms associated with the dehydration of BCD. In comparison with the undried samples (Figure 7.1) the endotherm associated with the melting of TPH was more evident, but greatly broadened in the curves for the mixtures. This could indicate that the presence of water facilitates the inclusion of TPH in the BCD cavity. The results are summarized in Tables 7.1 and 7.2.

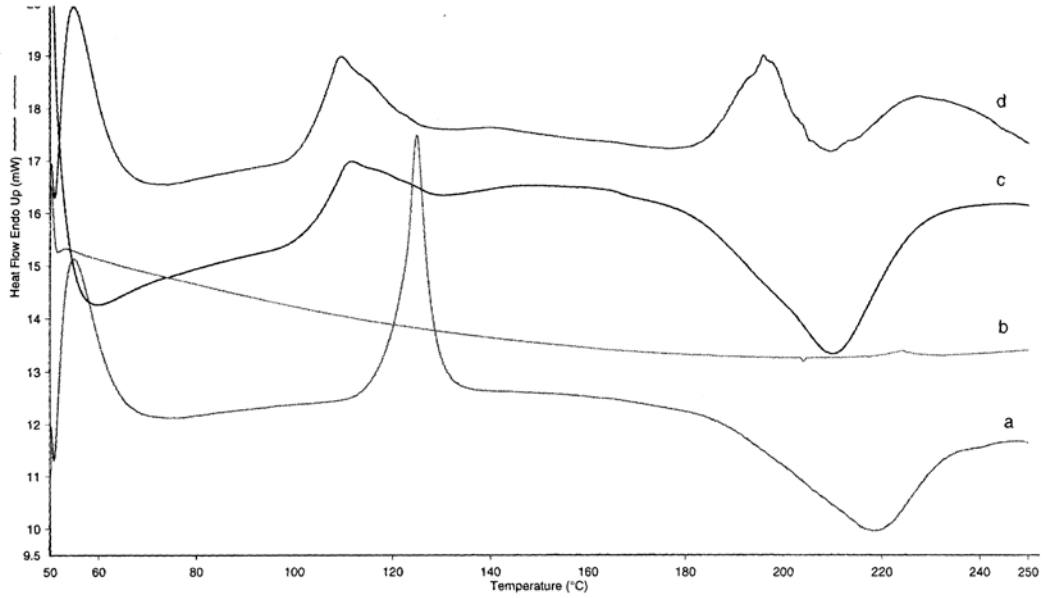

Figure 7.3 DSC curves for (a) dried TPH (b) dried BCD (in an uncrimped aluminium pan) (c) a dried samples of a 1:1 mass ratio (equivalent to 3.4:1.0 molar ratio physical mixture of TPH and BCD in sealed pressure pan and (d) a dried samples of a 1:1 molar ratio physical mixture of TPH and BCD in a sealed pressure pan, heated at 10 ^{o}C min^{-1} in flowing nitrogen.

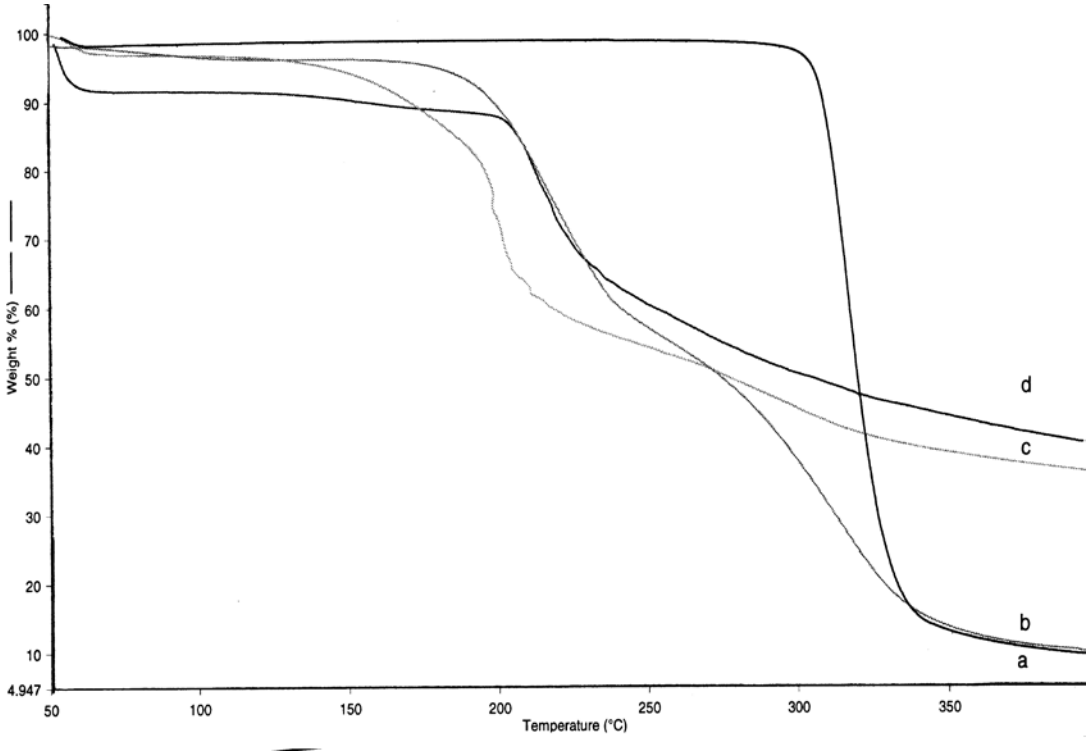

Figure 7.4 TG curves for (a) dried TPH, (b) dried BCD, (c) a dried sample of a 1:1 mass ratio physical mixture of TPH and BCD and (d) a dried sample of a 1:1 mole ratio physical mixture of TPH and BCD, heated at 10 ^{o}C min^{-1} in flowing nitrogen, using platinum pans.

7.2. Hot-stage microscopy of mixtures of TPH and BCD

The photomicrographs of a 1:1 mass (1.0:0.54 molar ratio) physical mixture of TPH and BCD are shown in Figure 7.5. A similar series for the 1:1 molar ratio physical mixture of TPH and BCD is shown in Figure 7.6. In both series (a) shows the sample at room temperature, (b) shows that slight movement of particles has occurred due to loss of water from BCD. The particles of TPH start melting at (c) and degradation continues until at (h) (about 280 ^{o}C) a black residue remains.

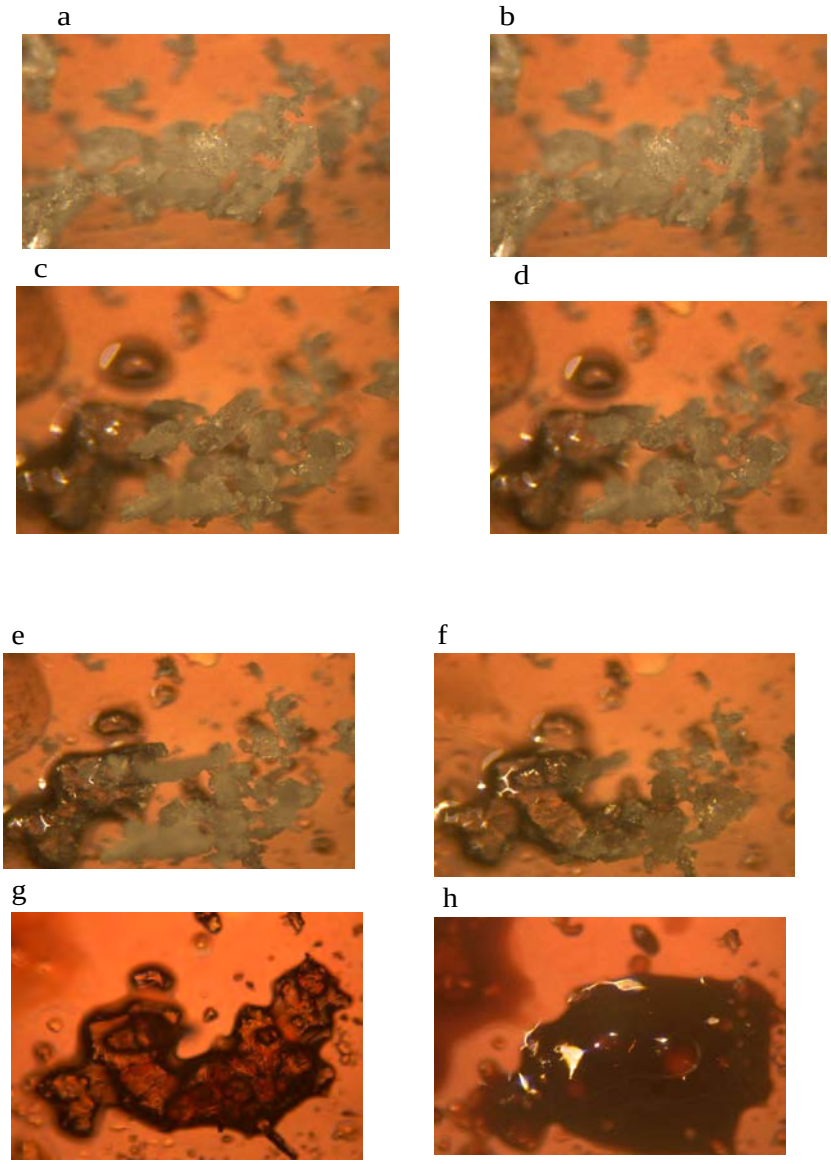

Figure 7.5 Photomicrographs of crystals of a 1:1 mass ratio physical mixture of BCD and glucose taken during HSM analysis. (a) 25 ^{o}C, (b) 75 ^{o}C, (c) 98 ^{o}C, (d) 111 ^{o}C, (e) 124 ^{o}C, (f) 196 ^{o}C, (g) 256 ^{o}C and (h) 279 ^{o}C.

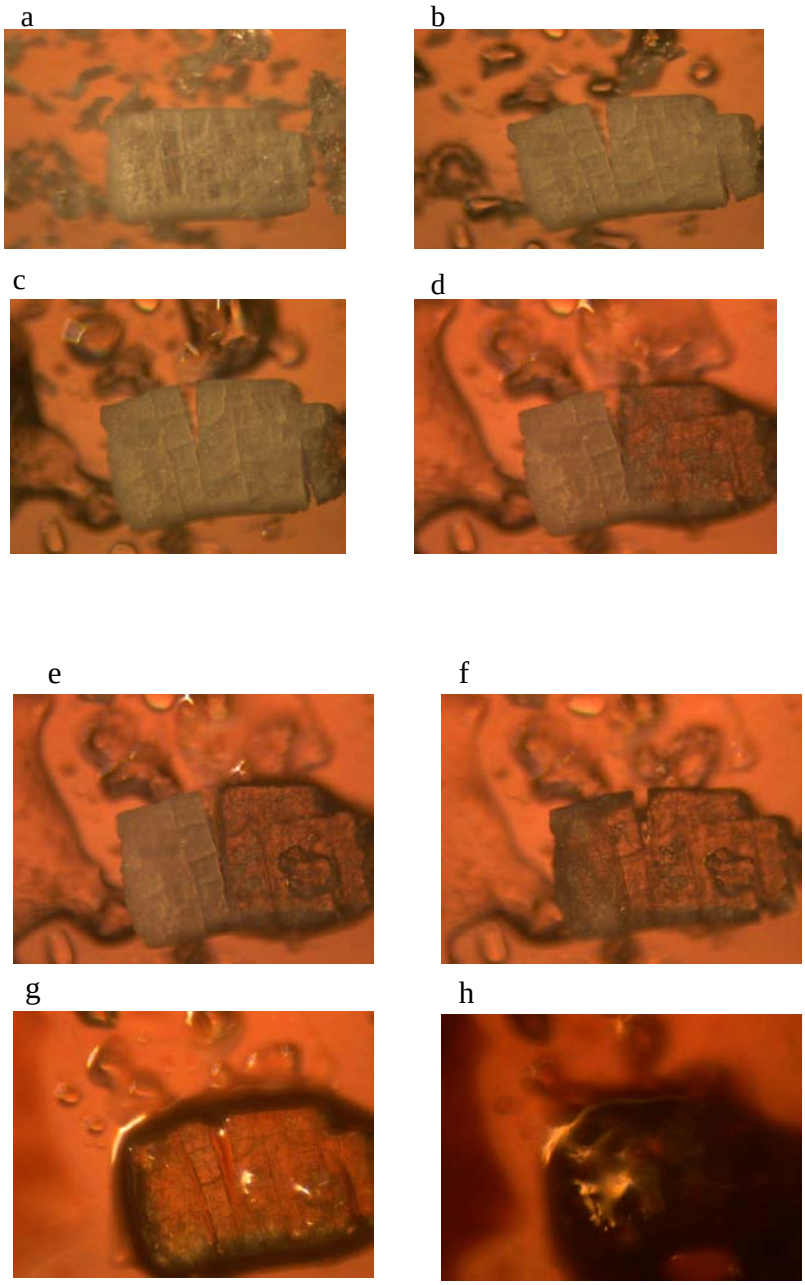

Figure 7.6 Photomicrographs of crystals of a 1:1 molar ratio physical mixture of TPH and BCD taken during hot-stage microscopy. (a) 25 ^{o}C, (b) 99 ^{o}C, (c) 121 ^{o}C, (d) 205 ^{o}C, (e) 233 ^{o}C, (f) 256 ^{o}C, (g) 269 ^{o}C and (h) 282 ^{o}C.

Table 7.1 Summary of the thermal behaviour of physical mixtures of TPH and BCD

Sample	TPH melting onset temperature /EC	Expected ΔH melting / kJ mol^{-1}	Observed ΔH melting / kJ mol^{-1}	Initial mass - loss (50 - 100EC)
TPH	123	-	37	4.9
BCD	-	-	-	12.5
1:1 mass ratio TPH and BCD	99	37	30	8.3
1:1 molar ratio TPH and BCD	91	37	25	10.0

Table 7.2 Summary of the thermal behaviour of dried physical mixtures of TPH and BCD

Sample	TPH melting onset temperature /EC	Expected ΔH melting / kJ mol^{-1}	Observed ΔH melting / kJ mol^{-1}	Initial mass - loss (50 - 100EC)
TPH	121		33	3.33
BCD	-	-	-	-
1:1 mass ratio TPH and BCD	109	33	36	2.30
1:1 molar ratio TPH and BCD	104	33	47	2.46

8. THE THERMAL BEHAVIOUR OF MIXTURES OF TPH AND GLUCOSE

8.1. DSC and TG studies

The DSC curves of 1:1 mole ratio and 1:1 mass ratio (equivalent to a 0.54:1 mole ratio) physical mixtures of TPH and glucose, together with the DSC curves for pure TPH and pure glucose are shown in Figure 8.1. The curve for the 1:1 mass ratio mixture shows a broad endotherm at 105 ^{o}C compared to the melting of TPH at 122 ^{o}C and glucose at 157 ^{o}C. The DSC curve for the 1:1 mole ratio mixture, i.e. with a higher mass proportion of TPH, shows similar lowering of the onset temperature of melting of TPH. The exotherm of TPH at about 220 ^{o}C is still visible in the DSC curves for the mixture of TPH and glucose.

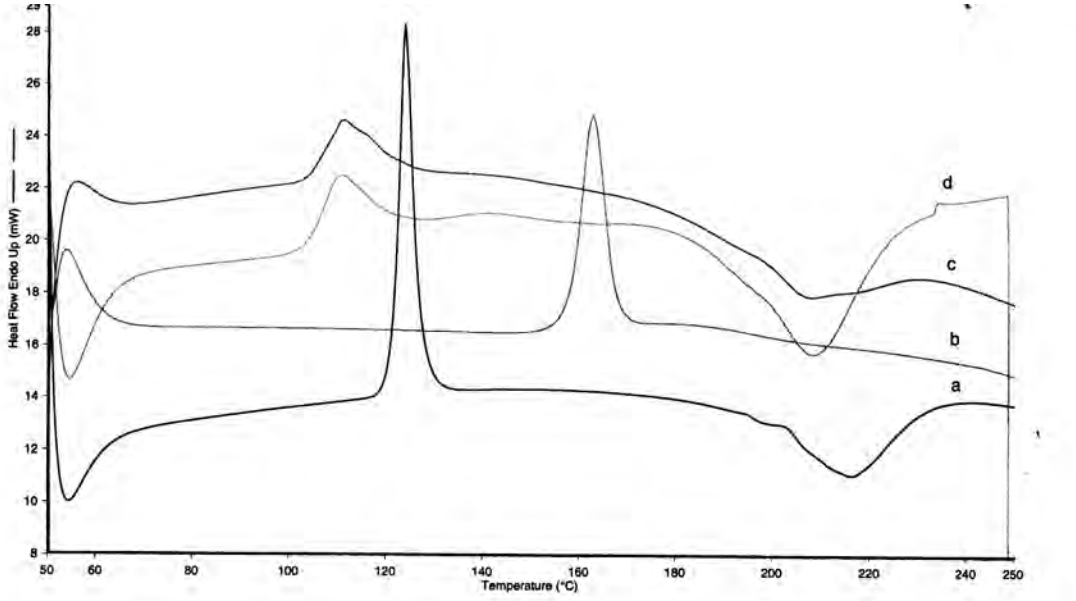

Figure 8.1 DSC curves for (a) TPH (b) glucose (c) a 1:1 mass ratio (equivalent to a 0.54:1 molar ratio) physical mixture of TPH and glucose and (d) a 1:1 molar ratio physical mixture of TPH and glucose, heated in sealed pressure pans, at 10 ^{o}C min^{-1} in flowing nitrogen.

The TG curves for the 1:1 mass and 1:1 molar ratio physical mixtures of TPH and glucose are compared to those of pure TPH and glucose in Figure 8.2. The 1:1 mass ratio physical mixture of TPH and glucose shows an initial-mass loss of 1.8 % while for the 1:1 molar ratio mixture with a higher content of TPH the mass-loss is about 2.5 %. The two other stages of mass-loss are still observed in the curves for the mixtures

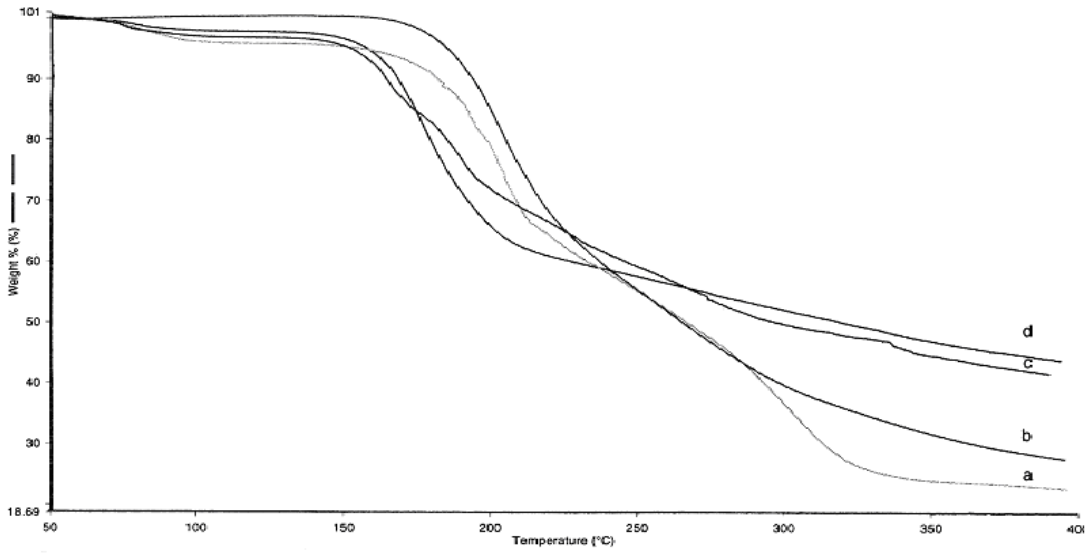

Figure 8.2. TG curves for (a) TPH, (b) glucose, (c) a 1:1 mass ratio (equivalent to a 0.54:1.0 molar ratio) physical mixture of TPH and glucose and (d) a 1:1 mole ratio physical mixture of TPH and glucose (heated at 10 ^{o}C min^{-1} in flowing nitrogen, using platinum pans).

The thermal behaviour of the TPH/glucose mixtures is summarized in Table 8.1.

Samples of TPH, glucose and of the mixtures of TPH and glucose were dried in a desiccator over P_2O_5. The DSC and TG curves are shown in Figures 8.3 and 8.4, respectively.

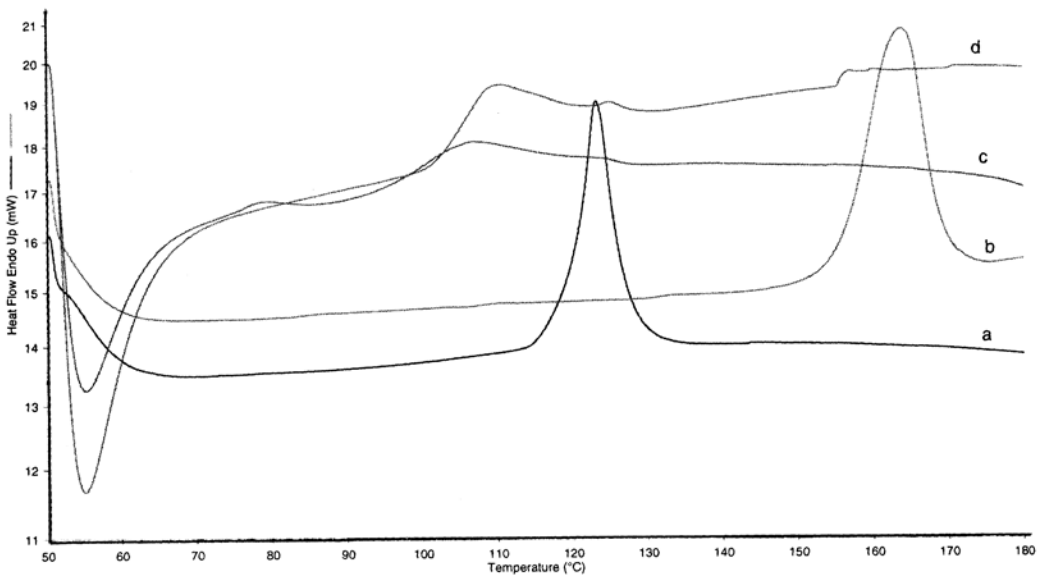

Figure 8.3 DSC curves for (a) dried TPH (b) dried glucose (c) a dried sample of a 1:1 mass ratio (equivalent to a 0.54:1 molar ratio) physical mixture of TPH and glucose and (d) a dried sample of a 1:1 molar ratio physical mixture of TPH and glucose (heated in sealed pressure pans, at 10 ^{o}C min^{-1} in flowing nitrogen).

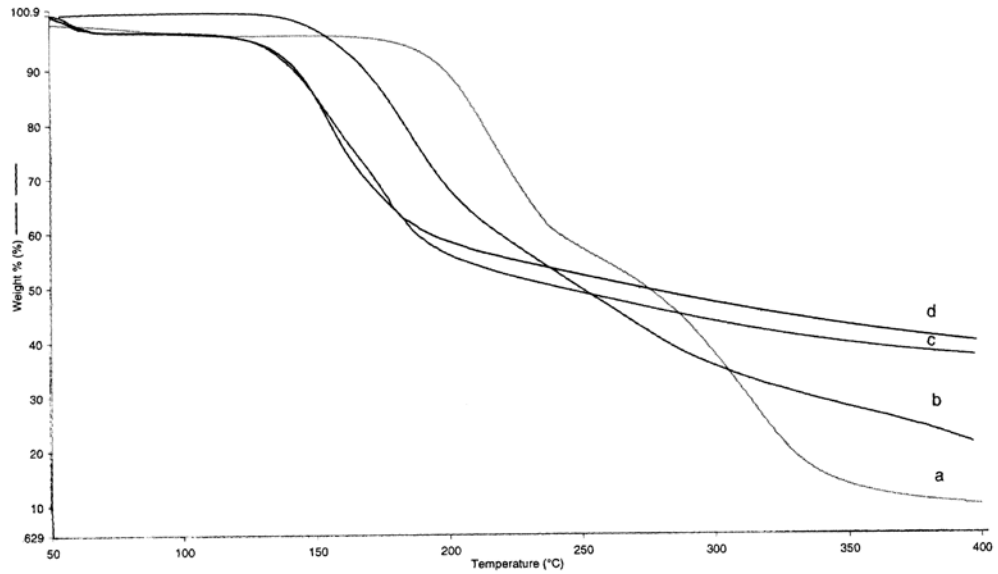

Figure 8.4. TG curves for (a) dried TPH, (b) dried glucose, (c) a dried sample of a 1:1 mass ratio (equivalent to a 0.54:1.0 molar ratio) physical mixture of TPH and glucose and (d) a dried sample of a 1:1 mole ratio physical mixture of TPH and glucose (heated at 10 ^{o}C min^{-1} in flowing nitrogen, using platinum pans.

The drying process does not appear to have a significant effect on the subsequent thermal behaviour.

8.2. Hot-stage microscopy of physical mixtures of TPH and glucose

Photomicrographs of the 1:1 mass ratio physical mixtures of TPH and glucose are shown in Figure 8.5 and a similar set for the 1:1 molar ratio mixture is shown in Figure 8.6. At room temperature (a) it is difficult to identify the individual constituents. In (c) at 106 ^{o}C the particles of TPH started melting and in (h) at 157 ^{o}C the mixture of TPH and glucose is completely molten.

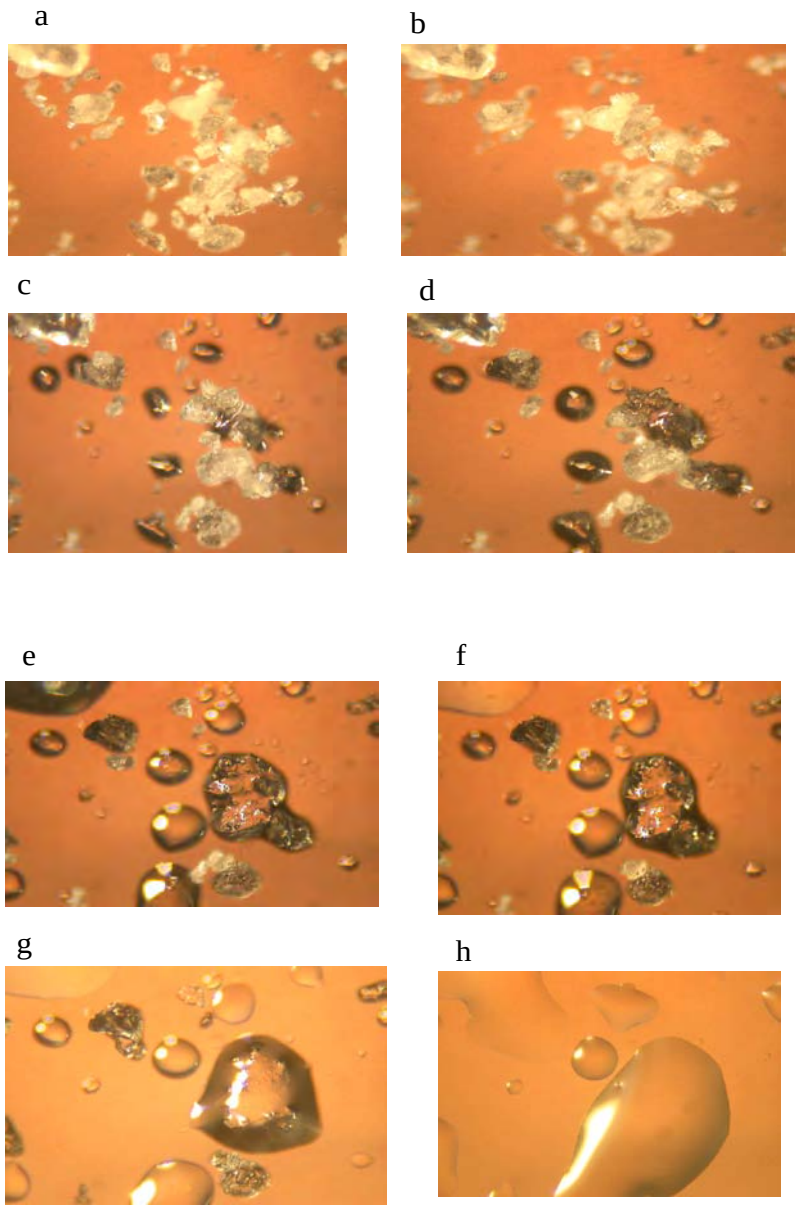

Figure 8.5 Photomicrographs of crystals of a 1:1 mass ratio physical mixture of TPH and glucose taken during hot-stage microscopy at (a) 25 ^{o}C, (b) 31 ^{o}C, (c) 106 ^{o}C, (d) 122 ^{o}C, (e) 139 ^{o}C, (f) 141 ^{o}C, (g) 148 ^{o}C and (h) 157 ^{o}C.

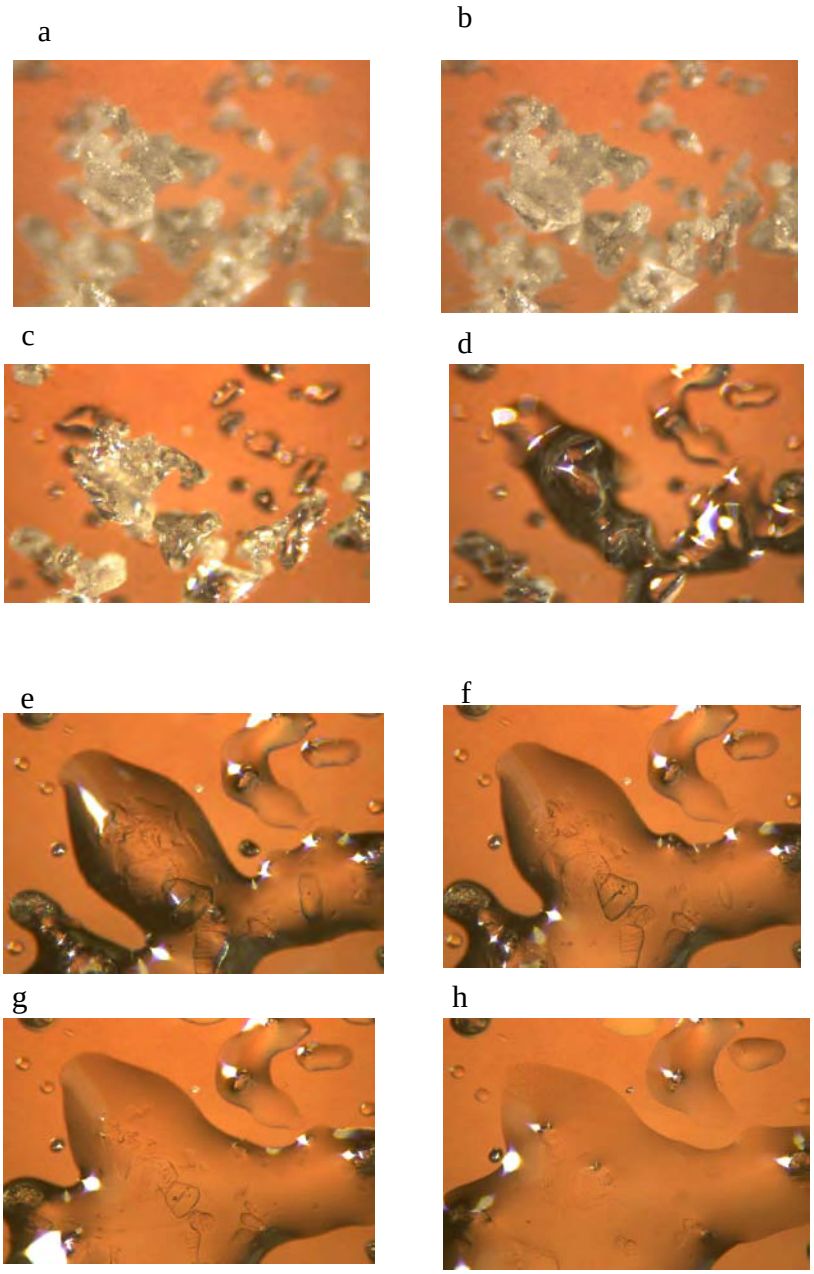

Figure 8.6 Photomicrographs of crystals of a 1:1 molar ratio physical mixture of TPH and glucose taken during hot-stage microscopy. at: (a) 25 ^{o}C, (b) 29 ^{o}C, (c) 93 ^{o}C, (d) 124 ^{o}C, (e) 138 ^{o}C, (f) 143 ^{o}C, (g) 151 ^{o}C and (h) 155 ^{o}C.

Table 8.1 Summary of the thermal behaviour of physical mixtures of TPH and glucose

Sample	Melting onset temperature /EC	Expected ΔH melting of TPH / kJ mol^{-1}	Observed ΔH melting of TPH / kJ mol^{-1}	Initial mass - loss (50 - 100EC)
TPH	123		37	3.8
Glucose	157			0.1
1:1 mass ratio TPH and glucose	104	37	43	1.8
1:1 molar ratio TPH and glucose	106	37	53	2.5

9. X-RAY POWDER DIFFRACTION STUDIES OF TPH AND ITS MIXTURES WITH BCD AND GLUCOSE

9.1. The pure compounds

The X-ray powder diffraction patterns (recorded as described in Section 4.4.4) for (a) TPH, (b) BCD and (c) glucose are shown in Figure 9.1. All three have distinctive crystalline patterns.

The X-ray powder diffraction of the original TPH, a sample dried over P_2O_5 in a desiccator, and a sample of dried TPH re-exposed to water vapour for 1 day, are given in Figure 9.2.

The XRD patterns of the original BCD, a sample dried over P_2O_5, and a sample of dried BCD that had been re-exposed to water vapour for 1 day are given in Figure 9.3. The dehydration of BCD produced a much less-crystalline material but this was reversed considerably on re-exposure of the BCD to water vapour.

The X-ray powder diffraction patterns of the original glucose, a sample of glucose that had been dried over P_2O_5 in a desiccator for 15 days, and a sample of dried glucose that had been re-exposed to water vapour for 1 day, are shown in Figure 9.4. These treatments for glucose appeared to have very little effect on the diffraction patterns.

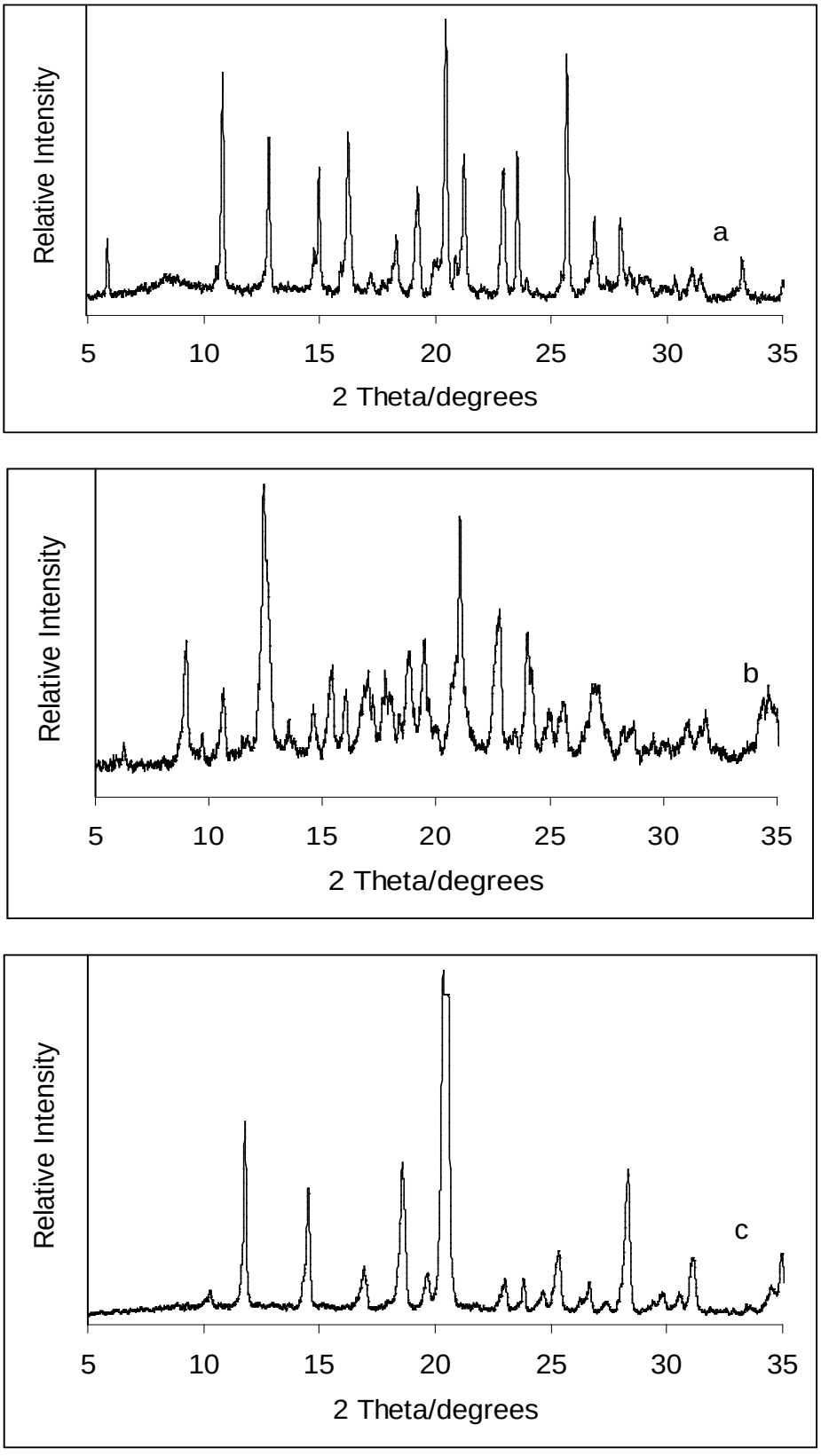

Figure 9.1 X–ray powder diffraction patterns of (a) TPH, (b) BCD and (c) glucose

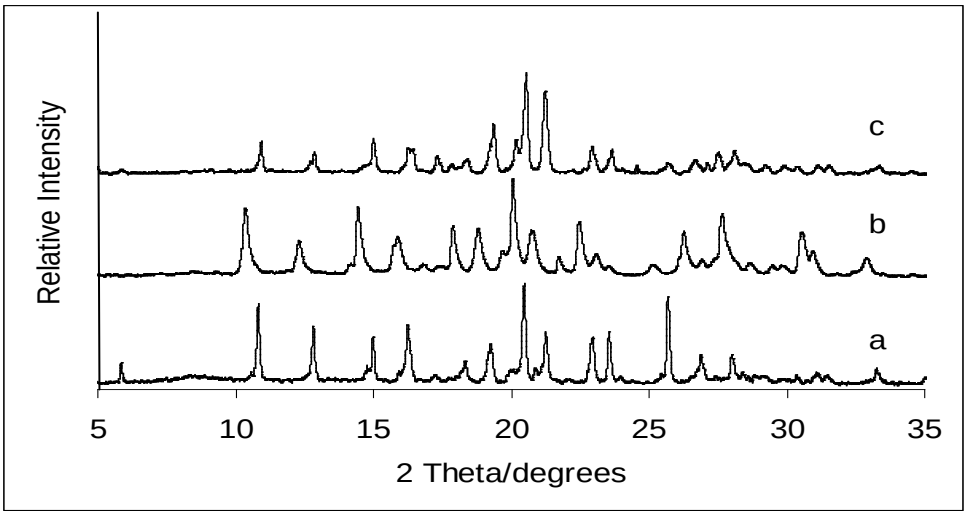

Figure 9.2 X-ray powder diffraction patterns of (a) TPH, (b) TPH dried over P_2O_5 in a desiccator for 15 days and (c) dried TPH after re-exposure to water vapour for 1 day.

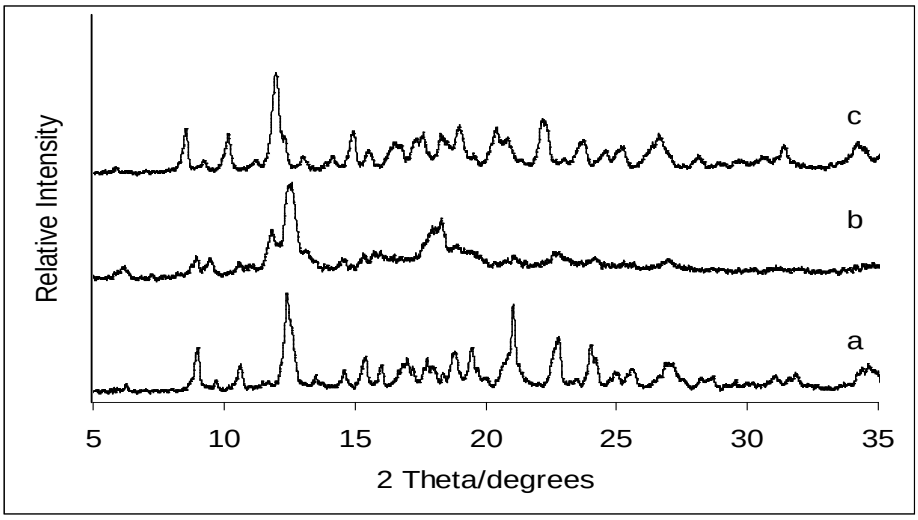

Figure 9.3 X-ray powder diffraction patterns of (a) BCD, (b) BCD dried over P_2O_5 in a desiccator for 15 days and (c) dried BCD after re-exposed to water vapour 1 for day.

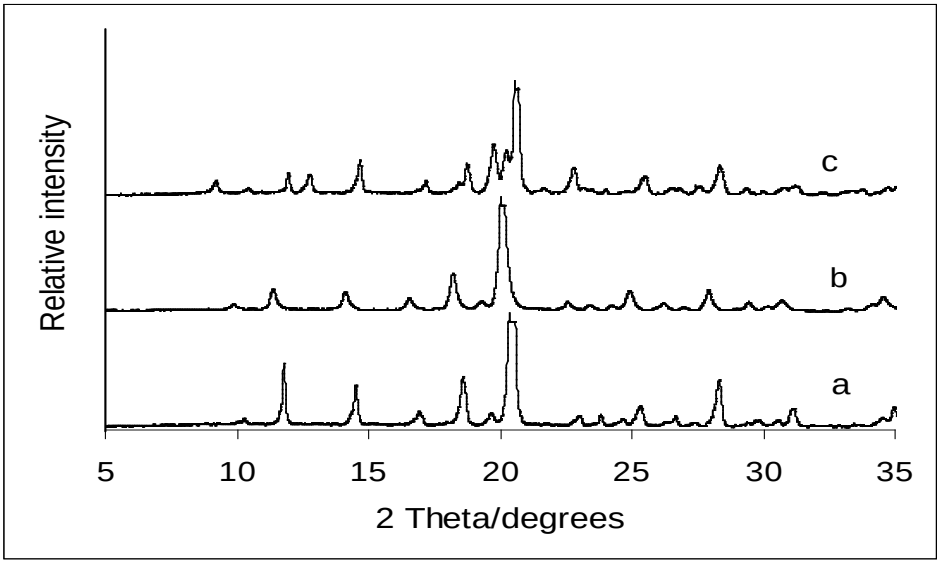

Figure 9.4 X-ray powder diffraction patterns of (a) glucose, (b) glucose dried over P_2O_5 in a desiccator for 15 days and (c) a sample of dried glucose re-exposed to water vapour for 1 day.

9.2. Mixtures of TPH and BCD

The X-ray powder diffraction patterns of the physical mixtures of TPH and BCD (prepared as described in Section 4.1) are shown in Figure 9.5 and are distinctly different from the pure components. The most intense peaks of the pure compounds are absent from the patterns of both the mixtures, but the patterns of the mixtures still indicate significant crystallinity. These results support the indication of the thermal studies (Section 7) that interaction, possibly the formation of an inclusion complex, occurs even on physical mixing of TPH and BCD. The pattern (d) for the mixture with the higher TPH content is closer to that of TPH itself (a). Pattern (c), shows the addition, in the appropriate proportions, of the individual patterns of TPH and BCD. Patterns (d) and (e) for the mixtures differ from pattern (c) indicating that physical mixing produces a compound with a different, less-crystalline structure.

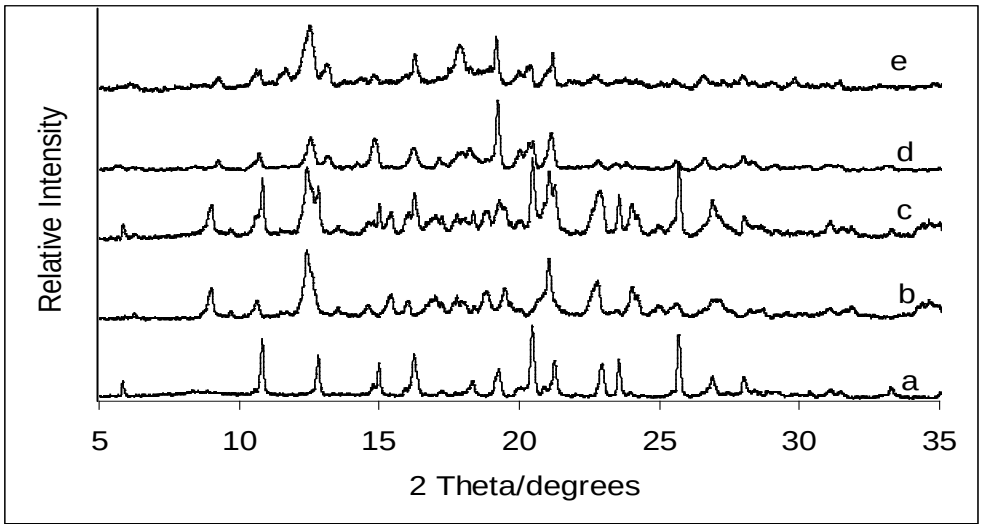

Figure 9.5 X-ray powder diffraction patterns of (a) TPH, (b) BCD, (c) addition of the individual XRD patterns of TPH and BCD, (d) a 1:1 mass ratio (equivalent to a 3.4:1.0 molar ratio) physical mixture of TPH and BCD and (e) a 1:1 molar ratio physical mixture of TPH and BCD.

The X-ray powder diffraction patterns of dried samples of the pure compounds and the mixtures are shown in Figure 9.6. The main changes on drying have occurred, as expected, in the pattern for BCD (b) and also in (d) which is the mixture with the higher proportion of BCD. The changes observed do support the probable role of H_2O in the TPH/BCD interaction (see Section 7).

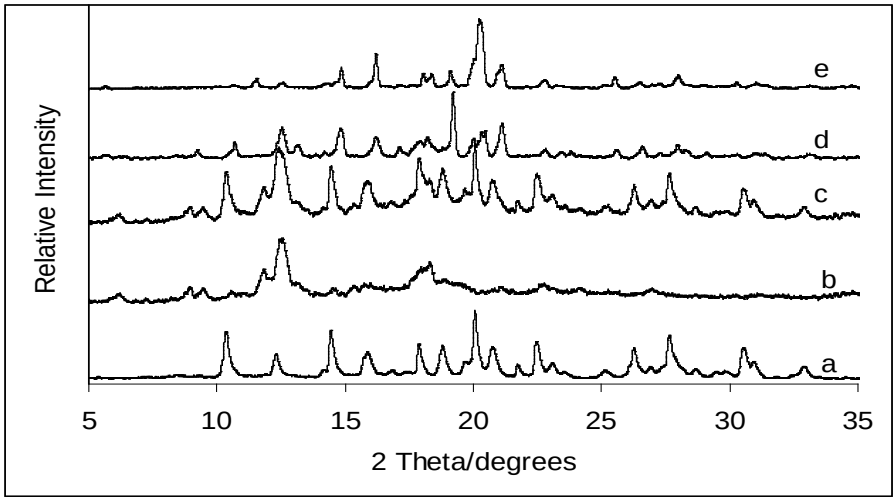

Figure 9.6 X-ray powder diffraction patterns of (a) dried TPH, (b) dried BCD, (c) the addition of the individual XRD patterns of dried TPH and dried BCD (d) a dried sample of a 1:1 mass ratio physical mixture of TPH and BCD and (e) a dried sample of a 1:1 molar ratio physical mixture of TPH and BCD.

9.3. Mixtures of TPH and glucose

The X-ray powder diffraction patterns (Figure 9.7) of the two physical mixtures of TPH and glucose differ significantly from each other and some features of the glucose pattern are evident in the patterns of both mixtures. The more intense peaks of the TPH pattern are not evident in the patterns of the mixtures and patterns (d) and (e) do not resemble the added individual patterns of TPH and glucose (c). These results support the indications from the studies of the thermal behaviour (Section 8) that interaction occurs between TPH and glucose.

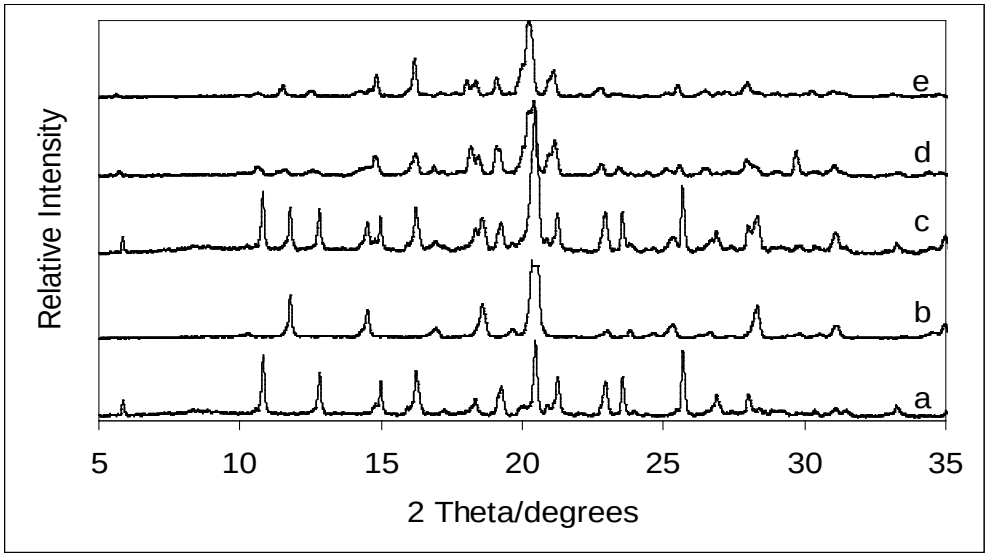

Figure 9.7 X-ray powder diffraction patterns of (a) TPH, (b) glucose, (c) the added of the individual XRD patterns of TPH and glucose, (d) a 1:1 mass ratio (equivalent to a 0.54:1.0 molar ratio) physical mixture of TPH and glucose and (e) a 1:1 molar ratio physical mixture of TPH and glucose.

The X-ray powder diffraction patterns of dried samples of TPH, glucose and TPH/glucose mixtures are shown in Figure 9.8 and confirm that the drying of these samples does not produce significant changes.

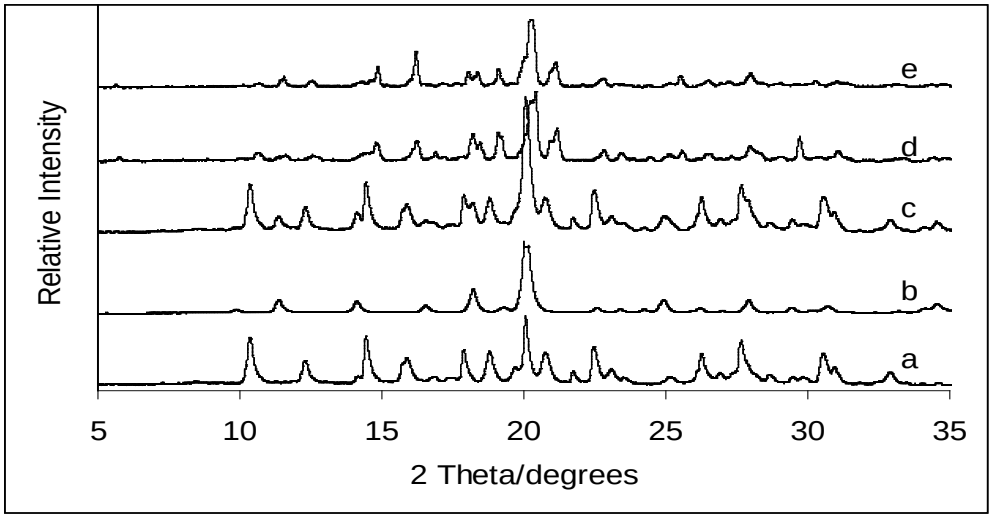

Figure 9.8 X-ray powder diffraction patterns of (a) dried TPH, (b) dried glucose, (c) the addition of the individual XRD patterns of dried TPH and dried glucose, (d) a dried sample of a 1:1 mass ratio physical mixture of TPH and glucose and (e) a dried sample of a 1:1 mole ratio physical mixture of TPH and glucose.

9.4. Mixtures of glucose and BCD

Figure 9.9 shows the X-ray powder diffraction patterns of the physical mixtures of glucose and BCD. In the 1:1 mass ratio mixture (equivalent to a 0.16:1.00 mole ratio of glucose and BCD), the most intense peak of glucose is still evident, while in the 1:1 mole ratio physical mixture the glucose peak is not as intense, due to the higher proportion of BCD. These results support the thermal behaviour studies (Section 5) where indications are that glucose is not included in the BCD cavity.

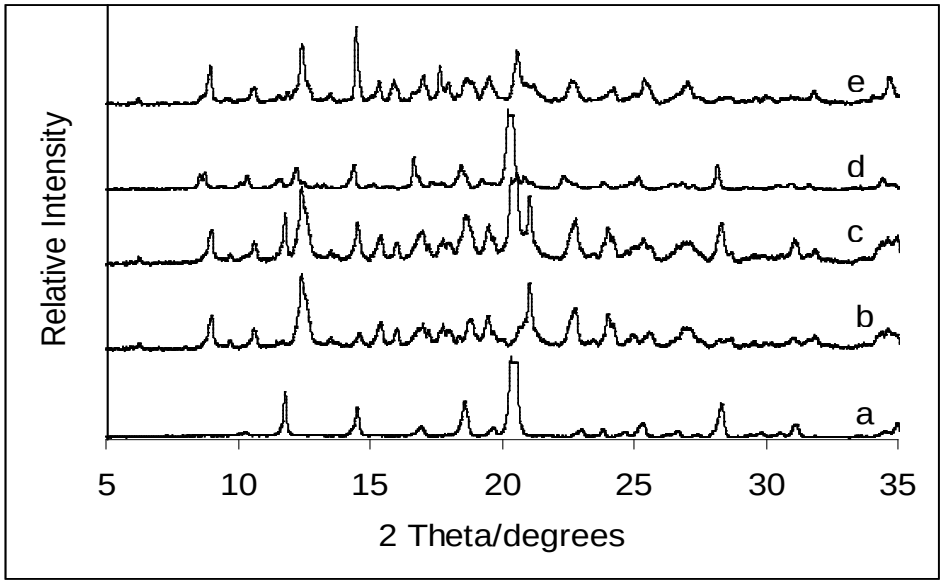

Figure 9.9 X-ray powder diffraction patterns of (a) glucose, (b) BCD, (c) the addition of the individual XRD patterns of glucose and of BCD, (d) a 1:1 mass ratio (equivalent to a 0.16:1.00 mole ratio) physical mixture of glucose and BCD and (e) a 1:1 mole ratio physical mixture of glucose and BCD.

10. INFRARED SPECTROSCOPIC STUDIES OF TPH AND ITS MIXTURES WITH BCD AND GLUCOSE

10.1. The pure compounds

The infrared absorption spectrum of a sample of TPH, by taking 1/3 portion of TPH in 2/3 KBr over the range 4000-400 cm^{-1} is shown Figure 10.1 [46]. The main absorption bands and their assignment are given in Table 10.1, compared with the values obtained in this study (see Figure 10.2)

Table 10.1 Infrared absorption results for TPH

Absorption maximum /cm^{-1}) Literature [3]	Absorption maximum /cm^{-1} Experimental	Assignment
3480	3477	OH stretch (hydrate)
2958	2959	CH stretch (-CH_3)
2960	2961	NH^+ stretch
1630	1631	C = C stretch
1582	1582	C = stretch (aromatic)
1562	1563	C = C stretch (pyridine)
1462	1462	-CH_3 asym. bend
1386	1386	-CH_3 sym. bend
1358	1359	C-N stretch (tert. amine)
846	847	= C-H rock
824	825	Para subst. benzene
776	775	1-subst pyridine

Table 10.2 Infrared absorption results for BCD [47]

Absorption maximum /cm^{-1}) Literature [40]	Absorption maximum /cm^{-1}) Experimental	Assignment
3384	3400	OH-stretching
2928	2927	C-H - stretching
1600	1598	- C-C stretching, aromatic ring
1411	1411	-OH in plane bending
1366	1365	-CH bending
1300	1299	-CH bending/wagging
1157	1156	-C-O-C glucosidic stretching
1079	1078	C-C and C-O stretching
1031	1030	C-C and C-O stretching
950-530	947-530	Cyclodextrin ring

The infrared spectra of the original TPH (a) and of a sample that had been dried in a desiccator over P_2O_5 for 15 days (b) and of a sample of dried TPH that had been re-exposed to water vapour for 1 day (c), are compared in Figure 10.2. The main absorption bands, their assignments and comparative literature values are shown in Table 10.1. Similar procedures were carried out for samples of BCD (See Figure 10.3) and glucose (See Figure 10.4). Apart from changes in intensity caused by the amounts present in the KBr, the drying process does not appear to have significantly changed the TPH spectrum. The drying process decreases the water absorption bands in the spectrum of BCD but does not remove the water completely. After re-exposure to water vapour, the absorption band of dried BCD had been broadened again. By comparison, the water content of the glucose is apparently more readily removed, and after re-exposure to water vapour is again evident. The main absorption bands and their assignment are given in Table 10.3 for BCD and in Table 10.4 for glucose.

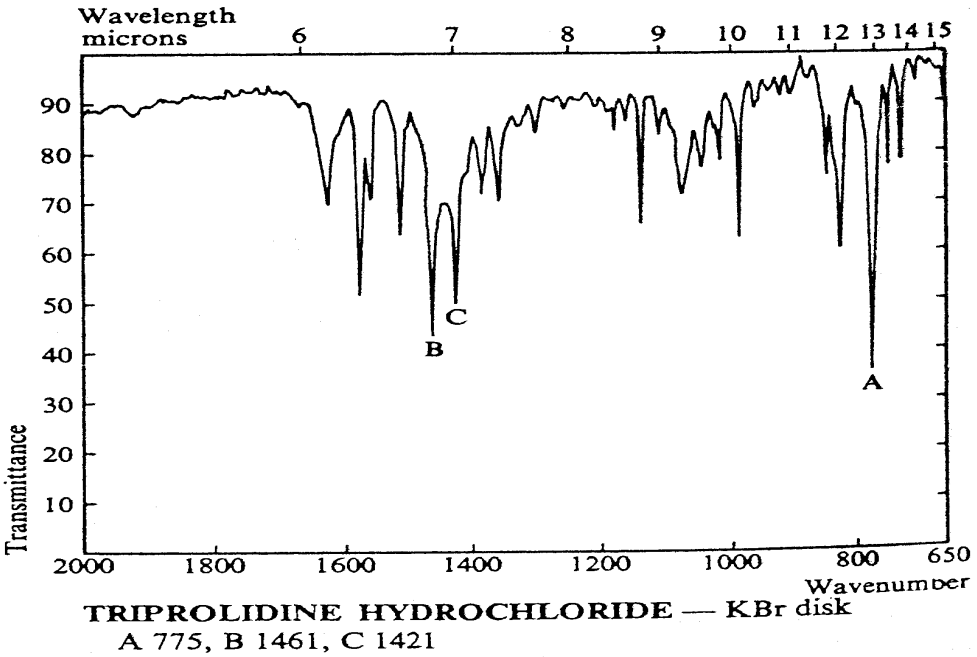

Figure 10.1 Infrared spectrum of TPH [2,4].

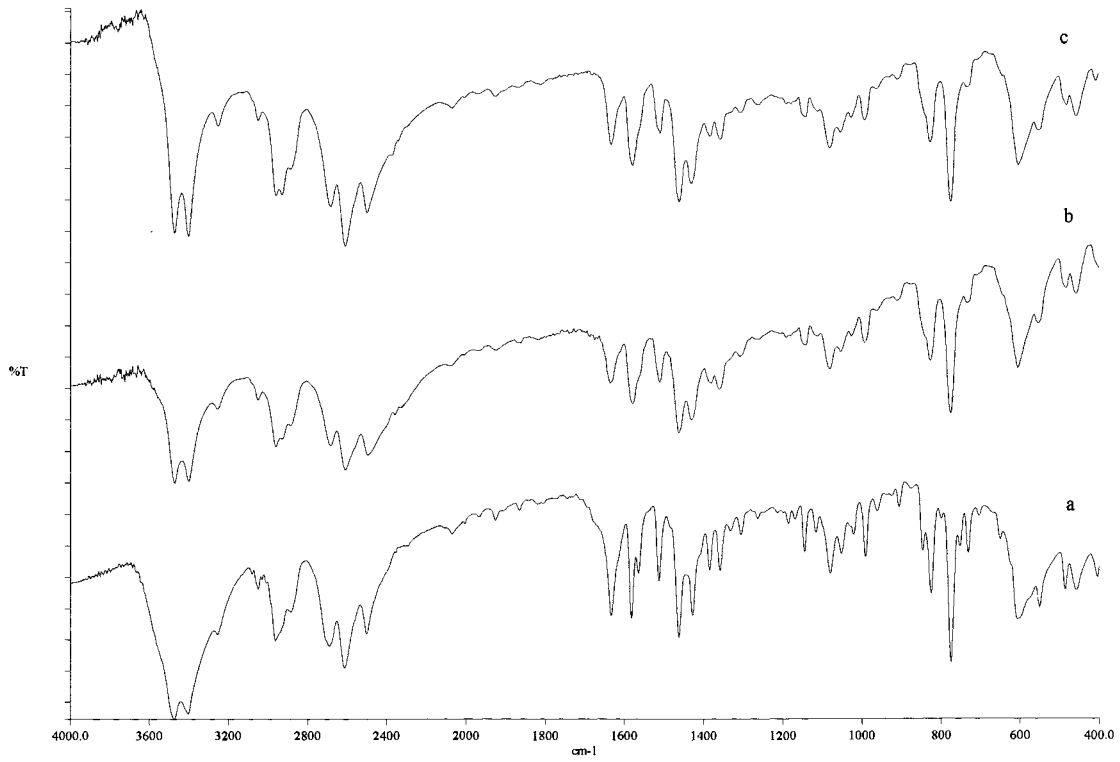

Figure 10.2 Infrared spectra of (a) TPH, (b) TPH dried over P_2O_5 in a desiccator for 15 days and (c) dried TPH after re-exposure to water vapour for 1 day.

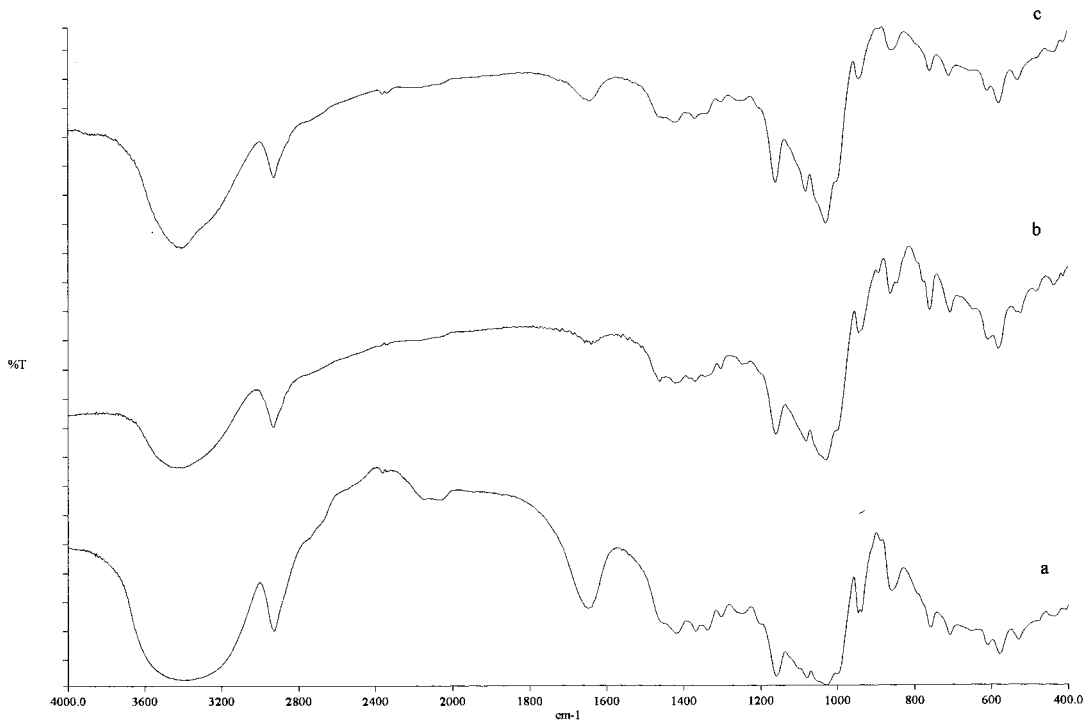

Figure 10.3 Infrared spectra of (a) BCD, (b) BCD dried over P_2O_5 in a desiccator for 15 days and (c) a dried BCD after re-exposure to water vapour for 1 day.

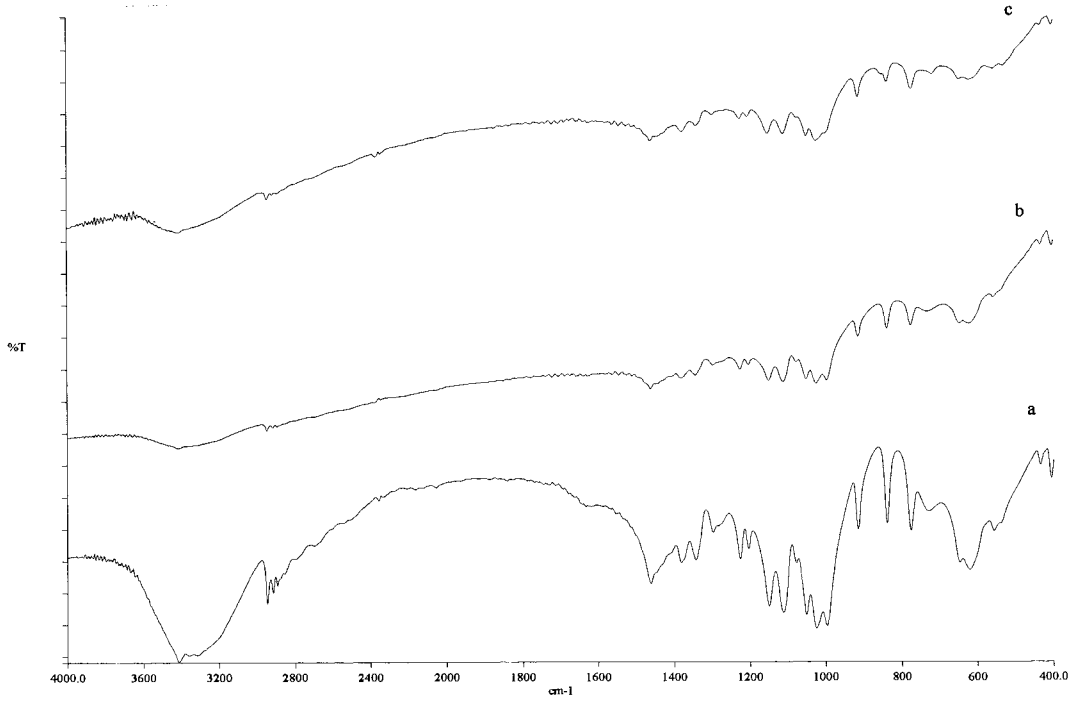

Figure 10.4 Infrared spectra of (a) the original glucose, (b) a sample of glucose dried over P_2O_5 in a dessicator for 15 days and (c) a sample of glucose after re-exposure to water vapour for 1 day

10.2. Mixtures of TPH and BCD

Figure 10.5 shows the IR spectra of the physical mixtures of TPH and BCD compared with the spectra of the pure components. Figure10.6 shows a similar set of spectra for dried samples of the components and mixtures. Fourier transform infrared spectroscopy is often used to assess the interaction between guest and cyclodextrin molecules in the solid-state [48-50]. The characteristic absorption bands of cyclodextrins tend to be minimally affected by inclusion complexation and if the mass of the included drug component is less than about 25% of the complex, any changes in the absorption bands of the drug will be obscured by the host spectrum. These changes are most often shifts, reductions or broadening in intensity of characteristic absorption bands [51-53]. The most noticeable changes seen in the spectra in Figure 10.5 are those connected with the water absorptions in the BCD spectrum. The broad band from 3800 to 3000 cm^{-1} and the slightly sharper band around 1680 cm^{-1} in spectrum (b) are not prominent in the spectra of the mixtures (c) and (d). This observation would support the replacement of water in the BCD cavity by TPH. An alternative explanation could be interaction between the HCl fragment of TPH and water from the BCD. There also appears to be a change in the intensity, broadening and shift of the-C=C- pyridine and other aromatic assignments suggesting a possible site for interaction between the TPH and BCD. The results (see also Section 14) suggest inclusion of TPH in the BCD cavity.

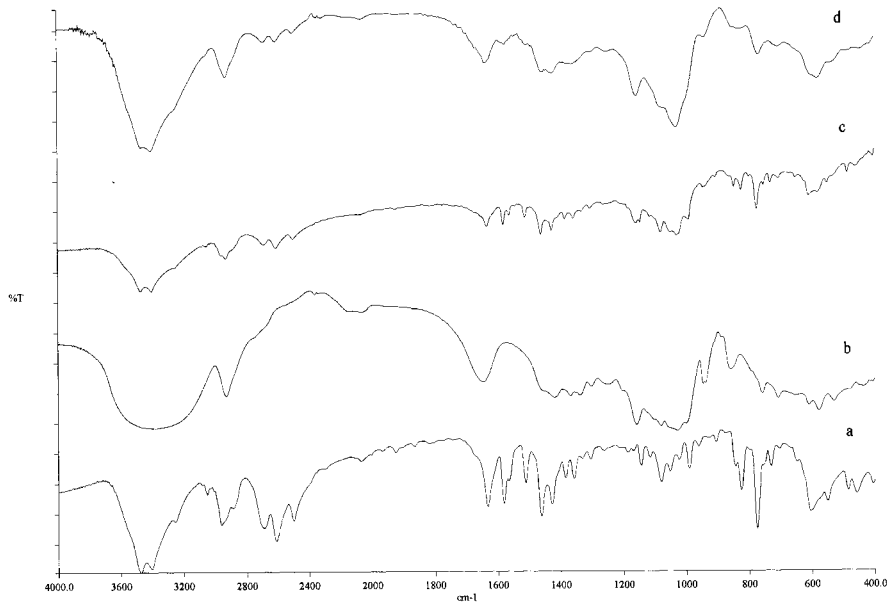

Figure 10.5 Infrared spectra of samples of (a) TPH, (b) BCD, (c) a 1:1 mass ratio (equivalent to a 3.4:1.0 mole ratio) physical mixture of TPH and BCD and (d) a 1:1 mole ratio physical mixture of TPH and BCD.

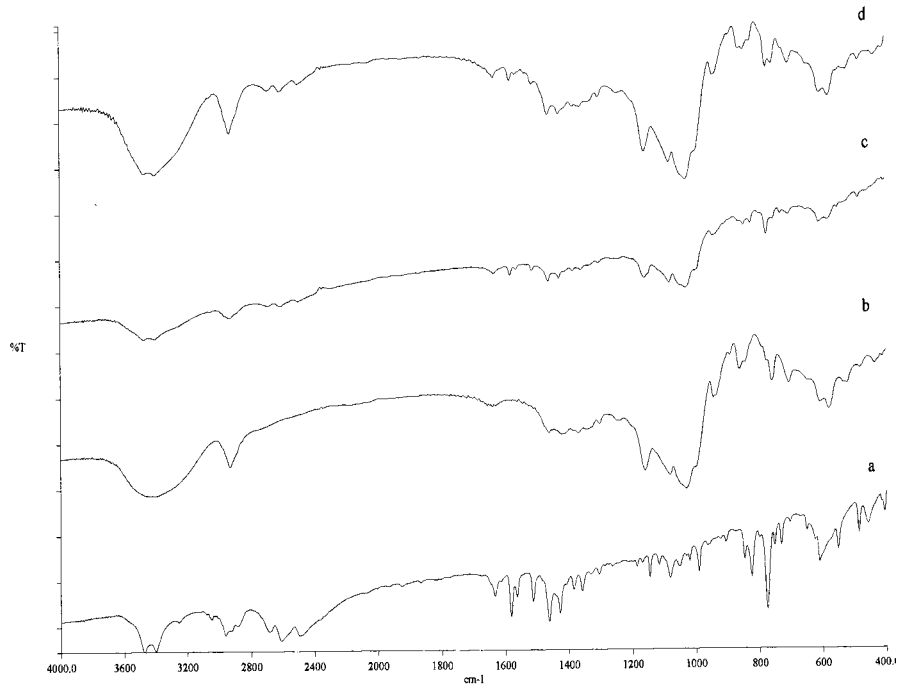

Figure 10.6 Infrared spectra of (a) dried TPH, (b) dried BCD, (c) a dried sample of a 1:1 mass ratio (equivalent to a 3.4:1.0 mole ratio) physical mixture of TPH and BCD and (d) a dried sample of a 1:1 mole ratio physical mixture of TPH and BCD

10.3. Mixtures of TPH and glucose

Figure 10.7 and 10.8 show the IR spectra of the original and dried samples of 1:1 mass ratio and 1:1 mole ratio physical mixtures of TPH and glucose, compared with the spectra of the pure components. The spectrum of dried glucose differs from that of the original glucose sample in the 4000 to 3000 cm^{-1} region and the absorptions in the lower wavenumber region are sharper in the dried samples. The TPH features are also much sharper in the spectra of the dried mixtures.

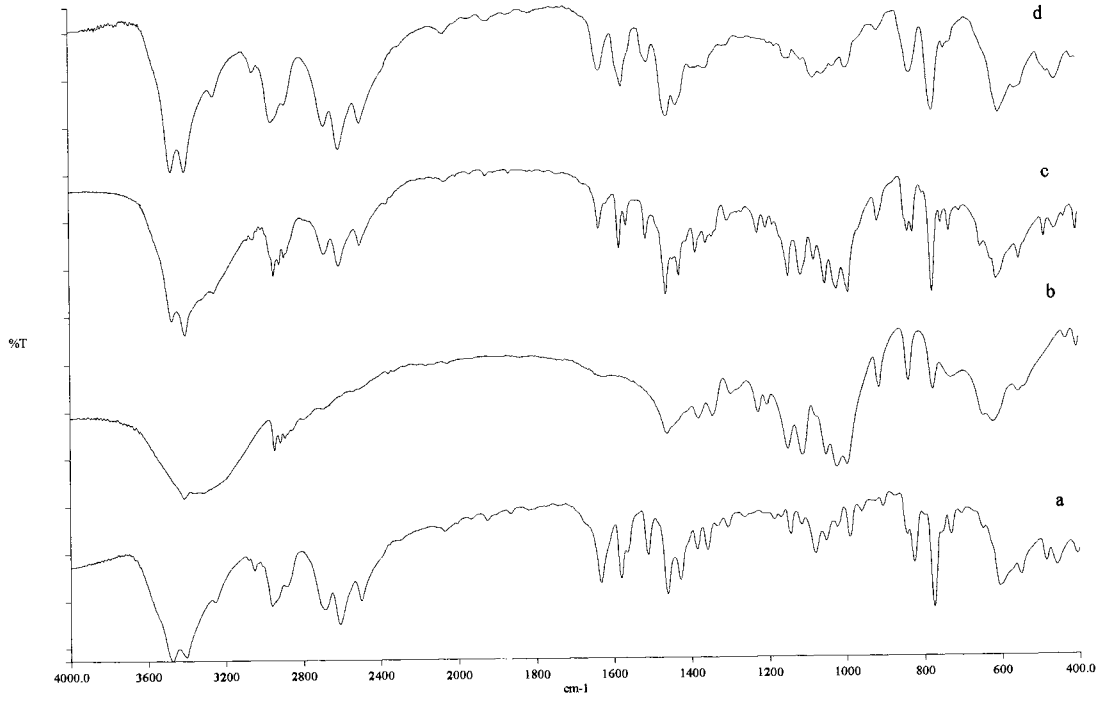

Figure 10.7 Infrared spectra of samples of (a) TPH, (b) glucose, (c) a 1:1 mass ratio (equivalent to a 0.54:1.0 mole ratio) physical mixture of TPH and glucose and (d) a 1:1 mole ratio physical mixture of TPH and glucose

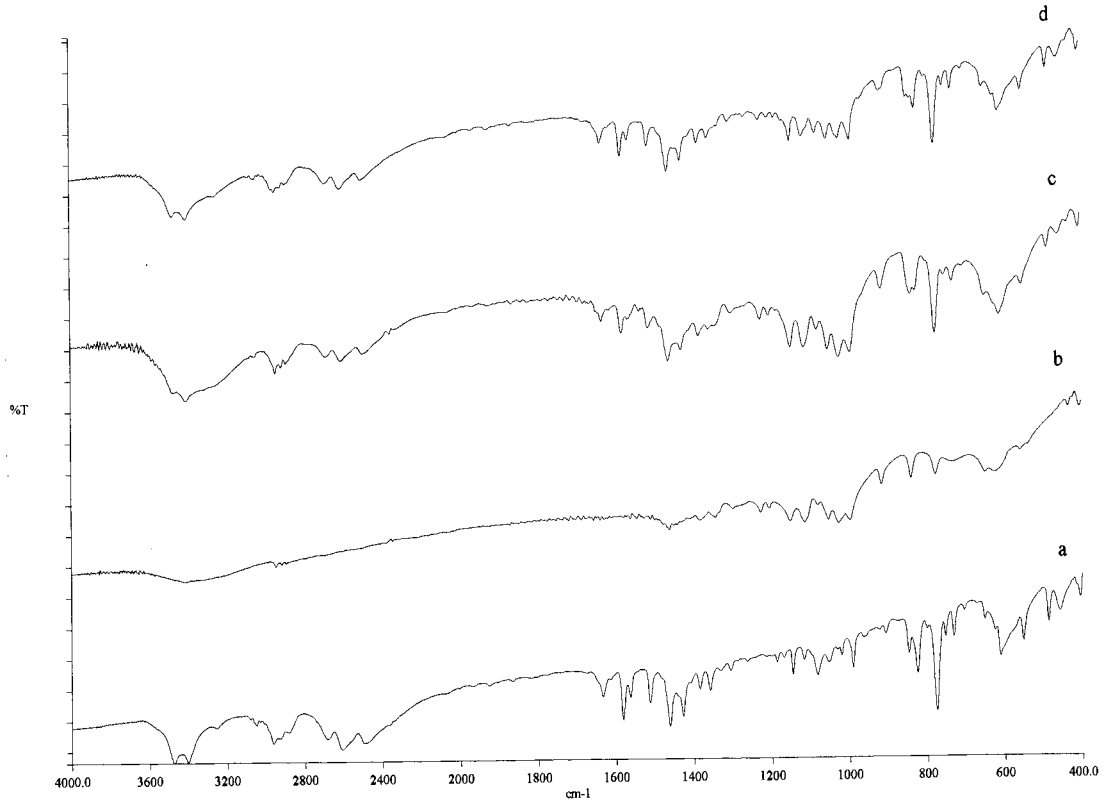

Figure 10.8 Infrared spectra of (a) dried TPH, (b) dried glucose, (c) a dried sample of a (equivalent to a 0.54:1.0 mole ratio) physical mixture of TPH and glucose and (d) a dried sample of a 1:1 mole ratio physical mixture of TPH and glucose

10.4. Mixtures of BCD and glucose

Figure 10.9 shows the IR spectra of the samples of 1:1 mass ratio and 1:1 mole ratio physical mixtures of glucose and BCD, compared with those of the original glucose and BCD. Features of spectra of both glucose and BCD are still evident in the physical mixtures of glucose and BCD. Molecular modelling of glucose and BCD (see Section 14) shows that glucose could be included in the BCD cavity.

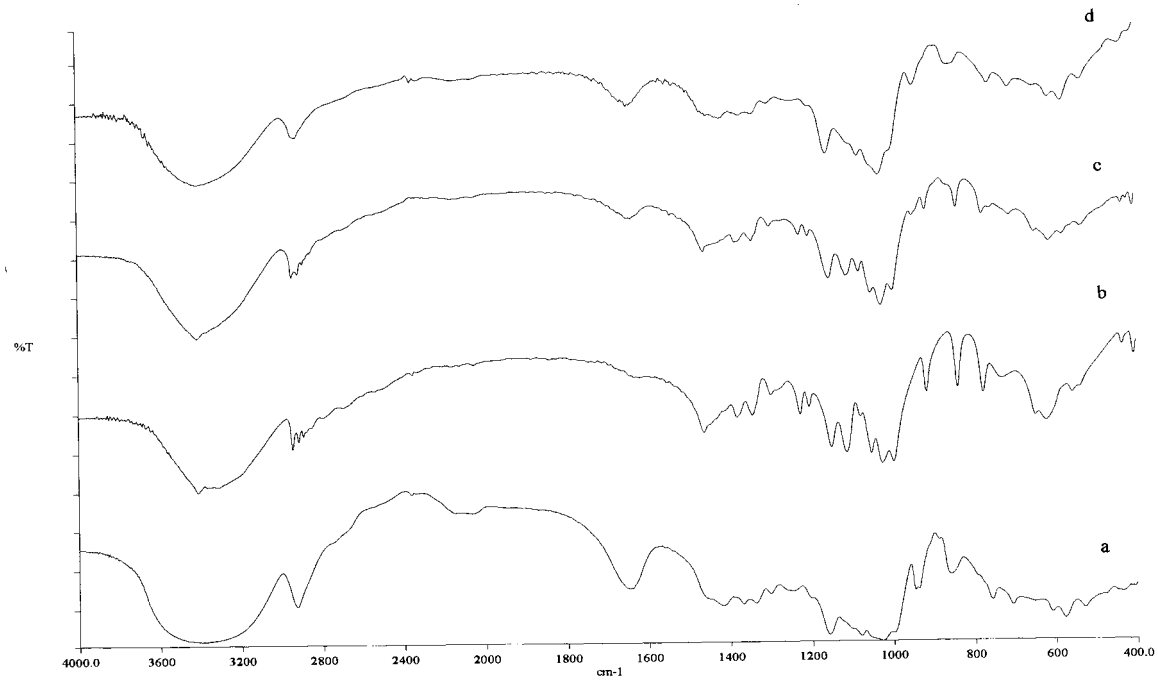

10.9 Infrared spectra of samples of (a) BCD, (b) glucose, (c) a 1:1 mass ratio (equivalent to a 0.16:1.00 mole ratio) physical mixture of glucose and BCD and (d) a 1:1 mole ratio physical mixture of glucose and BCD.

11. SOLID-STATE PHOTOSTABILITY OF TPH

11.1. Photostability studies

Solid samples of TPH and of physical mixtures of TPH with either cyclodextrin or glucose were spread evenly in thin layers in petri-dishes, covered with polyethylene film and irradiated using an Atlas Sun Test CPS+ (Atlas Material Technology BV, Germany) fitted with a Xenon lamp and a solar ID 65 filter. The medium irradiance level was used at 550 watts/m^2 for the time periods specified and the temperature was maintained at 40°C, as described in section 4.3. "Dark control" samples were treated similarly but covered with aluminium foil (see Section 4.3.1)

The behaviour of the irradiated samples, compared to the original samples, was evaluated using TG, DSC, XRD and IR. A validated HPLC method was used to quantitate the amount of drug remaining after irradiation (see Appendix A). Samples of the irradiated solids were dissolved to give aqueous solutions containing 0.01 mg ml^{-1} of the original TPH and injected in triplicate.

11.2. Photodegradation of solid TPH

The results of the HPLC analyses of samples of solid TPH, irradiated for various times in a petri-dish covered with plastic foil and "dark control" samples covered with aluminium foil, are listed in Table 11.1 and plotted in Figure 11.1.

Table 11.1 HPLC analyses of samples of solid TPH irradiated for various times compared with analyses for "dark control" samples covered with aluminium foil.

Irradiation time/hours	% drug remaining	dark control %
0	100	100
4	98	99
8	96	98
12	94	98
16	91	97
20	90	96

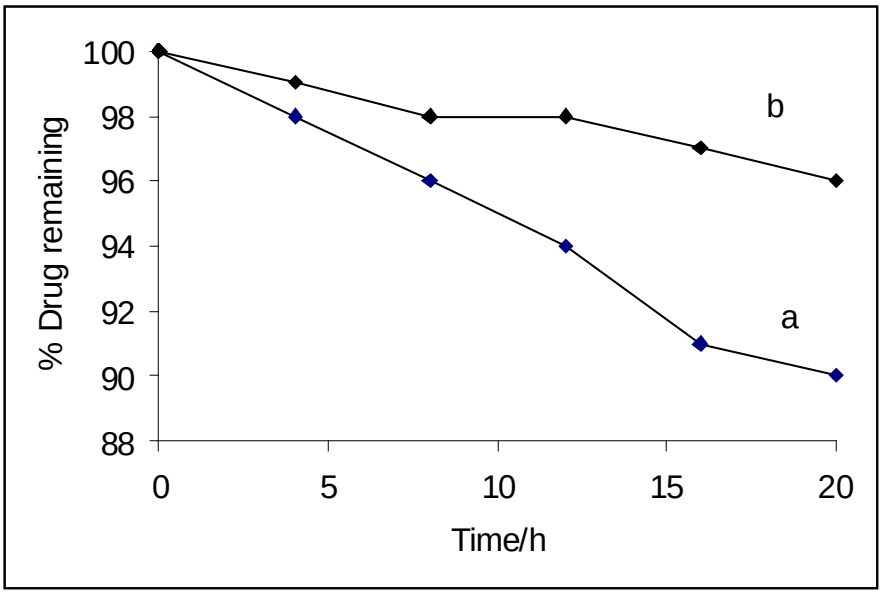

Figure 11.1 Photodegradation of (a) solid TPH after irradiation using an Atlas Suntest lamp at 40 ^{o}C at 550 W m^{-2} for the times indicated, compared with (b) dark control samples.

The amount of photodegradation under these harsh conditions is quite small and the dark control results suggest that some of the degradation is of thermal origin.

11.3. DSC and TG results for irradiated TPH

The DSC curves for the original TPH and TPH samples irradiated for 4, 8, 12, 16 and 20 hours (heated in flowing nitrogen at 10 ^{o}C min^{-1} using sealed pressure pans) are shown in Figure 11.2. Interpretation of the DSC curve of TPH has been discussed in Section 5. The curves for TPH irradiated for 4 and 8 hours show sharp endotherms (melting) at 122 to 123 ^{o}C and the curves for TPH irradiated for 12, 16 and 20 hours show broader endotherms with onsets 121, 119 and 117 ^{o}C. The ΔH values calculated for the melting endotherm are given in Table 11.2 and show a decrease in ΔH with irradiation time. This indicates that during irradiation some degradation or isomerisation has occurred. TG curves for irradiated TPH show slight degradation, (see Figure 11.3).

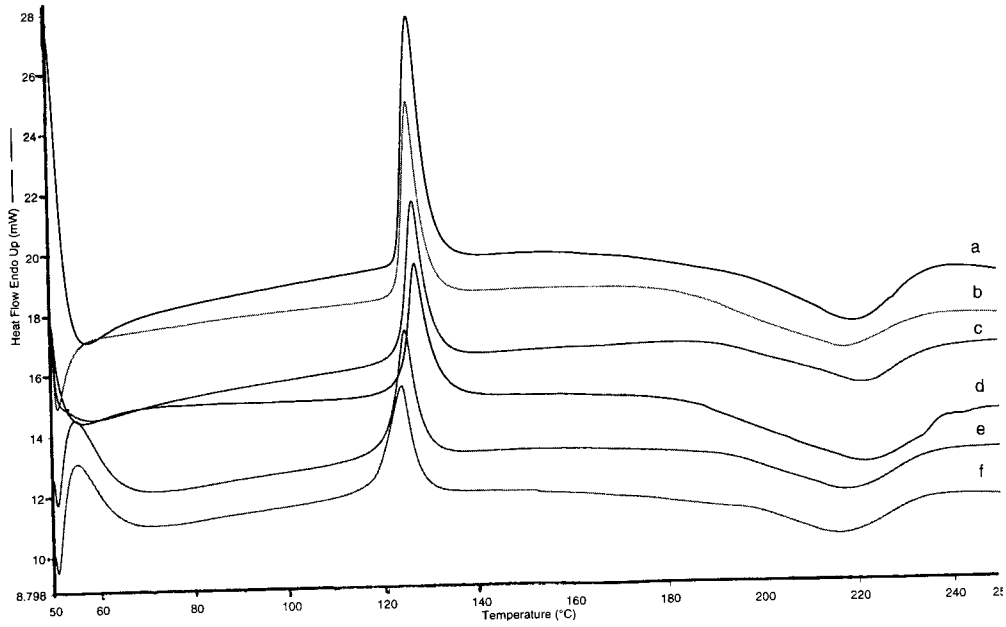

Figure 11.2 DSC curves for (a) original TPH and for samples of TPH irradiated for (b) 4, (c) 8, (d) 12, (e) 16 and (f) 20 hours, (heated at 10 ^{o}C min^{-1} in flowing nitrogen) using sealed pressure pans.

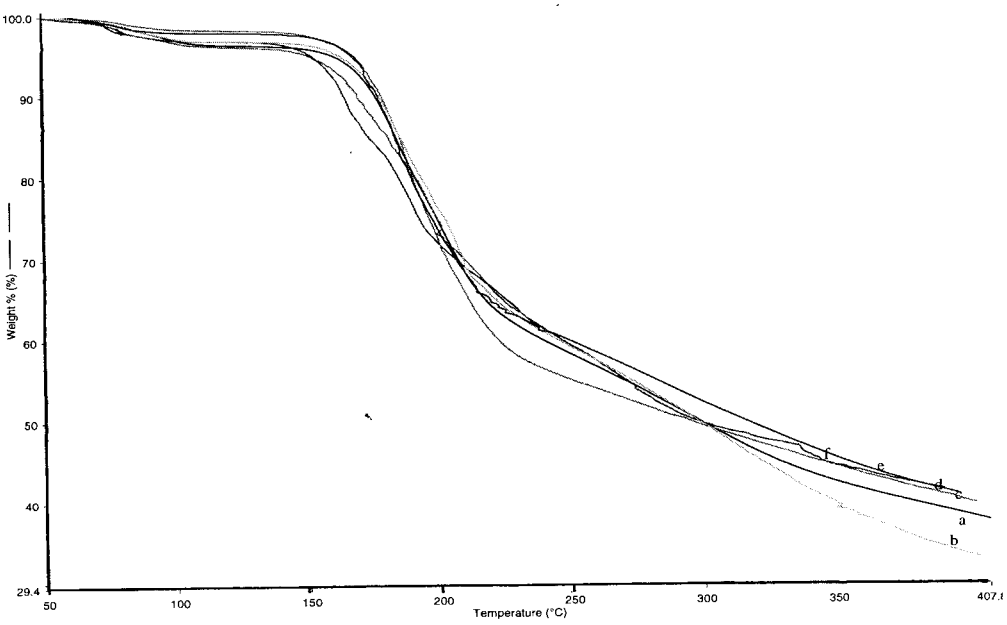

Figure 11.3 TG curves for (a) original TPH and for samples of TPH irradiated for (b) 4, (c) 8, (d) 12, (e) 16 and (f) 20 hours, heated at 10 ^{o}C min^{-1} in flowing nitrogen using, open platinum pans.

Table 11.2 Summary of the DSC results for the original TPH and irradiated TPH.

Irradiation time/h	Onset temperature of DSC endotherm /EC	Expected ΔH / kJ mol^{-1}	Observed ΔH / kJ mol^{-1}	ΔH/ J g^{-1}
0	124		37	117
4	123	37	32	107
8	122	37	32	98
12	121	37	28	91
16	119	37	33	100
20	117	37	32	95

11.4. X-ray powder diffraction patterns of irradiated TPH

The X-ray powder diffraction patterns of TPH and of samples of TPH irradiated for 4, 8, 12, 16 and 20 hours are compared with those of pure TPH and the dark control sample, covered during irradiation with aluminium foil, in Figure 11.4 and Figure 11.5.

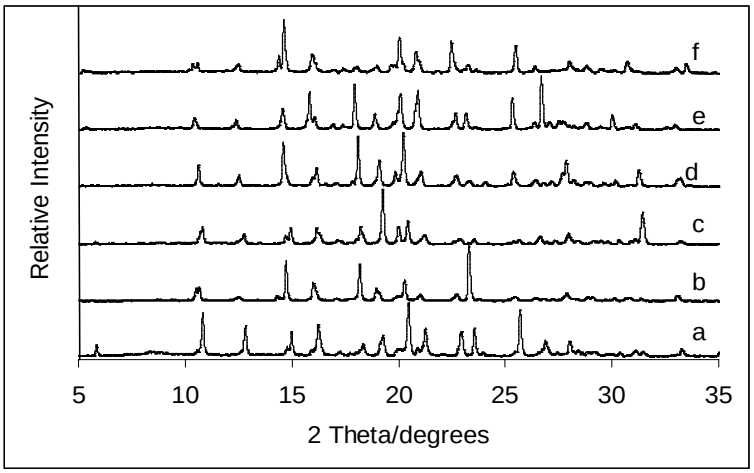

Figure 11.4 X-ray powder diffraction patterns of (a) TPH and of samples of TPH irradiated for (b) 4, (c) 8, (d) 12, (e) 16 and (f) 20 hours.

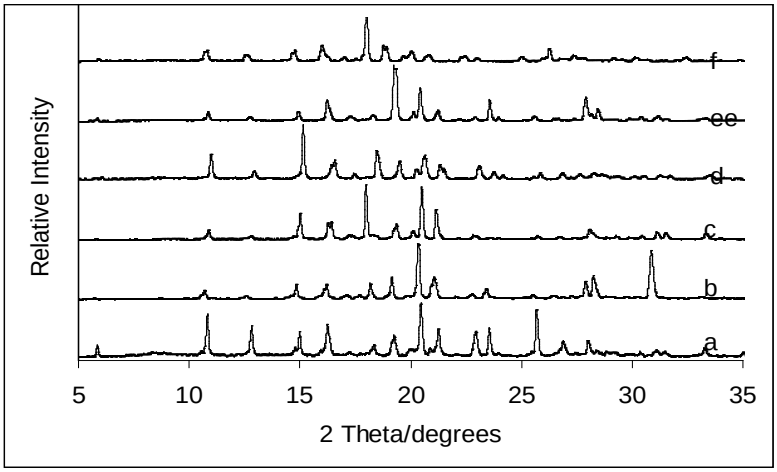

Figure 11.5 X-ray powder diffraction patterns of (a) TPH and of dark control samples of TPH irradiated for (b) 4, (c) 8, (d) 12, (e) 16 and (f) 20 hours.

In Figure 11.4 the patterns for the irradiated samples show that changes of crystal structure from the original have occurred during irradiation and that these changes continue with increasing dose. In Figure 11.5 the patterns for the dark control samples show that the temperature rise during irradiation has had an effect on the TPH even after 4 hours. It is interesting that the XRD pattern of the dark control sample after irradiation for 20 hours differs from that of the original TPH and also from that of the sample exposed to the irradiation for 20 hours. These results indicate that thermal and photodegradation occur concurrently under these conditions.

11.5. X-ray powder diffraction patterns of irradiated BCD

The X-ray powder diffraction patterns of samples of the original BCD and of samples of BCD that had been irradiated for 4, 8, 12, 16 and for 20 hours are shown in Figure 11.6 and the corresponding dark control samples of BCD in Figure 11.7. Some slight changes in crystal structure are produced by irradiation and by the thermal effects during irradiation of BCD.

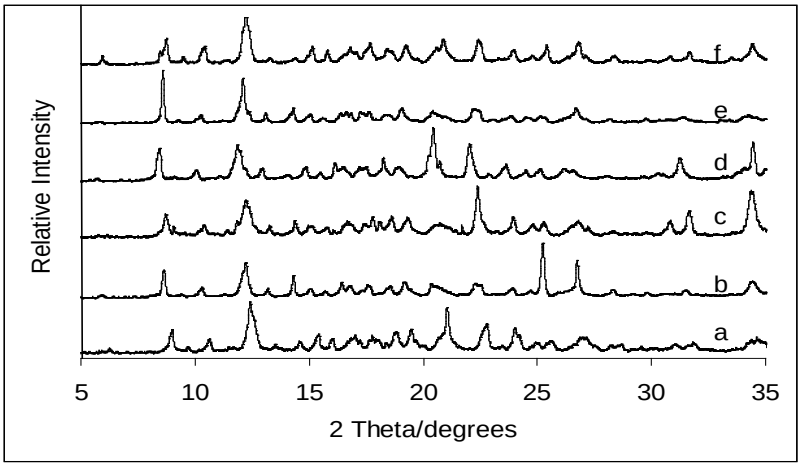

Figure 11.6 The X-ray powder diffraction patterns of (a) BCD and of samples of BCD irradiated for (b) 4, (c) 8, (d) 12, (e) 16 and (f) 20 hours.

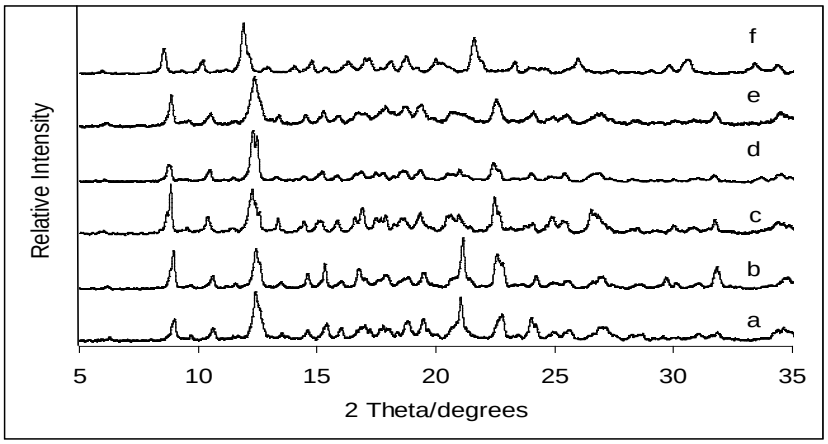

Figure 11.7 The X-ray powder diffraction patterns of (a) BCD and of dark control samples of BCD irradiated for (b) 4, (c) 8, (d) 12, (e) 16 and (f) 20 hours.

11.6. X-ray powder diffraction patterns of irradiated glucose

The patterns for the original glucose and for samples of glucose that had been irradiated for 4, 8, 12, 16 and for 20 hours are shown in Figure 11.8 and the patterns for the corresponding dark control samples of glucose are shown in Figure 11.8.

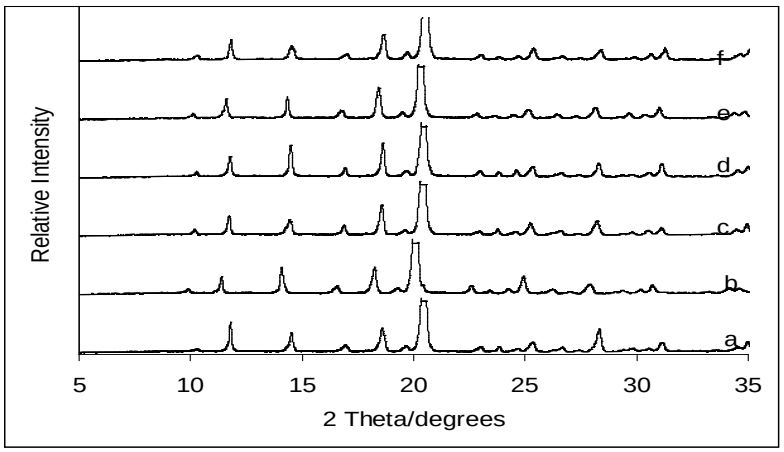

Figure 11.8 The X-ray powder diffraction patterns of (a) glucose and of samples of glucose irradiated for (b) 4, (c) 8, (d) 12, (e) 16 and (f) 20 hours.

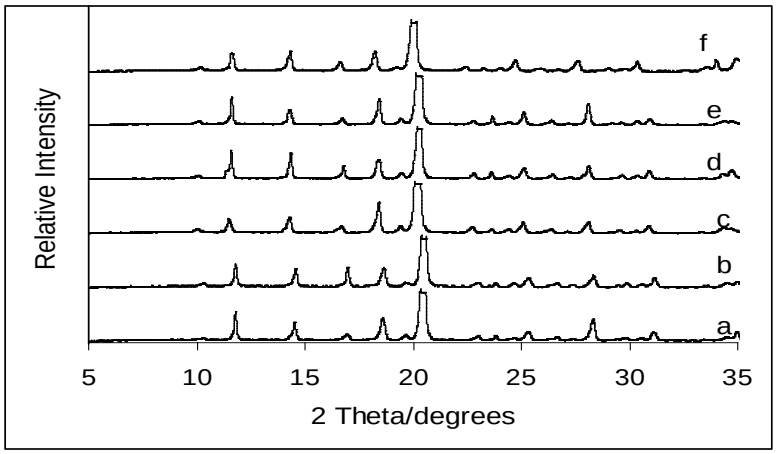

Figure 11.9 The X-ray powder diffraction patterns of (a) glucose and of dark control samples of glucose irradiated for (b) 4, (c) 8, (d) 12, (e) 16 and (f) 20 hours.

The effects of irradiation on the X-ray powder diffraction patterns of glucose were minimal. These results are of value in interpreting the effects of irradiation on physical mixtures of TPH and BCD and of TPH and glucose (see Section 12).

11.7. Infrared spectra of irradiated TPH

The infrared spectra of samples of irradiated TPH were compared with those of the original TPH, as well of the dark control samples of TPH, as shown in Figure 11.10 and Figure 11.11. The IR spectra show significant decreases in the absorption bands after irradiation.

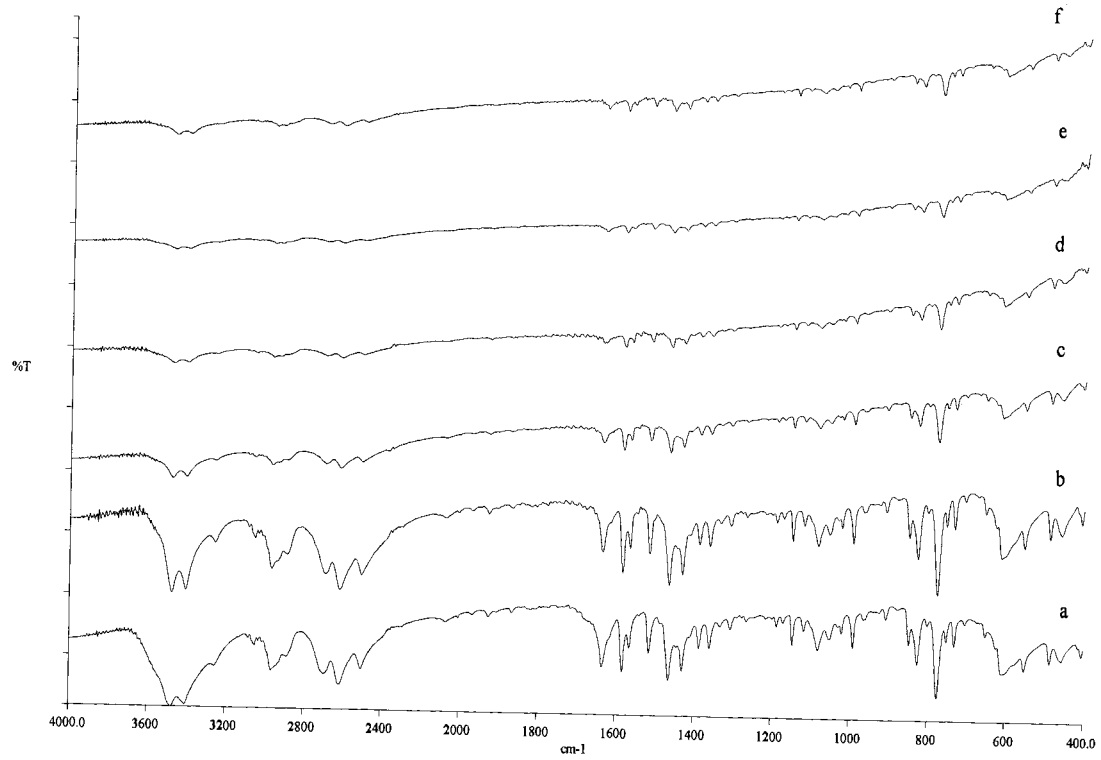

Figure 11.10 Infrared spectra of (a) TPH and of samples of TPH irradiated for (b) 4, (c) 8, (d) 12, (e) 16 and (f) 20 hours.

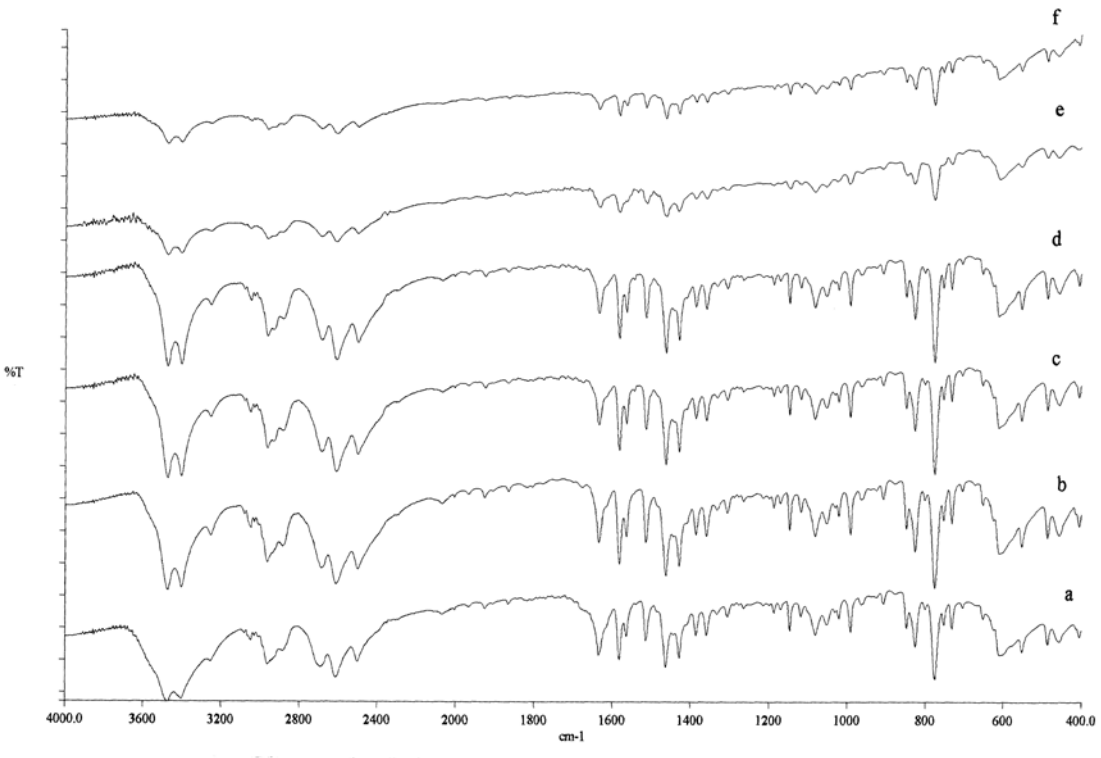

Figure 11.11 Infrared spectra of (a) TPH and of samples of TPH in dark control using aluminium foil irradiated for (b) 4, (c) 8, (d) 12, (e) 16 and (f) 20 hours.

11.8. Infrared spectra of irradiated BCD

Infrared spectra of samples of the original BCD and of samples of BCD irradiated for 4, 8, 12, 16 and for 20 hours are shown in Figure 11.12 and the spectra of the corresponding dark control samples of BCD are shown in Figure 11.13. The changes in absorption bands produced after irradiation are minimal.

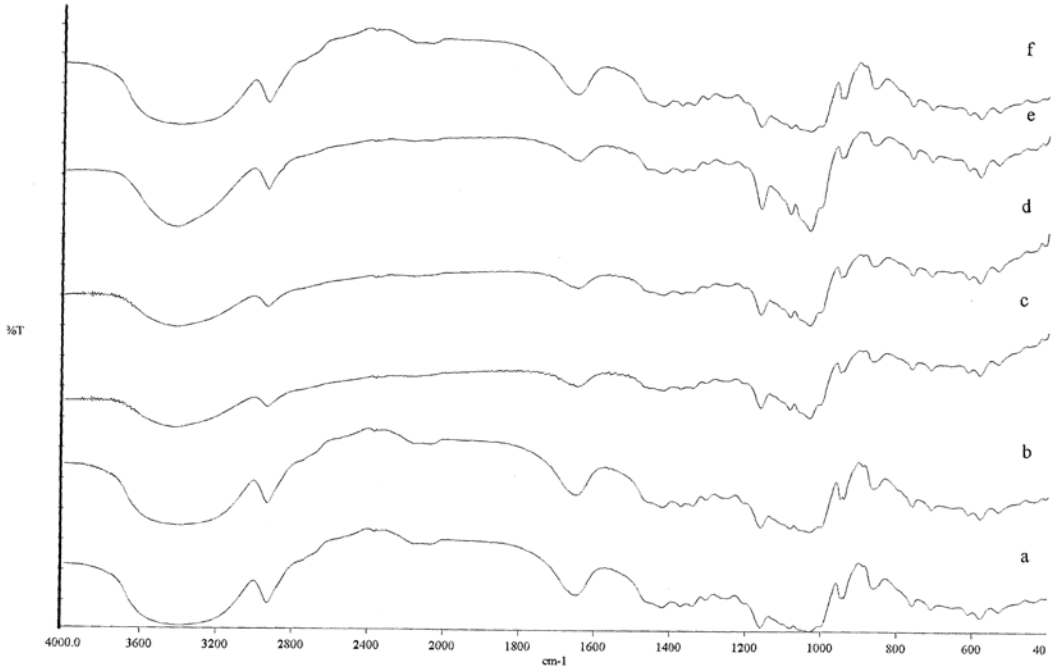

Figure 11.12 Infrared spectra of (a) BCD and of samples of BCD irradiated for (b) 4, (c) 8, (d) 12, (e) 16 and (f) 20 hours.

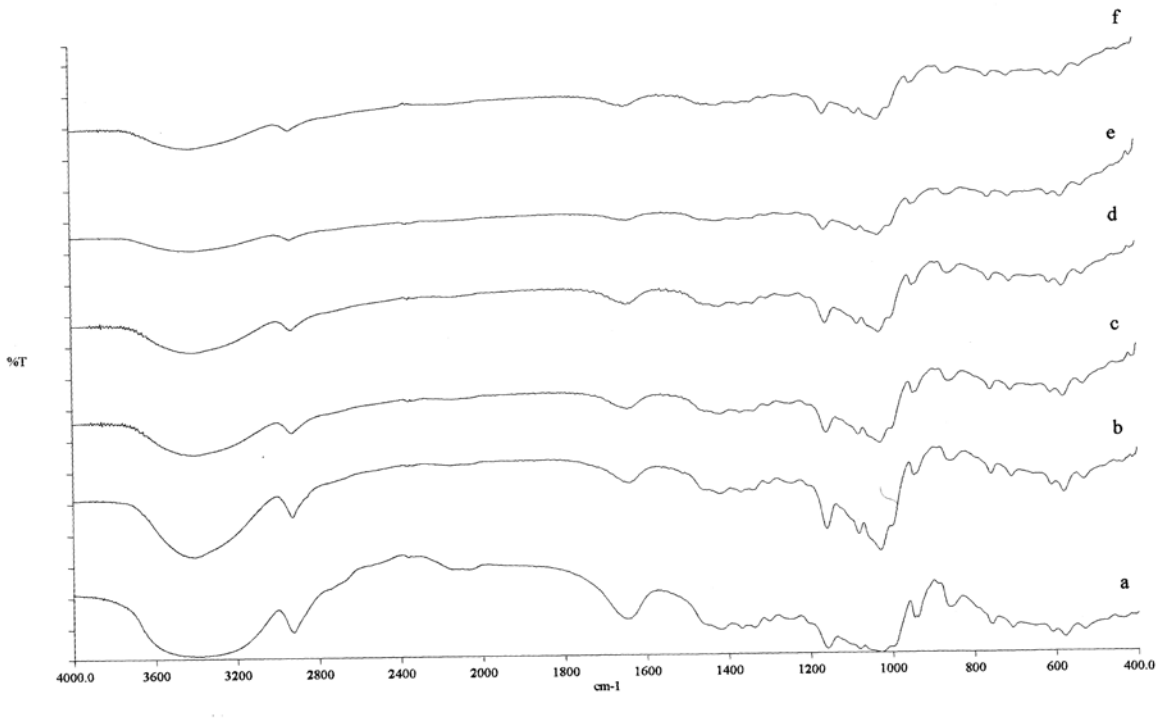

Figure 11.13 Infrared spectra of (a) BCD and of samples of BCD in dark control using aluminium foil irradiated for (b) 4, (c) 8, (d) 12, (e) 16 and (f) 20 hours.

11.9. Infrared spectra of irradiated glucose

Figure 11.14 shows the spectra for the original glucose and for samples of glucose that had been irradiated for 4, 8, 12, 16 and for 20 hours. Figure 11.15 shows the spectra of the corresponding dark control samples of glucose. The changes in absorption bands produced after irradiation are minimal.

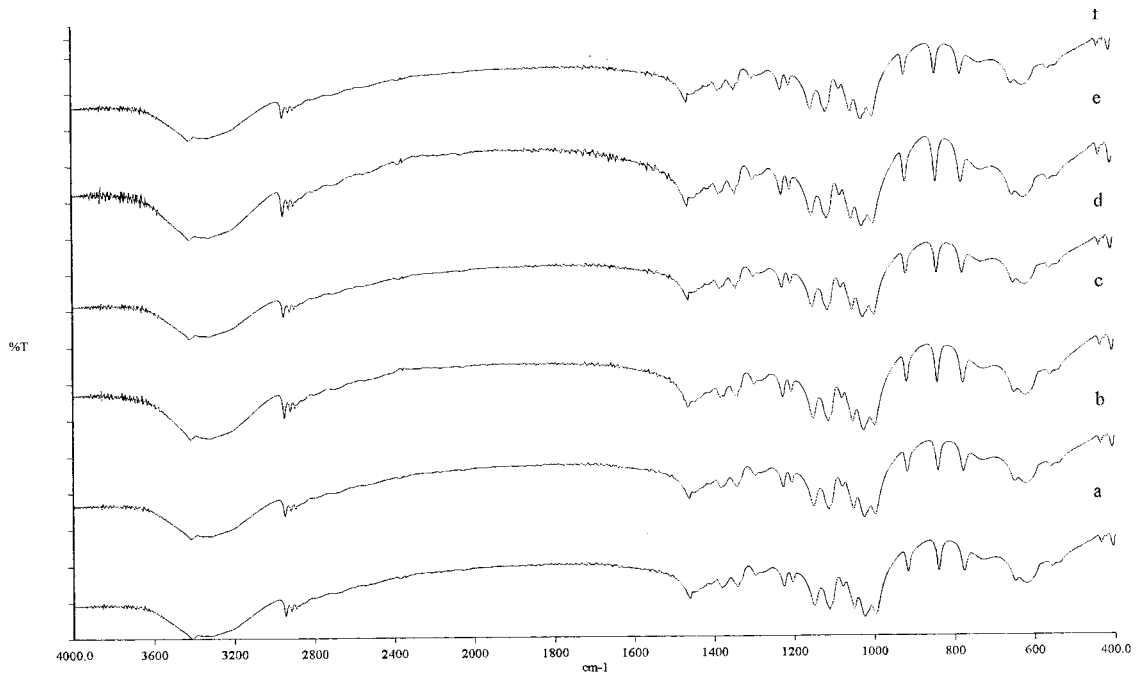

Figure 11.14 Infrared spectra of (a) glucose and of samples of glucose irradiated for (b) 4, (c) 8, (d) 12, (e) 16 and (f) 20 hours.

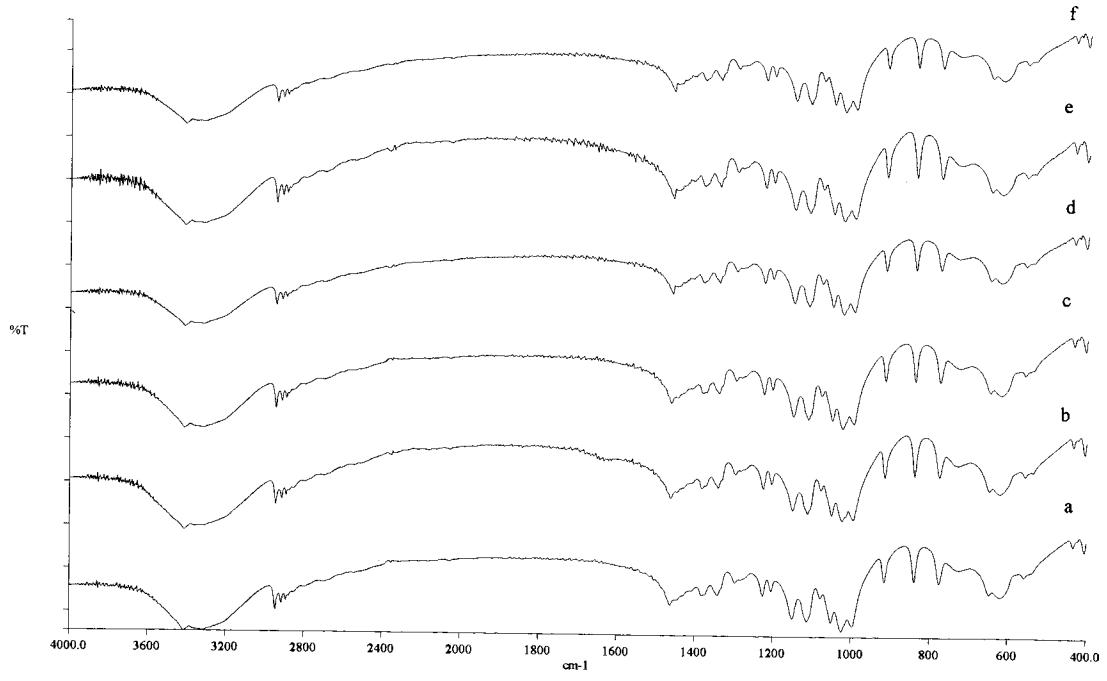

Figure 11.15 Infrared spectra of (a) glucose and of dark control samples of glucose irradiated for (b) 4, (c) 8, (d) 12, (e) 16 and (f) 20 hours.

11.10. Conclusions

Irradiation of solid TPH under the harsh conditions described produced little photodegradation. Results for the dark control samples suggested the possibility of some thermal contribution to the degradation resulting from the increased temperature during irradiation. The HPLC analyses were the most sensitive means of detecting degradation and these results were supported by the X-ray powder diffraction patterns and infrared spectra. Thermal analysis techniques did not have sufficient sensitivity.

12. THE PHOTOSTABILITY OF PHYSICAL MIXTURES OF TPH WITH BCD AND WITH GLUCOSE.

12.1. Introduction

The preparation of the physical mixtures is described in Section 4. Their thermal behaviour is described in Sections 7 and 8. For the irradiation studies the 1:1 mass ratio mixtures were used.

The conditions used for irradiation of the mixtures (Atlas Sun test CPS+ lamp at 550 W m^{-2} at 40 ^{o}C for the times specified) were the same as used for irradiation of pure TPH in the solid state (Section 11). Samples were evenly spread in thin layers in petri-dishes and covered with polyethylene film. "Dark control" samples were treated similarly but covered with aluminium foil (see Section 4.3.1).

The behaviour of the irradiated mixtures, compared to the original mixtures, was evaluated using TG, DSC, XRD and IR. A validated HPLC method was used to quantitate the amount of drug remaining in the mixture after irradiation (see Appendix A). Samples of the irradiated mixtures were dissolved to give aqueous solutions containing 0.01 mg ml^{-1} of the original TPH (0.02 mg ml^{-1} of the original 1:1 mass ratio mixtures) and injected in triplicate.

In interpreting the results for the photostability of mixtures of TPH and BCD and of TPH and glucose, the results given in Section 11 for BCD and for glucose, which showed minimal effects on these compounds when they were irradiated under the same conditions in the solid state, were of use.

12.2. Photostability of irradiated mixtures

12.2.1. TPH/BCD

HPLC analyses of the irradiated physical mixtures of TPH and BCD are compared with results for TPH alone in Table 12.1 and illustrated in Figure 12.1.

Table 12.1 HPLC analyses of a 1:1 mass ratio physical mixture of TPH and BCD irradiated for various times, compared with results for TPH alone.

	TPH alone	TPH/BCD mixture
Irradiation time/hours	% drug remaining	% drug remaining
0	100	100
4	98	99
8	96	96
12	94	95
16	91	93
20	90	92

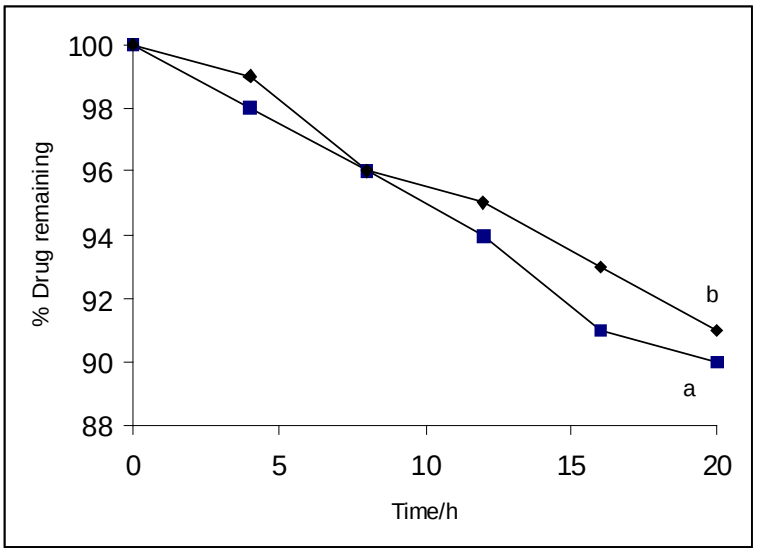

Figure 12.1 Photodegradation of (b) a 1:1 mass ratio physical mixture of TPH and BCD irradiated using an Atlas Suntest lamp at 40 ^{o}C at 550 W m^{-2} for the times indicated, compared with (a) the results for TPH alone. (Note: the points are joined for clarity.)

12.2.2. TPH/glucose

Results for similar experiments on irradiated physical mixtures of TPH and glucose are compared with results for TPH alone in Table 12.2 and illustrated in Figure 12.2.

Table 12.2 HPLC analyses of a 1:1 mass ratio physical mixture of TPH and glucose irradiated for various times, compared with results for TPH alone.

	TPH alone	TPH/glucose mixture
Irradiation time/hours	% drug remaining	% drug remaining
0	100	100
4	98	99
8	96	96
12	94	95
16	91	93
20	90	92

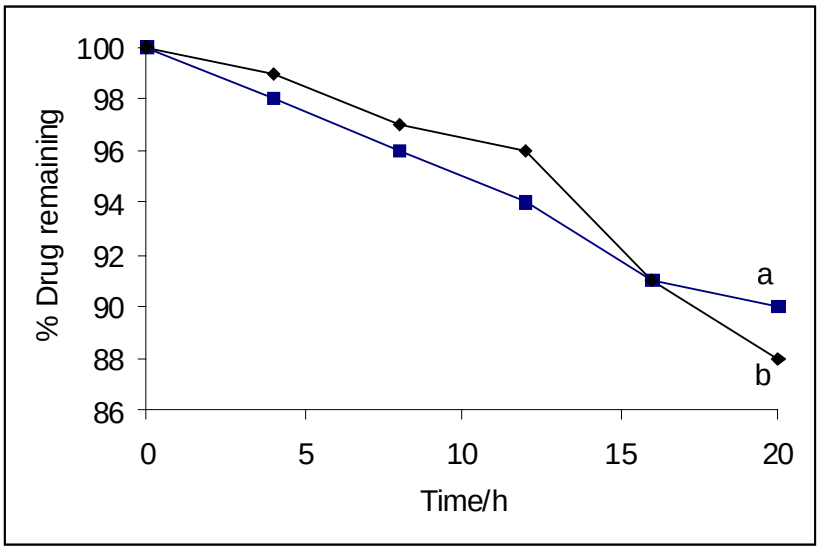

Figure 12.2 Photodegradation of (b) a 1:1 mass ratio physical mixture of TPH and glucose irradiated using an Atlas Suntest lamp at 40 ^{o}C at 550 W m^{-2} for the times indicated, compared with (a) the results for TPH alone. (Note: the points are joined for clarity.)

Neither the presence of BCD or of glucose has a significant effect on the limited amount of photodegradation of TPH in the solid state.

12.3. DSC and TG results for irradiated mixtures of TPH and BCD

DSC curves for a sample of the original 1:1 molar ratio physical mixture of TPH and BCD and of samples that had been irradiated for various times are compared in Figure 12.3. DSC curves for samples of the 1:1 mass ratio physical mixture of TPH and BCD after similar treatment are shown in Figure 12.4. The corresponding TG curves are shown in Figures 12.5 and 12.6.

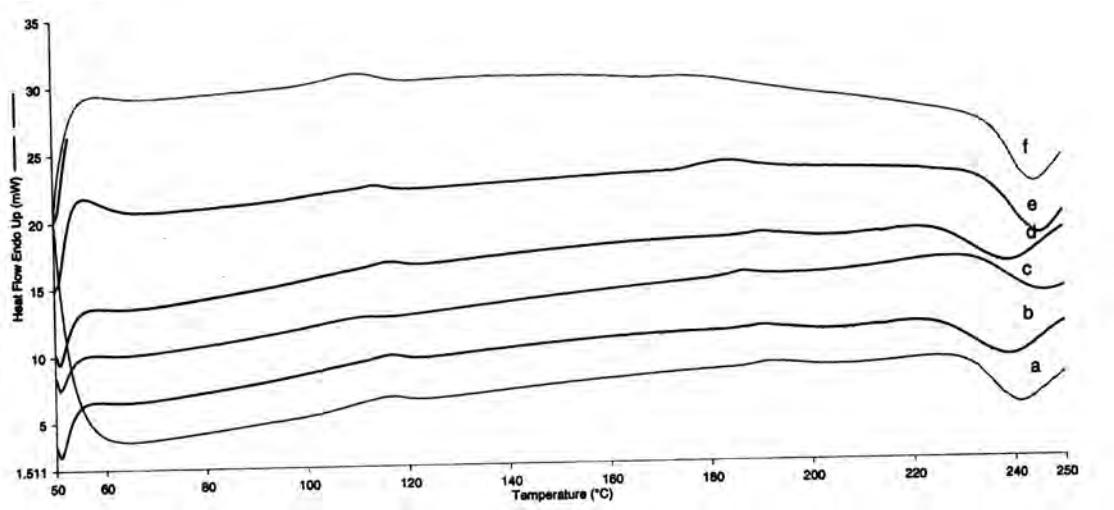

Figure 12.3 DSC curves for (a) a 1:1 molar ratio physical mixture of TPH/BCD and of samples of the mixture that had been irradiated for (b) 4, (c) 8, (d) 12, (e) 16 and (f) 20 hours (heating rate 10 ^{o}C min^{-1} in nitrogen).

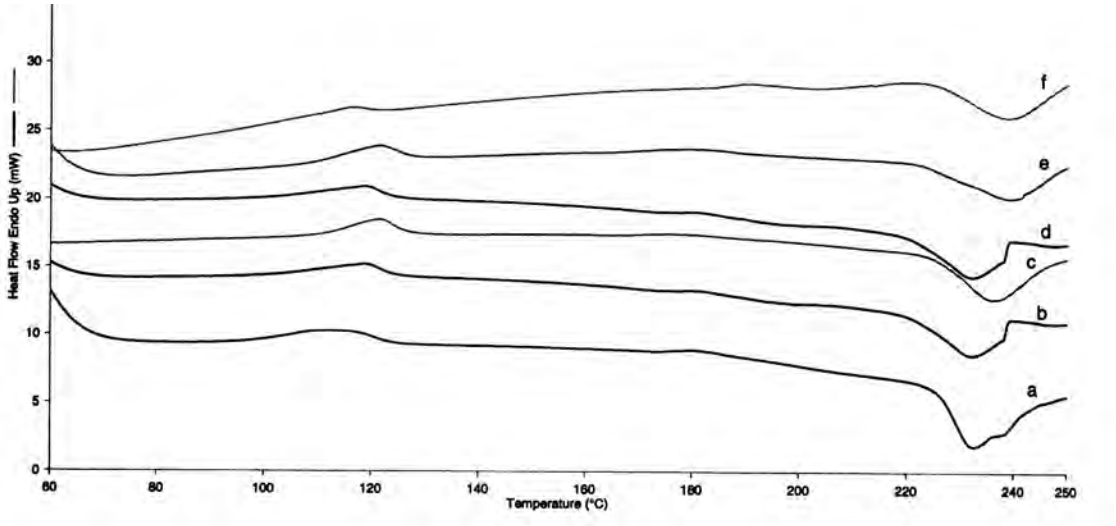

Figure 12.4 DSC curves for (a) a 1:1 mass ratio physical mixture of TPH/BCD and of samples of the mixture that had been irradiated for (b) 4, (c) 8, (d) 12, (e) 16 and (f) 20 hours (heating rate 10 ^{o}C min^{-1} in nitrogen).

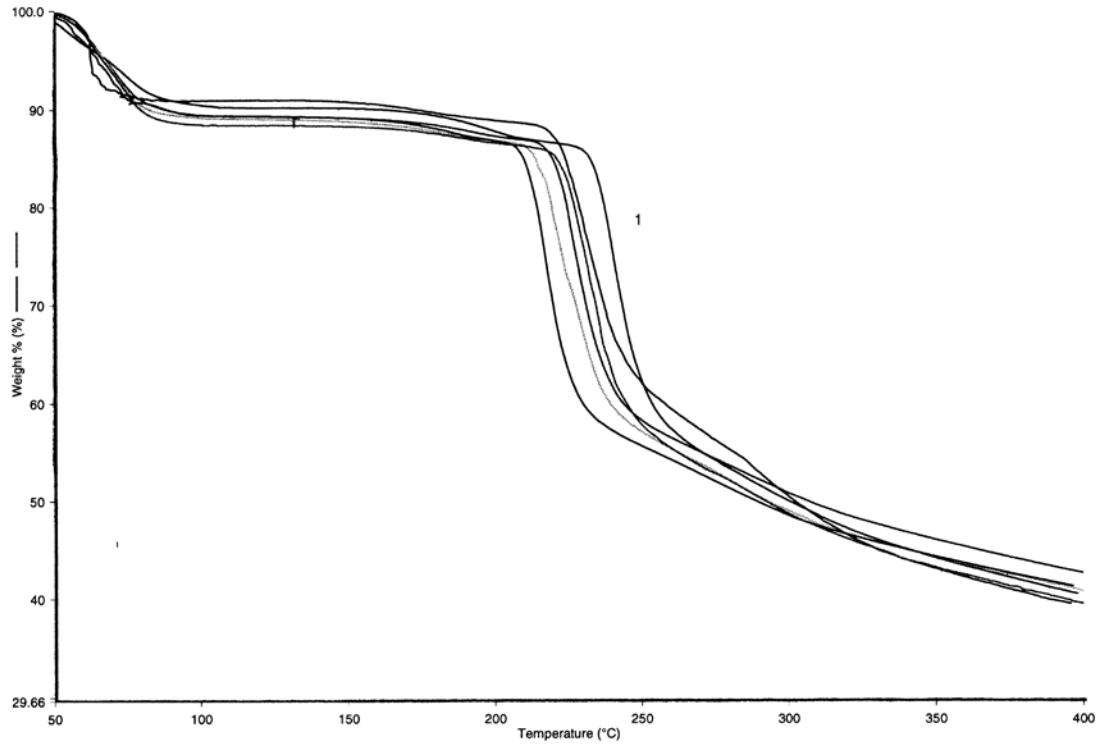

Figure 12.5 TG curves for (a) a 1:1 molar ratio physical mixture of TPH/BCD and of samples of the mixture that had been irradiated for (b) 4, (c) 8, (d) 12, (e) 16 and (f) 20 hours (heating rate 10 ^{o}C min^{-1} in nitrogen using platinum pans).

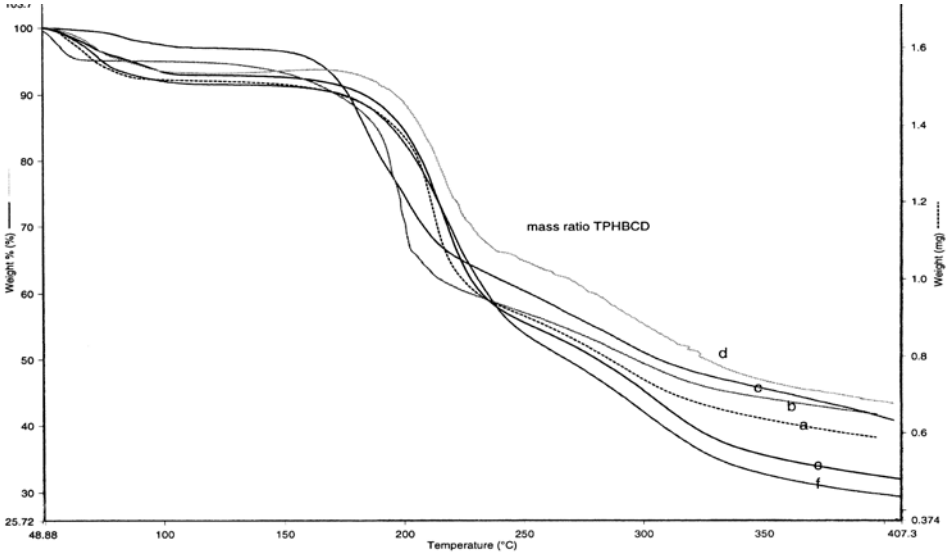

Figure 12.6 TG curves for (a) a 1:1 mass ratio physical mixture of TPH/BCD and of samples of the mixture that had been irradiated for (b) 4, (c) 8, (d) 12, (e) 16 and (f) 20 hours (heating rate 10 ^{o}C min^{-1} in nitrogen using platinum pans).

No systematic changes in thermal behaviour were observable directly from the DSC curves of samples after irradiation. The variations seen could be due to the problems of sampling of solid mixtures, particularly after irradiation when surfaces have received the greatest dose. A more quantitative comparison of melting behaviour in the mixtures is given in Table 12.3. There appears to be a general increase in onset temperature of melting and decrease in enthalpy of melting even at the lowest irradiation doses.

Table 12.3 Melting characteristics of TPH in physical mixtures with BCD before and after irradiation.

Sample _____ Irradiation time / h	Onset temperature of TPH melting / ^{o}C	ΔH of melting / J g^{-1}	Sample _____ Irradiation time / h	Onset temperature of TPH melting / ^{o}C	ΔH of melting / J g^{-1}
TPH/BCD 1:1 molar ratio	91	25	TPH/BCD 1:1 mass ratio	99	30
4	106	35	4	109	14
8	111	38	8	99	13
12	107	33	12	106	25
16	109	42	16	107	12
20	110	12	20	100	26

12.4. DSC and TG results for irradiated mixtures of TPH and glucose

A similar series of experiments was carried out on physical mixtures of TPH and glucose. The DSC curves for a sample of the original 1:1 molar ratio physical mixture and of samples that had been irradiated for various times are compared in Figure 12.7, and the DSC curves for samples of the 1:1 mass ratio physical mixture after similar treatment are shown in Figure 12.8. A comparison of melting behaviour in the mixtures is given in Table 12.4. The changes in onset temperature and enthalpy of melting are much less than for the TPH/BCD mixtures above.

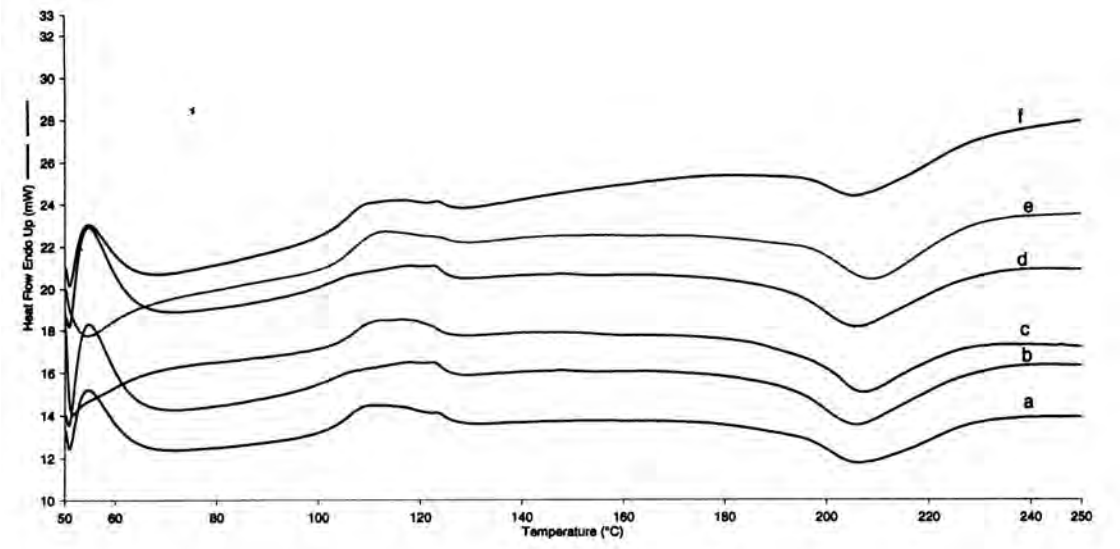

Figure 12.7 DSC curves for (a) a 1:1 molar ratio physical mixture of TPH/glucose and of samples of the mixture that had been irradiated for (b) 4, (c) 8, (d) 12, (e) 16 and (f) 20 hours (heating rate 10 ^{o}C min^{-1} in nitrogen).

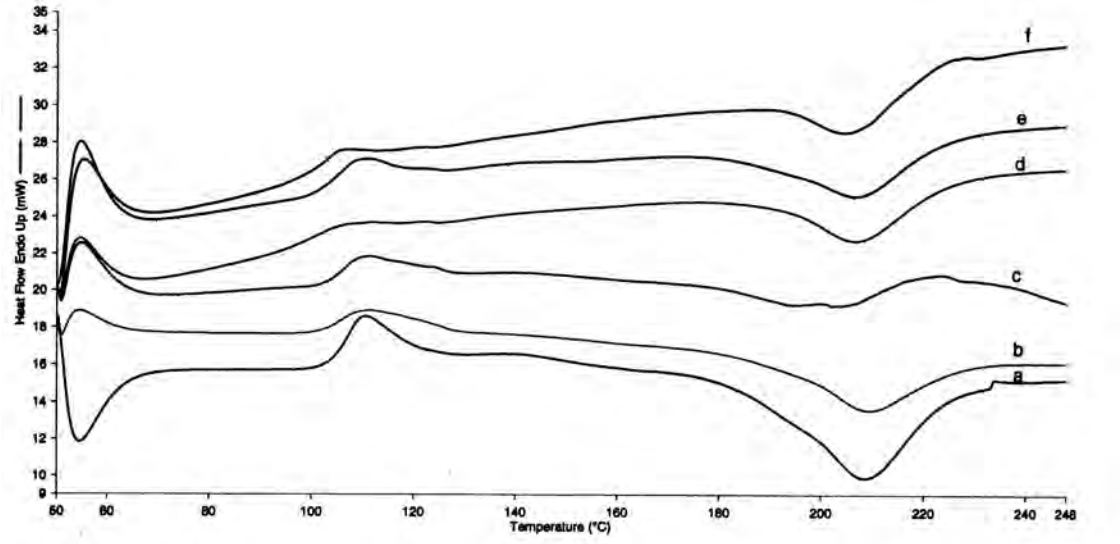

Figure 12.8 DSC curves for (a) a 1:1 mass ratio physical mixture of TPH/glucose and of samples of the mixture that had been irradiated for (b) 4, (c) 8, (d) 12, (e) 16 and (f) 20 hours (heating rate 10 ^{o}C min^{-1} in nitrogen).

Table 12.4 Melting characteristics of TPH in physical mixtures with glucose before and after irradiation for the times indicated.

Sample _____ Irradiation time / h	Onset temperature of TPH melting / ^{o}C	ΔH of melting / J g^{-1}	Sample _____ Irradiation time / h	Onset temperature of TPH melting / ^{o}C	ΔH of melting / J g^{-1}
TPH/glucose 1:1 molar ratio	106	102	TPH/glucose 1:1 mass ratio	104	64
4	98	71	4	102	75
8	104	72	8	104	69
12	99	65	12	97	56
16	103	70	16	101	76
20	102	81	20	99	62

12.5. DSC and TG results for irradiated mixtures of glucose and BCD

A further similar series of experiments was carried out on physical mixtures of glucose and BCD. The DSC curves for a sample of the original 1:1 molar ratio physical mixture and of samples that had been irradiated for various times are compared in Figure 12.9, and the DSC curves for samples of the 1:1 mass ratio physical mixture after similar treatment are shown in Figure 12.10. Results are summarised in Table 12.5. No significant systematic changes in melting behaviour are observed after irradiation.

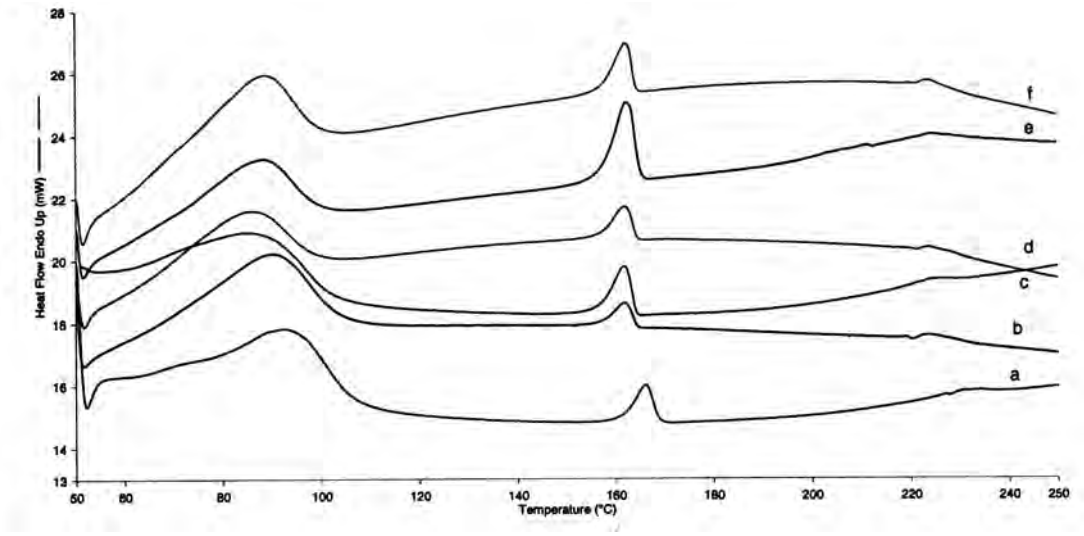

Figure 12.9 DSC curves for (a) a 1:1 molar ratio physical mixture of glucose and BCD and of samples of the mixture that had been irradiated for (b) 4, (c) 8, (d) 12, (e) 16 and (f) 20 hours (heating rate 10 ^{o}C min^{-1} in nitrogen).

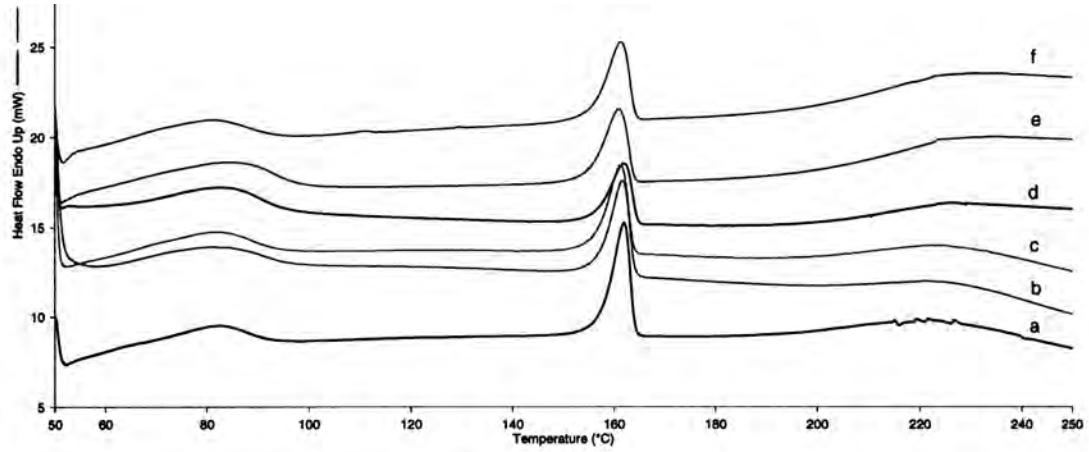

Figure 12.10 DSC curves for (a) a 1:1 mass ratio physical mixture of glucose and BCD and of samples of the mixture that had been irradiated for (b) 4, (c) 8, (d) 12, (e) 16 and (f) 20 hours (heating rate 10 ^{o}C min^{-1} in nitrogen).

Table 12.5 Melting characteristics of glucose in physical mixtures with BCD before and after irradiation.

Sample _____ Irradiation time / h	Onset temperature of glucose melting / ^{o}C	ΔH of melting / J g-1	Sample _____ Irradiation time / h	Onset temperature of glucose melting / ^{o}C	ΔH of melting / J g-1
Glucose/BCD 1:1 molar ratio	157	29	Glucose/BCD 1:1 mass ratio	157	109
4	157	20	4	156	98
8	157	27	8	156	95
12	157	21	12	156	66
16	157	41	16	155	86
20	157	18	20	155	91

12.6. X-ray powder diffraction patterns of irradiated mixtures of TPH and BCD

X-ray powder diffraction patterns of the original mixtures are reported in Section 9. The patterns of irradiated mixtures of TPH and BCD are compared with those of the unirradiated mixtures in Figures 12.11 and 12.12.

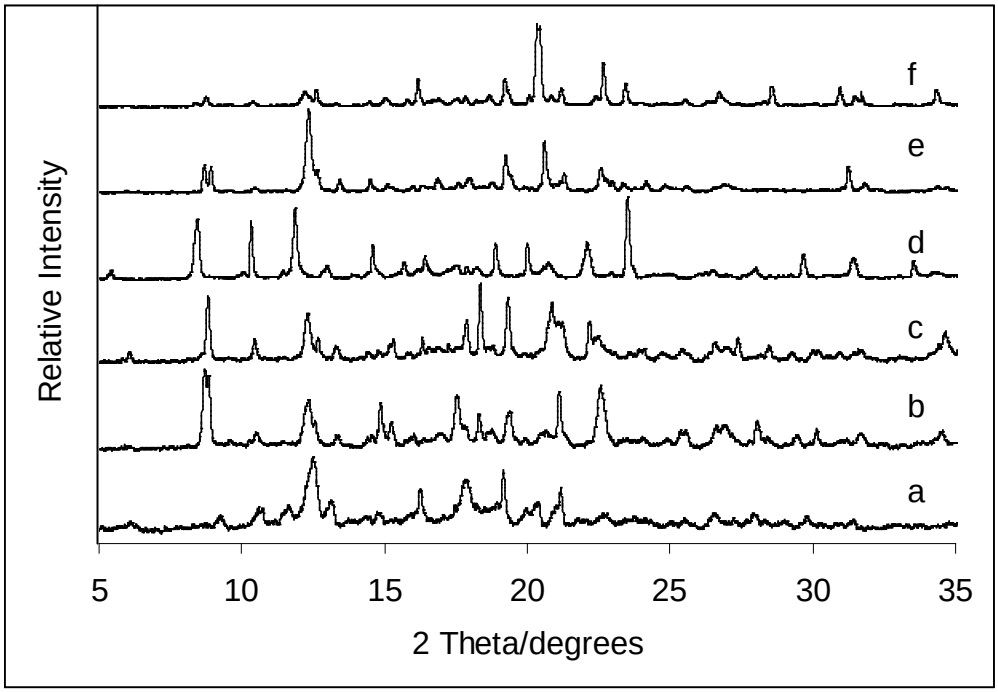

Figure 12.11 X-ray powder diffraction patterns of (a) a 1:1 mole ratio physical mixture of TPH and BCD and of samples of the mixture irradiated for (b) 4, (c) 8, (d) 12, (e) 16 and (f) 20 hours.

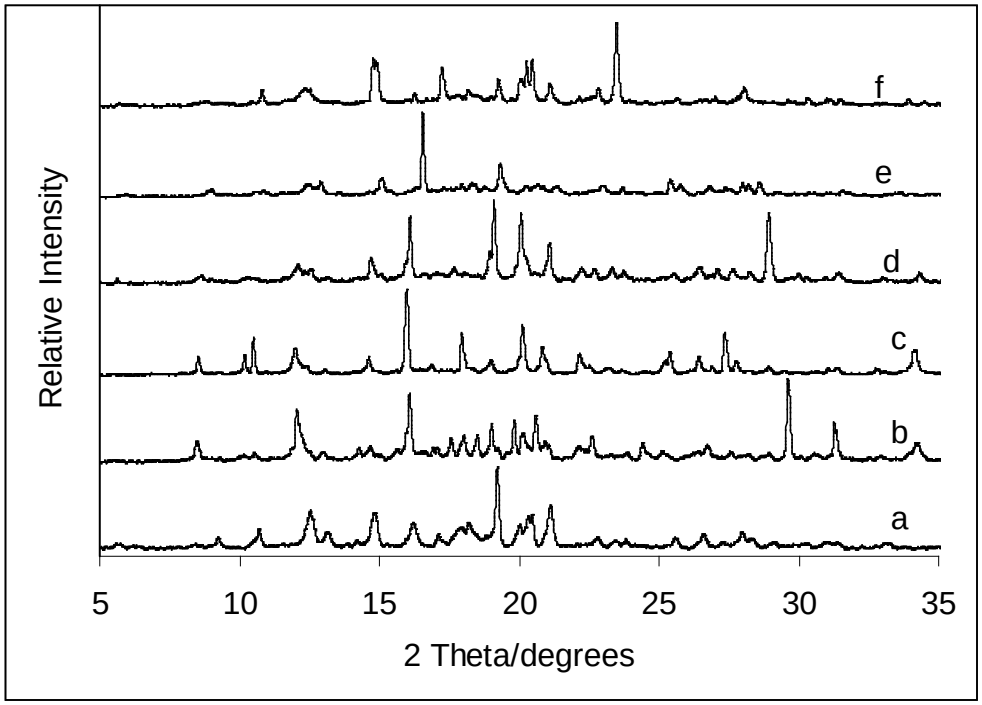

Figure 12.12 X-ray powder diffraction patterns of (a) a 1:1 mass ratio physical mixture of TPH and BCD (equivalent to a 3.4:1.0 mole ratio) and of samples of the mixture irradiated for (b) 4, (c) 8, (d) 12, (e) 16 and (f) 20 hours.

In Section 9 it was shown that physical mixing produces a compound with a different, less-crystalline structure than that of either TPH or BCD, represented by pattern (a) in Figure 12.12. This diffraction pattern changes with irradiation dose with the appearance and disappearance of peaks indicating significant but complex changes in crystal structure caused by irradiation. At the highest doses, patterns (e) and (f), there is an indication of some deterioration in crystallinity.

12.7. X-ray powder diffraction patterns of irradiated mixtures of TPH and glucose

The X-ray powder diffraction patterns of irradiated mixtures of TPH and glucose, shown in Figures 12.13 and 12.14, also indicate changes in crystal structure although the intense peak of glucose is still evident in the irradiated mixtures. The changes increase with increasing time of irradiation.

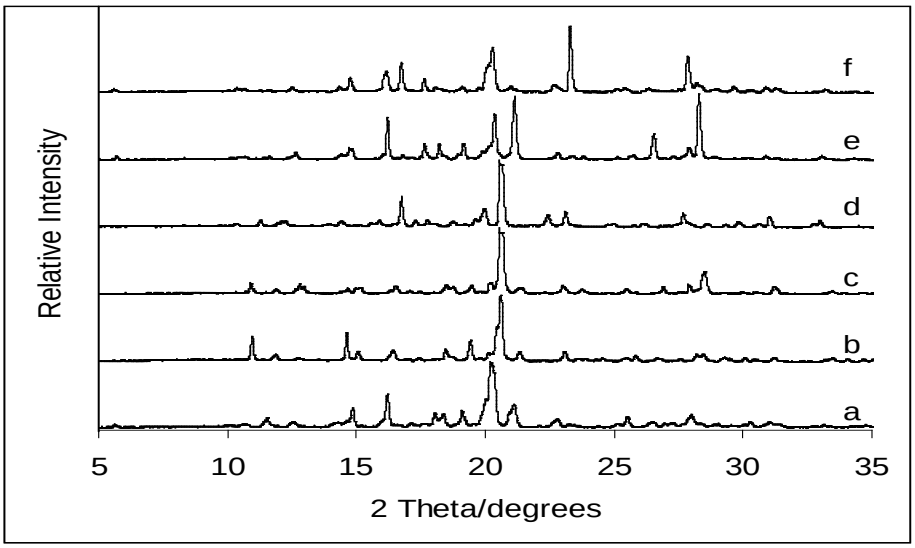

Figure 12.13 X-ray powder diffraction patterns of (a) a 1:1 mole ratio physical mixture of TPH and glucose and of samples of mixtures irradiated for (b) 4, (c) 8, (d) 12, (e) 16 and (f) 20 hours**.**

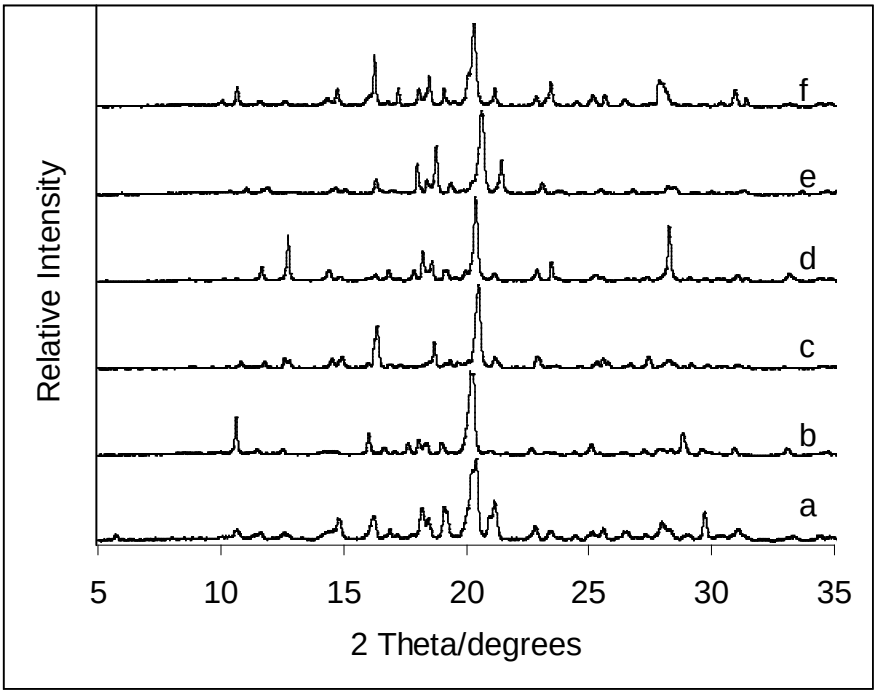

Figure 12.14 X-ray powder diffraction patterns of (a) a 1:1 mass ratio physical mixture of TPH and glucose (equivalent to a 0.54:1.00 mole ratio) and of samples of the mixture irradiated for (b) 4, (c) 8, (d) 12, (e) 16 and (f) 20 hours.

12.8. X-ray powder diffraction patterns of irradiated mixtures of glucose and BCD

The X-ray powder diffraction patterns of irradiated physical mixtures of glucose and BCD are shown in Figures 12.15 and 12.16. The changes in diffraction pattern with irradiation dose are not very marked.

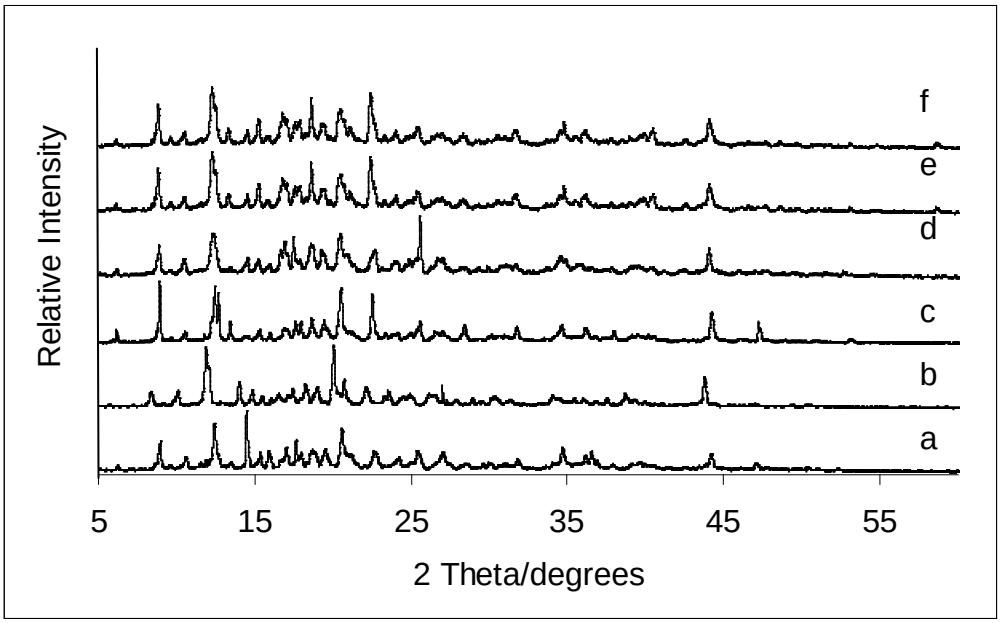

Figure 12.15 X-ray powder diffraction pattern of (a) a 1:1 mole ratio physical mixture of glucose and BCD and of samples of the mixture irradiated for (b) 4, (c) 8, (d) 12, (e) 16 and (f) 20 hours.

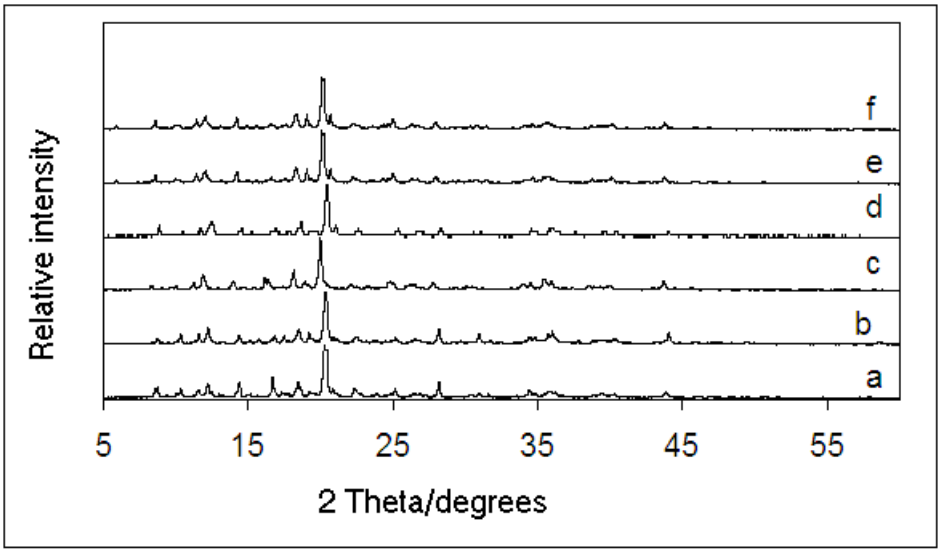

Figure 12.16 X-ray powder diffraction patterns of (a) a 1:1 mass ratio physical mixture of glucose and BCD (equivalent to a 6.3:1.0 mole ratio) and of samples of the mixture irradiated for (b) 4, (c) 8, (d) 12, (e) 16 and (f) 20 hours.

12.9. The IR spectra of irradiated mixtures of TPH and BCD

Infrared spectroscopic studies of the original mixtures are reported in Sections 9 and 10. The infrared spectra of irradiated physical mixtures of TPH and BCD are compared with the spectra of the unirradiated mixtures in Figures 12.17 and 12.18.

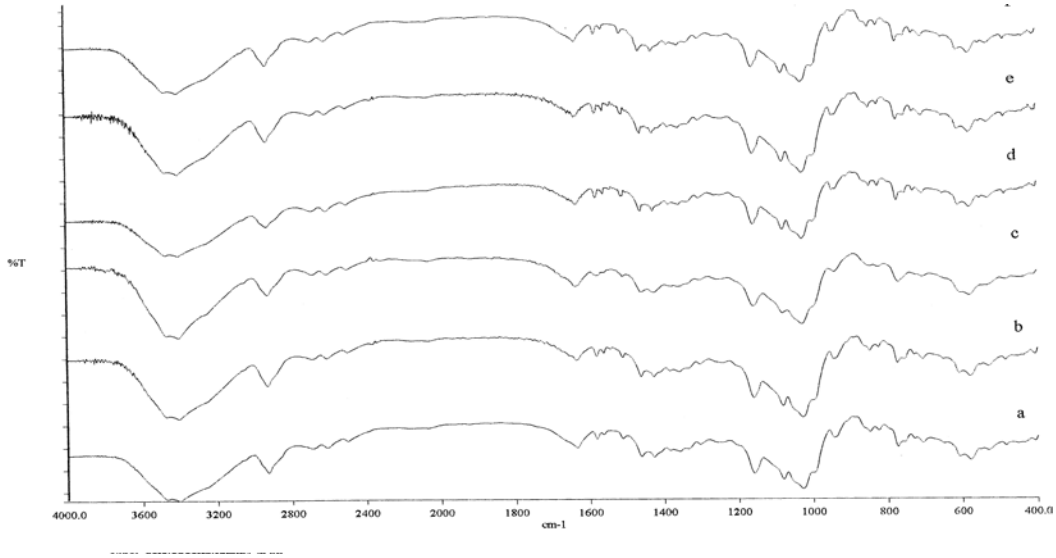

Figure 12.17 Infrared spectra of (a) a 1:1 mole ratio physical mixture of TPH and BCD and of samples of the mixture irradiated for (b) 4, (c) 8, (d) 12, (e) 16 and (f) 20 hours.

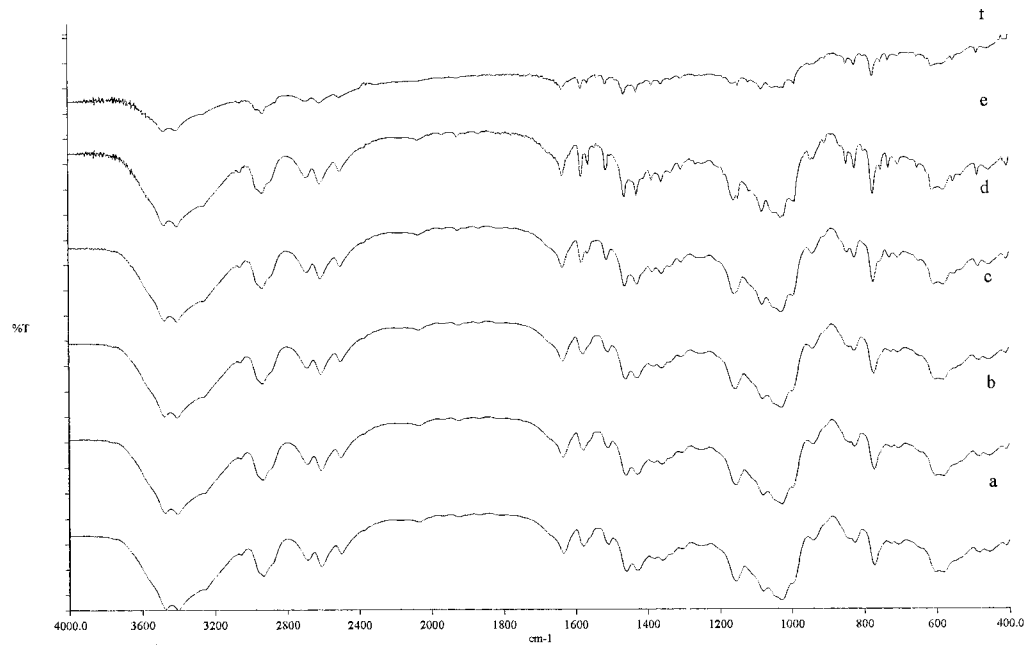

Figure 12.18 Infrared spectra of (a) a 1:1 mass ratio physical mixture of TPH and BCD (equivalent to a 3.4:1.0 mole ratio) and of samples of the mixture irradiated for (b) 4, (c) 8, (d) 12, (e) 16 and (f) 20 hours.

The results show broadening of bands and decreases in intensity, even disappearance of some IR bands, due to irradiation. The absorption bands at 3480 cm^{-1}, 1630 cm^{-1} and 776 cm^{-1} which are attributed to O-H stretching, C=C stretching and 1-substituted pyridine, respectively, decreased significantly after irradiation indicating that some degradation had taken place.

13. THE PHOTOSTABILITY OF TPH AND ITS MIXTURES WITH BCD AND WITH GLUCOSE IN AQUEOUS SOLUTION

13.1 Photostability studies

Aqueous solutions of TPH and of mixtures of TPH and BCD and of TPH and glucose were irradiated in clear glass ampoules and in dark brown ampoules covered with aluminium foil (as a control), under the same conditions as described in Section 4.3. The solution of TPH (0.01 mg ml^{-1}) was prepared as described in Section 4.3.2 and aqueous solutions of 1:1 mass ratio mixtures of TPH and BCD and of TPH and glucose were made up to a total concentration of 0.02 mg ml^{-1}.

An HPLC method, described and validated in Appendix A, was used to determine the amounts of TPH remaining after irradiation of the samples.

13.2 Photodegradation of an aqueous solution of TPH

The HPLC analysis results for the aqueous TPH solution (0.01 mg/ml) irradiated in clear and in "dark control" ampoules are shown in Table 13.1. In clear glass ampoules TPH shows some degradation and, after exposure for 20 hours, 84 % of the drug remained, while in the dark control ampoules degradation was less, with 93 % of the drug remaining after 20 hours exposure. This 7 % degradation may be attributed to thermal effects. These results are illustrated in Figure 13.1.

Table 13.1 HPLC analyses of samples of the aqueous TPH solution (0.01 mg/ml) irradiated for various times in clear ampoules and in "dark control" ampoules.

Irradiation time/hours	% drug remaining	Dark control %
0	100	100
4	97	99
8	96	96
12	93	95
16	87	94
20	84	93

A solution of the physical mixture of TPH and BCD shows 87 % TPH remaining, while physical mixture of TPH and glucose shows that glucose has increased decomposition of TPH (78 % TPH remaining).

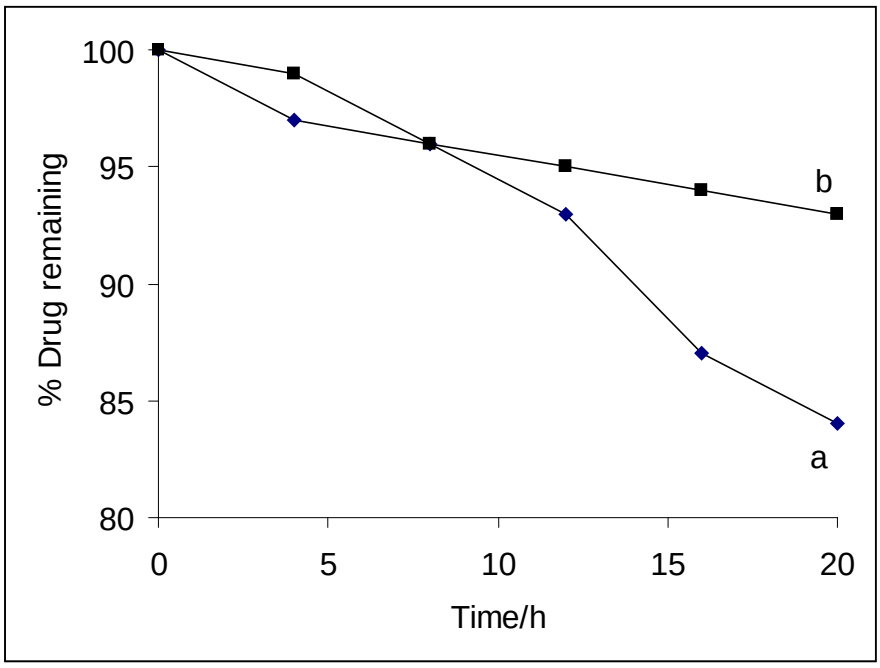

Figure 13.1 Photodegradation of an aqueous TPH solution (0.01 mg/ml) (a) after irradiation in clear glass ampoules and (b) under dark control conditions, using an Atlas Suntest lamp at 40 ^{o}C at 550 W m^{-2}, for the times indicated. (Note: the points are joined for clarity.)

13.3 Photodegradation of an aqueous mixture of TPH and BCD

Samples of an aqueous mixture of TPH and BCD were irradiated in clear ampoules in a similar manner to the solution of TPH alone. HPLC analysis of the mixture after irradiation for the times shown gave the results listed in Table 13.2 and illustrated in Figure 13.2. BCD does not seem to have a significant protective effect on the photodegradation of TPH.

Table 13.2 HPLC analysis of an aqueous mixture of TPH and BCD (0.02 mg/ml) irradiated for various times using clear ampoules compared with the results for TPH alone.

	TPH alone	TPH/BCD mixture
Irradiation time/hours	% drug remaining	% drug remaining
0	100	100
4	97	98
8	96	96
12	93	94
16	87	89
20	84	87

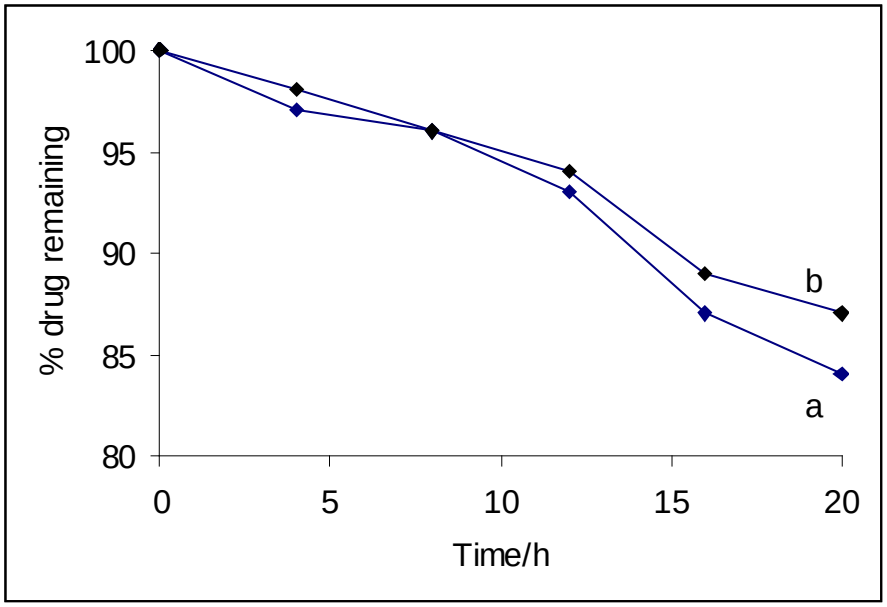

Figure 13.2 Photodegradation of (b) an aqueous mixture of TPH and BCD (0.02 mg/ml) after irradiation in clear ampoules, compared with (a) TPH alone (0.01 mg/ml), using an Atlas Suntest lamp at 40 ^{o}C at 550 W m^{-2}, for the times indicated. (Note: the points are joined for clarity.)

13.4 Photodegradation of an aqueous mixture of TPH and glucose

Similar irradiation experiments were done on an aqueous mixture of TPH and glucose. The results are listed in Table 13.3 and illustrated in Figure 13.3. There could be a slight accelerating effect of glucose on the photodegradation of TPH. Over longer times this might be more significant.

Table 13.3 HPLC analysis of an aqueous mixture of TPH and glucose (0.02 mg/ml) irradiated for various times in clear ampoules compared with the results for TPH alone.

	TPH alone	TPH/glucose mixture
Irradiation time /hours	% drug remaining	% drug remaining
0	100	100
4	97	97
8	96	92
12	93	90
16	87	86
20	84	78

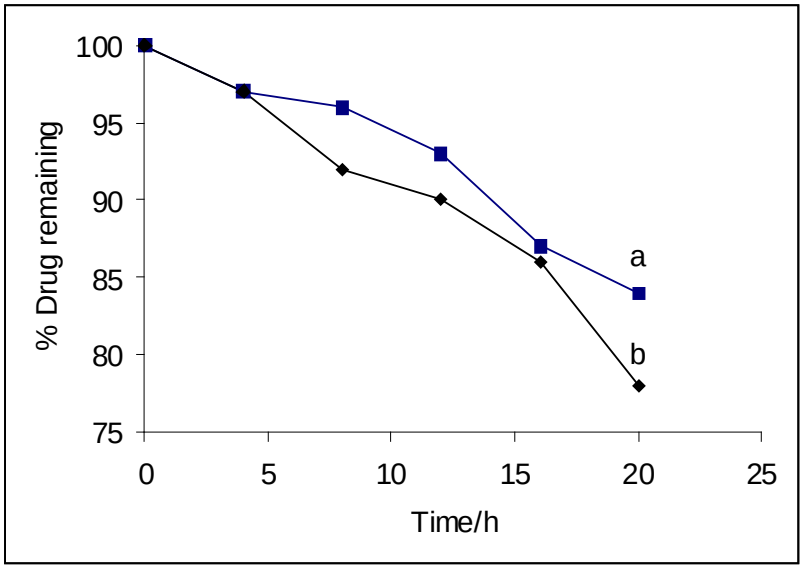

Figure 13.3 Photodegradation of (b) an aqueous mixture of TPH and glucose (0.02 mg/ml) after irradiation in clear ampoules, compared with (a) TPH alone (0.01 mg/ml), using an Atlas Suntest lamp at 40 ^{o}C at 550 W m^{-2}, for the times indicated. (Note: the points are joined for clarity.)

13.5. Conclusions

ICH guidelines [54] require that samples be exposed for not less than 1.2 million lux hours, with an integrated near ultraviolet energy of not less than 200 W h m^{-2}. In this study, ICH conditions are reached after 12 hours exposure with the percentage of TPH remaining being 93 % on its own and 94 % and 90 % in the presence of BCD and glucose, respectively, indicating a slight improvement in the photostability of TPH in combination with BCD. These results confirm that that TPH and the TPH/BCD mixture meet the TPH requirements for photostability testing, because the percentage of drug remaining is almost 95 % in these dilute solutions.

14. MOLECULAR MODELLING

14.1. Introduction

Molecular modelling was used to investigate the possible interactions, such as the formation of inclusion complexes where applicable, between TPH and BCD and between glucose and BCD.

{THERE MUST BE MORE DETAIL OF HOW AND WHAT YOU DID - e.g. PROGRAMS USED, METHODS WITHIN PROGRAMS, etc.)

Dynamics control was used to run the molecular modelling. The time step used was 0.0010 ps, at a required temperature of 300.00 K and 9000 steps were used. The total energy {EXPLAIN} was then recorded for each run.

14.2. Molecular structures

Figure 14.1 show the molecular structures of the E- and Z-isomers of triprolidine (HCl omitted). Figure 14.2 shows the molecular structures of glucose and beta-cyclodextrin.

{WHAT WAS DONE ABOUT THE HCl???}

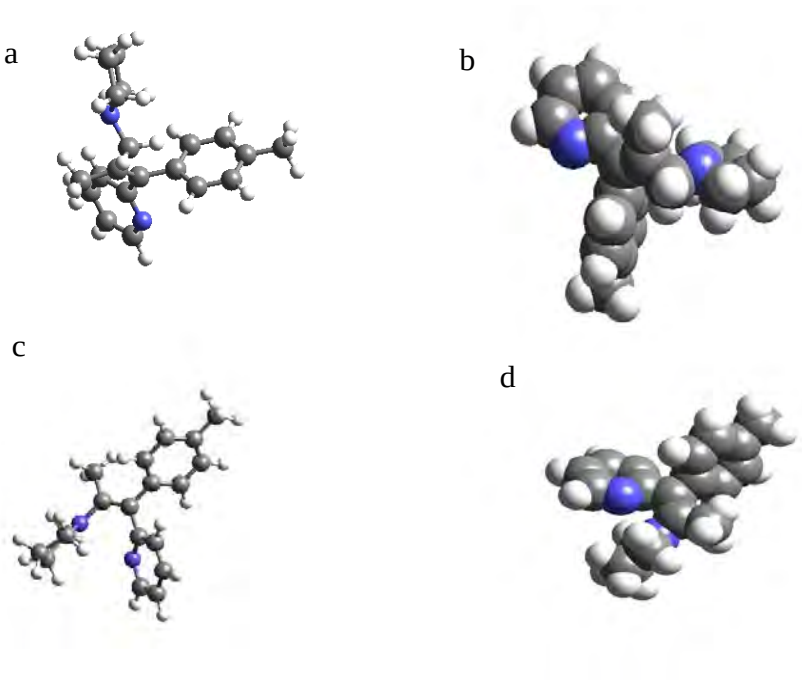

Figure 14.1 Molecular modelling of (a) and (b) the E-isomer of TPH, (c) and (d) the Z-isomer of TPH.

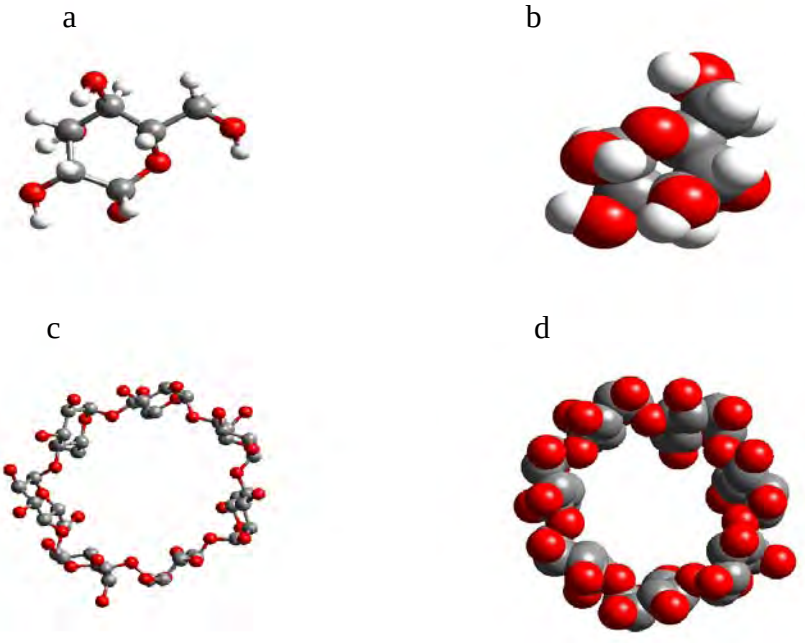

Figure 14.2 Molecular modelling of (a) and (b) glucose, (c) and (d) beta-cyclodextrin (BCD).

14.3. Possible inclusion complexes

Figure 14.3 shows the molecular structure of a possible inclusion complex of TPH and BCD, while Figure 14.4 shows a possible inclusion complex of glucose and BCD.

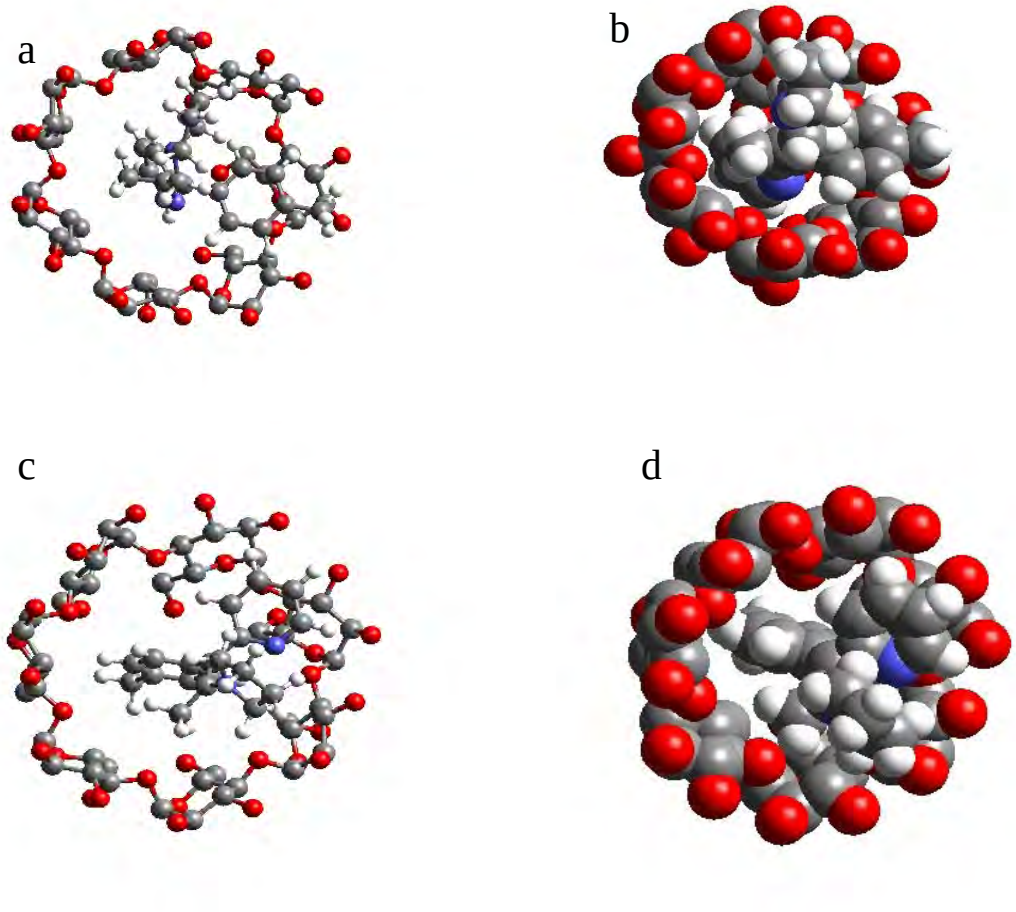

Figure 14.3 Molecular modelling (a) and (b) of possible inclusion of the E-isomer of TPH in the cavity of BCD, and (c) and (d) similar modelling of the possible inclusion of the Z-isomer of TPH in the BCD cavity.

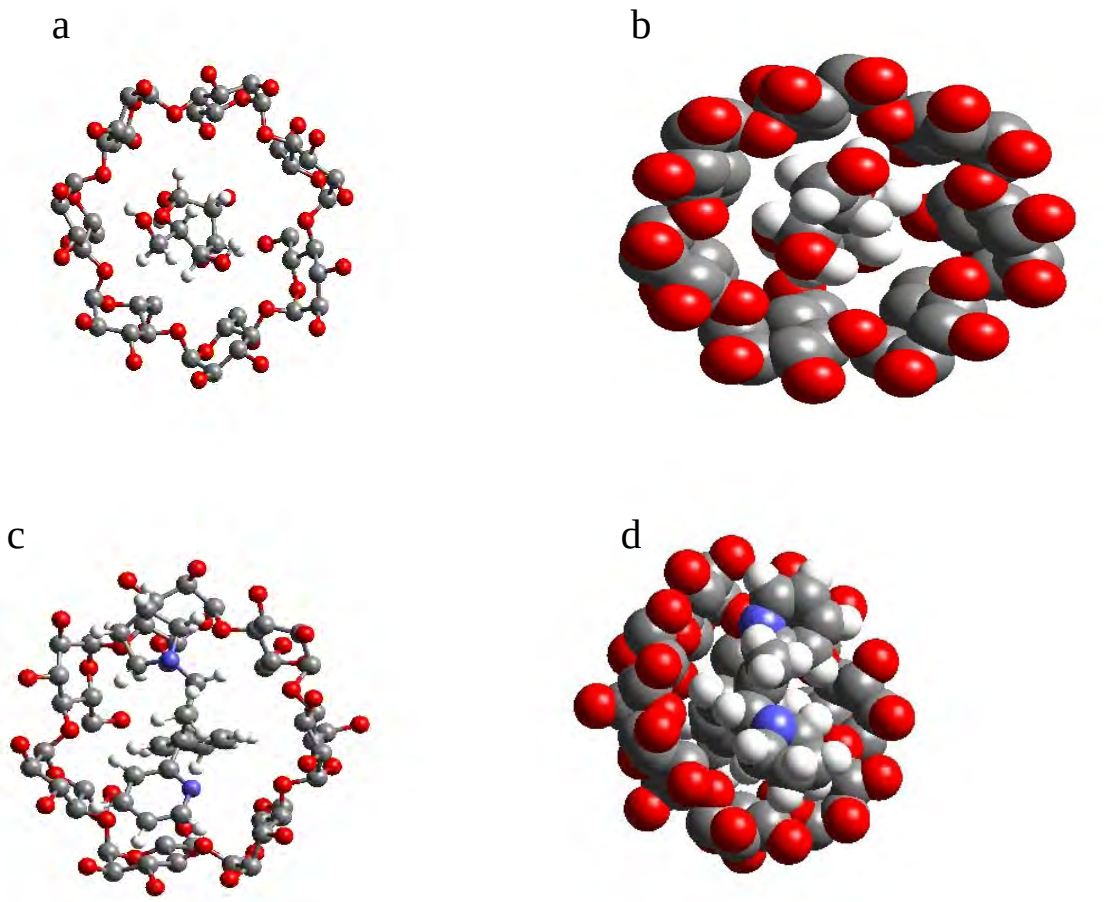

Figure 14.4 Molecular modelling (a) and (b) of a possible inclusion complex of glucose and BCD, (c) and (d) a possible inclusion complex of TPH and BCD.

{WHAT IS THE DIFFERENCE BETWEEN 14.4 (c) and (d) and 14.3 ????}

14. MOLECULAR MODELLING

14.1 Introduction

Molecular modelling was used in a very qualitative manner to investigate possible interactions, such as the formation of inclusion complexes, between TPH and BCD and between glucose and BCD.

Computer modelling is a powerful tool [55] and it has been especially valuable in examining the potential complexation of drugs with cyclodextrins. For example, Pose and his group [57] have modelled the interactions of sulfamethizole with β-cyclodextrin and the results indicate that the sulfamethizole group is able to enter the cavity of the cyclodextrin.

In this study, dynamics simulations were run using the Cerius2 software running on a Silicon Graphics O2 workstation. The starting conformer of the cyclodextrin used was obtained from the Cambridge Crystal Structure Database [40]. The neutral triprolidine (TP) molecule was investigated first. Minimized structures of TP were used in a variety of starting orientations at a starting distance of approximately 7 Å from the centre of the cyclodextrin. Upon simulation these provided a variety of conformations for each of the three situations in which the toluene, pyridine, or pyrrolidine groups were included in the cyclodextrin cavity.

The constant volume, constant energy equilibrium dynamics simulation was run at a temperature of 300 K for 10 000 steps, corresponding to a total simulation time of 10 ps. For each simulation, several of the lowest energy conformers obtained were examined and further minimized. Only the lowest energy conformers thus obtained were used for comparison. This provided three reasonable conformers corresponding to the three inclusion orientations.

The procedure was repeated with the protonated species (TPH^+) to obtain a further three possible inclusion complexes, and with glucose to obtain a single BCD-glucose inclusion complex.

14.2 Possible inclusion complex of glucose and BCD

Figure 14.1 shows the molecular structure of a possible inclusion complex of glucose and BCD. The glucose molecule fits well within the BCD cavity which corresponds to the results of previous work [56].

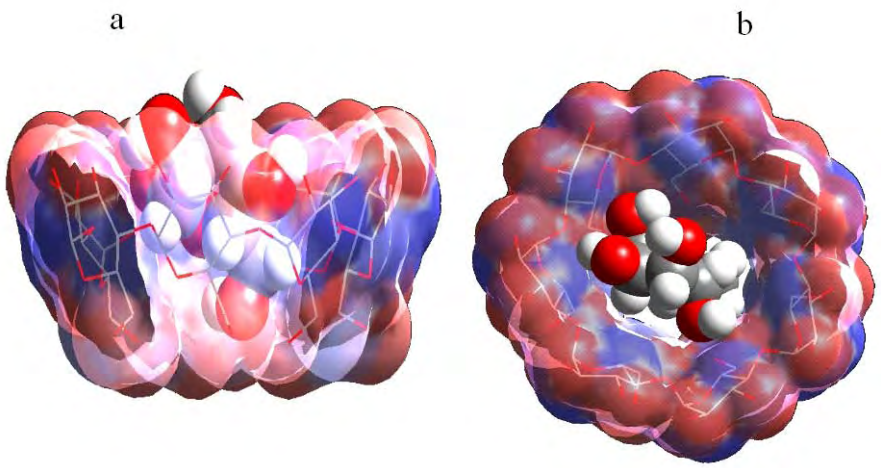

Figure 14.1 Molecular modelling of glucose-β-cyclodextrin complexation: (a) side view and (b) bottom view.

14.3. Possible inclusion complexes of TPH and BCD

Figures 14.2 and 14.3 show the molecular structure of a possible inclusion complex of the E-isomer of TPH with BCD. The initial modelling of the E-isomer of TPH was based on

the neutral triprolidine (TP) molecule and three different configurations were used for the approach of the TP molecule to the BCD cavity, namely with the pyridine, toluene or pyrrolidine groups entering first. The minimum total energies calculated were: pyridine first = 169.9 Kcal/mol; toluene first = 97.6 Kcal/mol, and pyrrolidine first = 99.4 Kcal/mol. Therefore, on the basis of modelling only, the toluene group is most likely to be readily accommodated in the BCD cavity. Attempts at modelling the approach of the E-isomer of the protonated TPH^+ molecule to the BCD cavity were also done in the three configurations. The minimum total energies calculated were, respectively, for pyridine, toluene and pyrrolidine first, 183.1, 182.1 and 181.5 Kcal/mol, which indicates that the presence of the proton hinders the inclusion of the E-isomer.

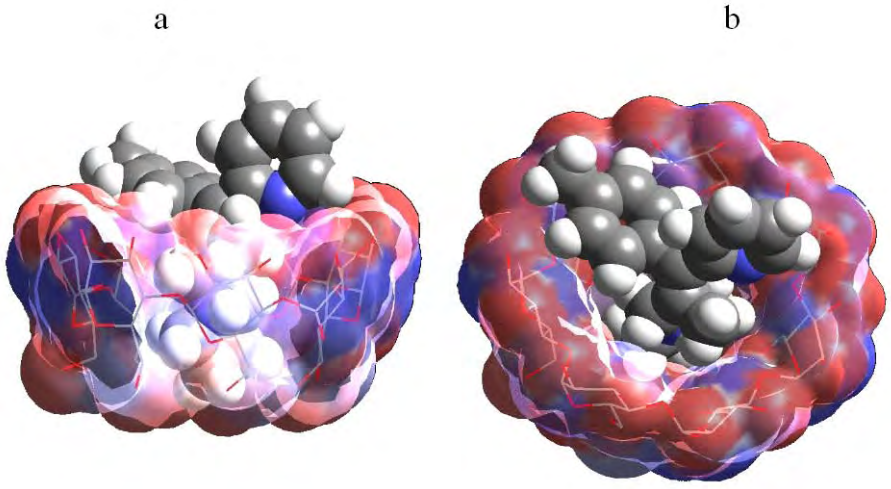

Figure 14.2 Molecular modelling of E-TP (pyrrolidine first)-β-cyclodextrin complexation (a) side view and (b) bottom view.

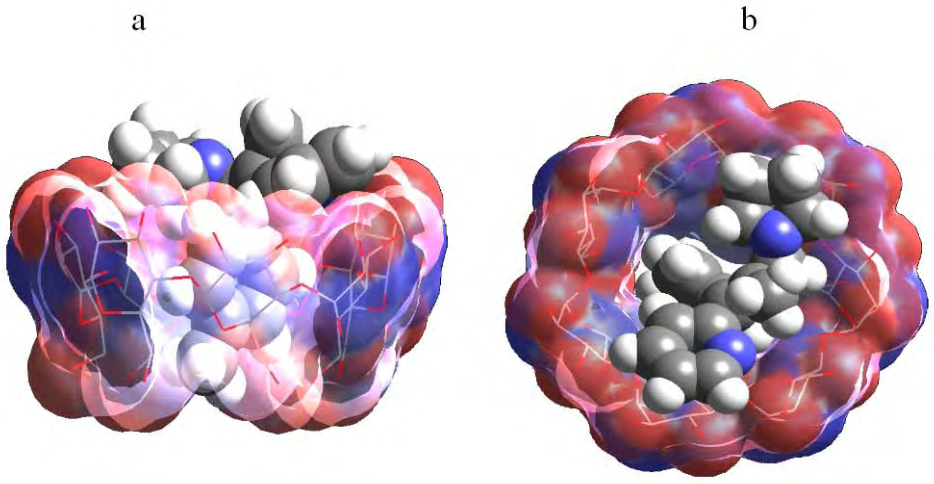

Figure 14.3 Molecular modelling of E-TP (toluene first)-β-cyclodextrin complexation (a) side view and (b) bottom view.

Figures 14.4 and 14.5 show similar modelling of the molecular structure of a possible inclusion complex of the Z-isomer of TP with BCD. The same three possible entry configurations: pyridine, toluene and pyrrolidine gave minimum total energies of: pyridine first = 96.1 Kcal/mol; toluene first = 95.2 Kcal/mol, and pyrrolidine first = 97.0 Kcal/mol. Again modelling shows that the toluene group is the most readily accommodated. The minimum total energies calculated for inclusion of the protonated Z-isomer of TPH^+ with HCl in the BCD cavity were, for pyridine, toluene and pyrrolidine first, respectively, 176.3, 173.9 and 174.8 Kcal/mol. Again, the presence of the proton hinders inclusion. The results suggest a slightly better inclusion for the Z-isomer in which the toluene group is included in the cavity of BCD than for the E-isomer in a similar configuration.

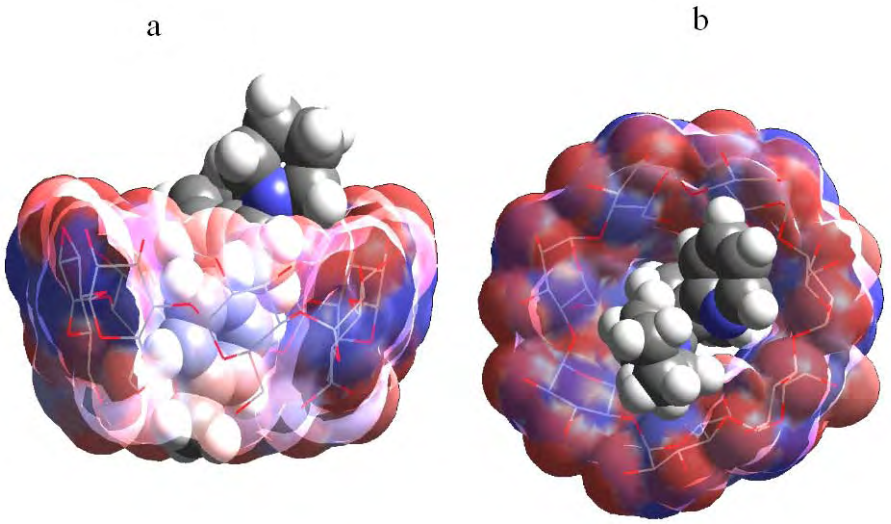

Figure 14.4 Molecular modelling of Z-TP (toluene first)-β-cyclodextrin complexation (a) side view and (b) bottom view.

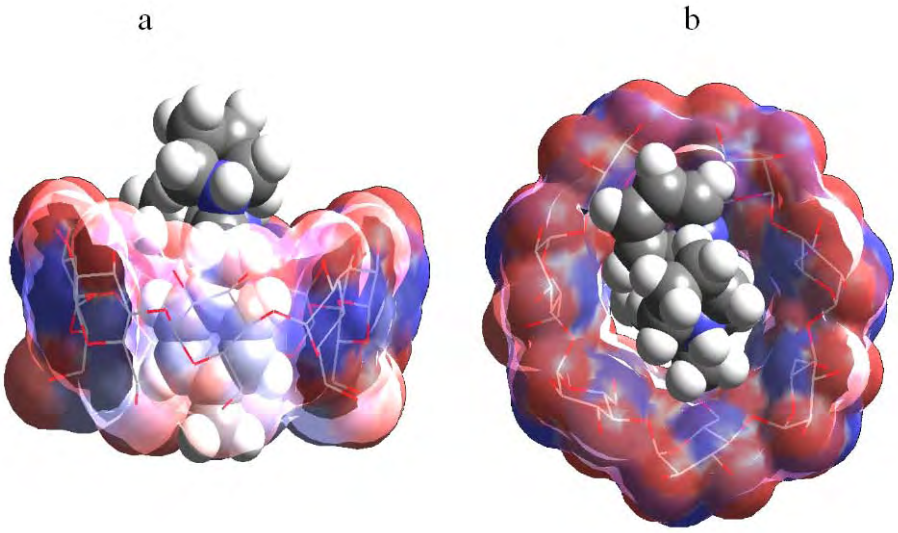

Figure 14.5 Molecular modelling of Z-TPH$^+$ (toluene first)-β-cyclodextrin complexation (a) side view and (b) bottom view.

14.4. Conclusions

Molecular modelling can only indicate which molecular configurations are most likely on the basis of potential energies and which configurations are highly unlikely. Other methods, such as spectroscopy and X-ray crystallography, are needed to determine whether such configurations actually occur. The results obtained here suggest that the neutral triprolidine molecule is most likely to be accommodated in the BCD cavity with the toluene portion of the molecule entering first. There is also an indication that the Z-isomer should be accommodated slightly more readily than the E-isomer. Protonation of triprolidine makes inclusion less favourable.

15. CONCLUSIONS

15.1. The thermal stability of triprolidine hydrochloride (TPH)

The DSC curves for TPH, using a sealed pressure pan, show a sharp melting endotherm at 122-123 ^{o}C which corresponds to the literature value of the melting point and a broad exotherm between 195 and 240 ^{o}C. The type of sample pan used affects the curves obtained. Heating to just beyond the melting point (125 ^{o}C), followed by cooling and reheating, showed that the melting transition is not readily reversible and may be accompanied by decomposition.

The TG curves for TPH show multi-step loss of components. The major mass-loss to a residue of about 20 % of the original mass of dried TPH by 400 ^{o}C occurs in two overlapping stages. The onset of the first stage of the major mass-loss occurs soon after the melting endotherm on the corresponding DSC curve. The mass-loss may be a combination of evaporation and decomposition of the liquid. By use of TG–FTIR, evolution of HCl from TPH was detected between 150 and 350 ^{o}C, which is the temperature range of the overall mass loss in the TG curve. For carefully dried TPH, formation of HCl gas was shown to occur between 220 and 260 ^{o}C, which corresponds to the second stage of mass-loss in the TG curve

Hot-stage microscopy of TPH showed that some melting is visible at temperatures as low as 82-84 ^{o}C and that evolution of some trapped gas occurs through the liquid surface.

TPH is thus reasonably stable to thermal degradation and protection from water vapour enhances the stability.

15.2. Thermal behaviour of. beta-cyclodextrin (BCD)

The DSC curves for BCD show a broad dehydration endotherm between 65 and 110 ^{o}C and a small exotherm at 220 ^{o}C which is not accompanied by a mass-loss. The TG curves show that the original BCD contains 12.5 % water which is lost in a single step.

BCD dried over P_2O_5 shows no dehydration endotherm. Re-exposure to water vapour results in regaining of 10 % water. Degradation of BCD occurs above 300 ^oC.

15.3. The thermal behaviour of glucose

The DSC curve for glucose shows a sharp melting endotherm with onset 158 ^oC. Glucose adsorbs water during exposure to water vapour and this is lost in a broad endothermic process between 50 and 100 ^oC.

15.4. The thermal behaviour of physical mixtures

15.4.1. TPH/BCD

The endotherm associated with the melting of TPH disappears almost completely in the DSC curves of the physical mixtures. The dehydration endotherm of BCD is also decreased significantly.

Disappearance of the melting endotherm for the drug, in the DSC curves for drug/cyclodextrin mixtures, is generally regarded as an indication that the drug may have been included in the CD cavity [57], although other explanations are possible, such as that the drug has been converted to an amorphous form in the presence of the cyclodextrin [56, 57]. The possibility of inclusion is supported by X-ray powder diffraction results in Section 9 and molecular modelling in Section 14. The results of molecular modelling suggest that TPH is most likely to be accommodated in the BCD cavity as a neutral TP molecule, with the toluene portion of the molecule entering first. There is also an indication that the Z-isomer should be accommodated slightly more readily than the E-isomer.

There is some indication that the presence of water facilitates the inclusion of TPH in the BCD cavity.

The two stages of mass-loss seen in the TG curves for the mixtures correspond to the decomposition of BCD followed by decomposition of the TPH at higher temperatures.

15.4.2. TPH/glucose

The DSC curves for the physical mixtures of TPH and glucose show considerable lowering of the onset temperature of melting of TPH in the presence of glucose.

15.4.3. Glucose/BCD

The DSC curves for mixtures of glucose and BCD show the features of the pure samples, although the glucose melting endotherm shows slight broadening. The lack of significant changes indicates little if any interaction between glucose and BCD in the solid state. These results are supported by XRD in Section 9 and IR in Section 10. Molecular modelling in Section 14 suggests that glucose could be included in the BCD cavity. Molecular modelling is really only of use in indicating molecules whose size or steric factors make it virtually impossible for the molecule to be accommodated in the cyclodextrin cavity. Even then there are possible ways in which different parts of a large molecule can be included in the cavities of a cluster of CD molecules. The fact that the size and shape of a molecule are suitable for inclusion in a CD cavity does not imply that such inclusion will actually occur.

15.5. X-ray diffraction patterns of TPH and its mixtures with BCD and glucose

TPH, BCD and glucose all have distinctive crystalline X-ray powder diffraction patterns. Dehydration of BCD produced a much less-crystalline material but this crystallinity is considerably restored on re-exposure of the dehydrated BCD to water vapour.

The patterns of the physical mixtures of TPH and BCD are distinctly different from the pure components but still indicate significant crystallinity. These results support the possible formation of an inclusion complex on physical mixing of TPH and BCD.

The patterns of the physical mixtures of TPH and glucose also differ from those of the individual components. Some features of the glucose pattern, but not the more intense peaks of the TPH pattern, are evident in the patterns of the mixtures. Studies of the thermal behaviour indicate an interaction of some kind, but obviously not the cyclodextrin-type of inclusion, between TPH and glucose.

The patterns of the physical mixtures of glucose and BCD are not all that different from a combination of the patterns of the components. Thermal studies also do not give a strong indication that glucose is included in the BCD cavity.

15.6. Infrared spectroscopic studies of TPH and its mixtures with BCD and glucose

FTIR spectroscopy has been used [49, 50] to assess the interaction between guest and cyclodextrin molecules in the solid-state. The characteristic absorption bands of cyclodextrins are often only affected (shifts, reductions or broadening in intensity [45, 46]) by inclusion complexation if the mass of the included drug component is greater than about 25 % of the complex. Changes in the absorption bands of the drug will usually be obscured by the spectrum of the host CD.

The most noticeable changes seen in the spectra of TPH/BCD mixtures involve the water absorptions in the BCD spectrum, suggesting either the possible replacement of water in the BCD cavity by TPH, or interaction between the HCl fragment of TPH and water from the BCD.

The IR spectra of mixtures of TPH and glucose and of glucose and BCD do not provide much information.

15.7. Solid-state photostability studies

An HPLC method was developed and validated for the quantitation of TPH and this was used to measure the extent of degradation of TPH in the solid state, in aqueous solution and in physical and in aqueous mixtures with BCD and with glucose.

In the solid state, the amount of degradation under the conditions of irradiation used (Atlas Suntest lamp at 40 ^{o}C at 550 W m^{-2}) reslted in about 10 % degradation after an exposure of 20 hours. Some of the degradation may be of thermal origin as indicated by the dark control reults.

DSC studies were not sensitive enough to provide reliable information on any degradation of TPH that may have occurred during irradiation under the specified conditions. X-ray powder diffraction patterns were altered by irradiation, but the sequence of patterns with increasing irradiation dose did not show systematic changes in particular diffraction lines. This could indicate a complex solid-state degradation process or the difficulty of obtaining a representative sample after irradiation of the solid. The X-ray powder diffraction patterns of BCD and of glucose showed very much smaller changes during irradiation and these changes may have been caused by the temperature effects as shown by the dark control results.

The infrared spectra of samples of irradiated TPH showed significant decreases of absorption bands after irradiation. Similar treatment of samples of BCD and of glucose produced minimal changes in the FTIR spectra with irradiation dose.

No systematic changes in thermal behaviour were observable from the DSC curves of physical mixtures of TPH and BCD after irradiation. The variations seen could be due to the problems of representative sampling of solid mixtures, particularly after irradiation when surfaces have received the greatest dose. A more quantitative comparison shows a general increase in onset temperature of melting and a decrease in enthalpy of melting even at the lowest irradiation doses.

The changes detectable by thermal studies of irradiated physical mixtures of TPH and glucose and of glucose and BCD were minimal.

Physical mixing of TPH and BCD produces a compound with a different, less-crystalline structure than that of either TPH or BCD. This diffraction pattern changes with irradiation dose, with the appearance and disappearance of peaks indicating significant but complex changes in crystal structure caused by irradiation. At the highest doses there is an indication of some deterioration in crystallinity.

The X-ray powder diffraction patterns of irradiated mixtures of TPH and glucose also indicated changes in crystal structure, although the intense peak of glucose is still evident in the irradiated mixtures. The changes increase with increasing time of irradiation.

Changes in the X-ray powder diffraction patterns of irradiated physical mixtures of glucose and BCD are not very marked.

The FTIR spectra of irradiated physical mixtures of TPH and BCD show broadening of bands and decreases in intensity, even disappearance of some IR bands, due to irradiation. These changes indicate that some degradation has taken place during irradiation.

15.8. The photostability of TPH and its mixtures with BCD and with glucose in aqueous solution

HPLC analysis of samples of an aqueous TPH solution (0.01 mg/ml) irradiated in clear ampoules showed that, after exposure under the specified conditions for 20 hours, 84 % of the drug remained compared with 93 % of the drug remaining in the dark control samples. From similar measurements on irradiated aqueous solutions of TPH and BCD, and of TPH and glucose, no significant protective effect of BCD on the photodegradation of TPH in aqueous solution was observed, but there could be a slight accelerating effect of glucose on the photodegradation of TPH.

TPH in aqueous solution is thus sensitive to irradiation, but under normal light photodegradation will be very slow and could be further hindered by use of amber ampoules.

15.9. General

The above results illustrate the stability of TPH, especially in the solid state. Although the potential for isomerization to the pharmaceutically inactive Z-isomer exists, these findings have shown that this transformation would require extreme light conditions. The study has also shown TPH to be compatible with both glucose and BCD, which are potential excipients both in solid and liquid dosage forms. The presence of these excipients in dosage forms will thus not adversely affect the stability and the therapeutic efficacy of TPH.

REFERENCES

1. British Pharmacopoeia, 1 (1998) 1334-1335.
2. United States Pharmacopoeia, 23 (1994) 1605-1607
3. British Pharmaceutical Codex, (1963) 867-868.
4. A. S. Benezra and Chen-Hwa Yang, Analytical Profiles Of Drug Substances, 8 (1979) 509-528.
5. A.F Casy, C. R Ganellin, A.D Mercer and C. Upton, J. Pharm. Pharmacol., 44 (1992) 791-795.
6. C.O. Wilson, O.G. Gisvaldo and R.F. Doerge, Textbook of Organic Medicinal and Pharmaceutical Chemistry, Raven-Lippincott, Philadelphia, 7th Edn, 1977, Chapter 18.
7. F.H. Metwally, J. Pharm. Biomed. Anal., 26 (2001) 265-272.
8. E. B Hansen, Jr., R. H Heflich, W. A Korfmacher, D.W Miller and C. E Cerniglia, J. Pharm. Sci., 77 (1988) 259-264.
9. R. L DeAngelis, M.F Kearney and R. M Welch, J. Pharm. Sci., 66 (1977) 841-843.
10. Sang-Chul Shin and Mi-Kyoung Yoon, Int. J. Pharm., 232 (2002) 131-137.
11. J.N. Delgado and W.A. Remers, Texbook of Organic Medicinal and Pharmaceutical Chemistry, J.B. Lippincott Co., Philadelphia, 9th Edn, 1991, pp.603-626.
12. H. van der Goot and H. Timmerman, Eur. J. Med. Chem., 35 (2000) 5-20.
13. R.R. Ison, F. M. Franks and K.S Soh, J. Pharm. Pharmacol., 25 (1973) 887-890.
14. E.G.C Clarke, Isolation and Identification of Drugs, The Pharmaceutical Press, London, 1975, p.588.
15. F. Giodarno, C. Novak, and J. Ramón Moyano, Thermochim. Acta., 380 (2001) 123-151.
16. D. Duchêne and D. Wouessidjewe, Drug Dev. Ind. Pharm., 16 (1990) 2487-2499.
17. J. Szejli, Comprehensive Supramolecular Chemistry, Ed. J.L. Atwood, Vol. 3, Pergamon, New York, 1996, Chapter 5.
18. J. Snopek, E. Smolková-Keulemansová, J. Cserháti, K.H. Gahm and A. Stalcup, Comprehensive Supramolecular Chemistry, Ed. J.L. Atwood, Pergamon, New York, 1996, Vol. 3, Chapter 18.

19. P.J. Crowley, Pharm. Sci. Technol. Today, 2 (1999) 237-243.
20. http://www.environment.google/triprolidine-stability.htm, Stability of triprolidine hydrochloride in liquid dosage form, 1997
21. V. Rhodes, Chiral Pharmaceuticals, Chimicaoggi, 20(10) (2002) p37-39
22. J. Tomaszewski and M. M Rumore, Drug Dev. Ind. Pharm., 20 (1994)119-139.
23. K. K. Midha, G. Mckay, M. J. Rawson and J. W. Hubbard, J. Pharm. Sci., 87 (1998) 797-802.
24. United States Pharmacopoeia, 25 (2002) 1772-1773.
25. S. Yoshioka and M. Uchiyama, J. Pharm. Sci., 75 (1986) 92-96.
26. R.C. Mackenzie, Differential Thermal Analysis, Vol. 2, Academic Press, London and New York, 1972, pp.453-470.
27. M.J. Arias, J.R. Moyano and J.M. Gines, Thermochim. Acta, 321 (1998) 33-41.
28. M. Worthington, Pharmaceutical Research Laboratories, South Africa, private communication.
29. H. Kitaoka and K. Ohya, J. Therm. Anal., 40 (1993)387-394.
30. M.M. Meier, M.T.B Luiz, B. Szpoganicz and V. Soldi, Thermochim. Acta., 375 (2001) 153-160.
31. A. Bayomi Mohsen, A. A Khalid and Al-Angary Abdulaziz, Int. J. Pharm, 243 (2002) 107-117.
32. Nianbing Li, Hongqun Luo, Sharopu Liu and Guonan Chen, Spectrochim. Acta, Part A, 58 (2002) 502-507.
33. R. Ficarra, S. Tommasini, D. Raneri, M. L Calabro, M. R DiBella, C. Rustichelli, M. C. Gamberi and P. Ficarra, J. Pharm. Biomed. Anal., 29 (2002) 1005-1014.
34. T. Utsuki, K. Imamura, F. Hirayama and K. Uekama, Eur. J. Pharm. Sci., 1 (1993) 81- 87.
35. A. Li Wan Po and W. J Irwin, J. Pharm. Pharmacol., 32 (1980) 25-29.
36. J.M. Moreno-Cerezo, M. Co′rdoba-Diaz and D. Co′rdoba-Borrego, J. Pharm. Biomed. Anal., 26 (2001) 417-426.
37. F. Hirayama, T. Utsuki, K. Uekama, M. Yamsaki and K. Harata, J. Pharm. Sci., 81 (1992) 817-822.
38. A. Lukta, Acta Poloniae Pharmaceutica, 59 (2002) 45.

39. J. Mielcarek and E. Daczkowska, J. Pharm. Biomed. Anal., 21 (1999) 393-398
40. The Cambridge Structural Database, the Cambridge Crystallographic Data Centre, Cambridge, UK, Structural reference code (TPROLC).
41. R.H. Pierson, A.N. Fletcher, Anal. Chem., 28 (1956) 1230.
42. M.E. Brown, B.D. Glass and M.S. Worthington, J. Therm. Anal. Calorim., 68 (2002) 631-646.
43. G. Bettinetti, A. Gazzaniga, P. Mura Giodano and M. Setti, Drug Dev. Ind. Pharm., 18 (1992) 39-53.
44. Y. Nakai, K. Yamamoto, T. Oguchi, E. Yonemochi, T. Hanawa, Chem. Pharm. Bull., 38 (1990) 1345-1348.
45. A. Abdel Rahman, S. I. Saleh, Y. Nakai, A.E. Aboutaleb and M.O. Ahmed, Eur. J. Pharm. Biopharm., 39 (1993) 82-86.
46. British Pharmacopoeia, 3 (1993) 689-690.
47. A. Farcas, Analele Stiintifice ale Universitatii “Al.I.Cuza” Iasi, Vol. XLV-XLVI, s. Fizica Starii Condensate, (1999-2000) 217-223.
48. O. Bekers, E.V. Uijtendaal, J.H. Beijnen, A. Bult, W.J.M. Underberg, Drug Dev. Ind. Pharm., 17 (1991) 1503-1549.
49. B.W. Muller and E. Albers, Int. J. Pharm., 79 (1992) 273-280.
50. Lin S.-Y Kao Y.-H, Int. J. Pharm., 56 (1989) 249-259.
51. G.A. El-Gendy, M. El-Gendy, Eur. J. Pharm. Biopharm., 39 (1993) 249-254.
52. I.-K. Chun, D.-S. Yun, Int.J. Pharm. 96 (1993) 91-103.
53. K. Uekama, S. Narisawa, F. Hirayama, M. Otagiri, Int. J. Pharm., 16 (1983) 327-338.
54. International Conference on Harmonisation (ICH), Photostability testing of new drug substances and products, ICH Committee, 1996, 1-7.
55. Jun-Jen Chen, MSc.Thesis, Rhodes University, 2000, p179-180.
56. W. Hirsch, T. Muller, R. Pizer and P.J. Ricatto, Can. J. Chem., 73 (1995) 12-15.
57. B. Pose-Vilarnavo, I. Perdamo-Lo′pez, M. Echezarreta- Lo′pez, P. Schroth-Pardo, E. Estrada and J.J. Torres-Labandeira, Eur. J. Pharm. Sci., 13 (2001) 328.
58. E. Katz, (ed.), Quantitative Analysis Using Chromatographic Techniques, John Wiley and Sons, New York, 1988, pp31-98.

59. D.R. Jenke, J. Liq.Chrom.Rel. Technol., 19 (1996) 1873-1891.
60. United State Pharmacopeia, 23 (1995) 1982-1983.
61. C.P. Tonseth and J. Dohl, Guidelines for Validation of Analytical Methods, Analytical Sciences R&D, Nycomed Imaging, 1st Edn, 1993, pp.35-57.
62. A.R. Buick, M.V. Doig, S.C. Jeal, G.S. Land and R.D. McDowall, J. Pharm. Biomed. Anal., 8 (1990) 629-637.
63. International Conference on Harmonisation (ICH), Validation of Analytical Methods, (1994) p1-5.
64. T.D. Wilson, J. Pharm. Biomed. Anal., 8 (1990) 389-400.
65. CDER (Center for Drug Evaluation and research); Review Guidance: Validation of Chromatographic Methods, (1994), CMC 1-30.
66. B.L Hogan, M. Williams, A. Iduculla, T. Veysoglu and E. Parente, J. Pharm. Anal., 23 (2000) 637-651.
67. G. S Clarke, J. Pharm. Biomed. Anal., 12 (1994) 648-652.
68. A.S.L. Mendez, M. Steppe and E.E.S. Schapval, J. Pharm. Biomed, (2003) 1-8.
69. L. Baur, H. Jehle and H. Wätzig, J. Pharm. Biomed. Anal., 22 (2000) 433-449.
70. R.L. Lundblad, Biotechnol.Appl. Biochem., 34 (2001) 1-3.

APPENDIX A

HPLC METHOD DEVELOPMENT AND VALIDATION

A1. Introduction

High Performance Liquid Chromatography (HPLC) is a powerful analytical technique because of its unique capability to separate complex mixtures [58]. A stability-indicating assay is established once the parent drug can be separated from all potential degradation products and excipients [59]. In this study, the HPLC method for TPH [60] has been validated to quantitate TPH in the presence of potential impurities, degradants (isomerization) and excipients (glucose and BCD). Some method development in terms of manipulation of the solvent ratios has been undertaken to illustrate that the USP method in this case is optimum.

A2. Method development

A2.1. Mobile phase

The mobile phases used were: (A) 15% of aqueous 52 mM ammonium acetate and 85% of 95% ethanol according to the USP method [60]. (This mobile phase was prepared by weighing accurately 0.24 g of ammonium acetate and dissolving this in 60 ml of water and 340 ml of absolute ethanol.) The effect on peak retention time was investigated by varying the solvent ratios. (B) 10% of 52 mM ammonium acetate and 90% of 95% ethanol. (C) 20% of 52 mM ammonium acetate and 80% of 95% ethanol. The retention times for TPH were: (A) 4.683 min (B) 4.681 min and (C) 4.686 min.

A2.2. Equipment

The modular HPLC system consisted of a Spectraseries P 100 isocratic solvent pump (Spectra Physics, USA), a M7125 20 :l fixed-loop injector (Rheodyne Inc., CA, USA), a 100 :l HPLC syringe (Hamilton Company, Reno, USA) a Lambda-Max M481 variable wavelength UV detector (Waters Assoc., Milford, MA, USA) and a Rikadenki flat-bed chart recorder (Kogyo Co. Ltd, Tokyo, Japan).

A2.3. Preparation of a stock solution of TPH

A stock solution containing 100 mg of triprolidine hydrochloride per 100 ml of 50/50 % ethanol and water was prepared to make up a final concentration of 0.01 mg/ml.

A2.4. Final chromatographic conditions

Mobile phase	15 % by volume of aqueous 52 mM ammonium acetate (pH 7.2) and 85 % of ethanol (95%)
Flow rate	1.0 ml/minute
Column	Novapak® Silica steel cartridge column (15 cm x 3.9 mm i.d., 4 :m particle size
Column temperature	Ambient
Detector setting	254 nm ; 2.0 AUFS
Chart speed	1 cm/minute

A3. Validation

Validation is a process of proving a method acceptable for its intended analytical application [61]. The analytical performance parameters used for validation [62] are: accuracy, linearity, specificity, range, limit of detection, limit of quantification and robustness.

A4. Accuracy

The accuracy of an analytical procedure expresses the closeness of agreement between the value obtained in the analysis and the accepted or true value [63] and is performed across a specified range which is recommended at 80 to 120 % of the label claim for an active drug substance or drug product [64]. The result can also be expressed as a percentage recovery [61] and should be between 98 and 102 % of the theoretical value [65]. A plot of of the recovered versus the known concentration should also have a slope of 1.00, an intercept of 0.00 and a correlation coefficient of 1.00 [68]. The accuracy of the triprolidine hydrochloride (TPH) determination by the HPLC method was tested by addition of known TPH concentrations of 0.008, 0.01 and 0.012 mg ml^{-1}, obtained by dilution of a stock solution with 50:50 ethanol and water. Each sample

was injected in triplicate and the concentration calculated using the following equation [69]:

$C_{spl} = C_{std} \times h_{spl}/h_{std}$

where C = concentration, h = peak height, spl = sample, and std = standard.

The results shown in Table A1 confirm the method to be accurate at 100 % recovery. A plot of the mean value of the drug recovered versus the known concentration (Figure A1) resulted in a correlation coefficient of 0.998, a slope of 0.959 and an intercept of 0.032, confirming the method to be accurate.

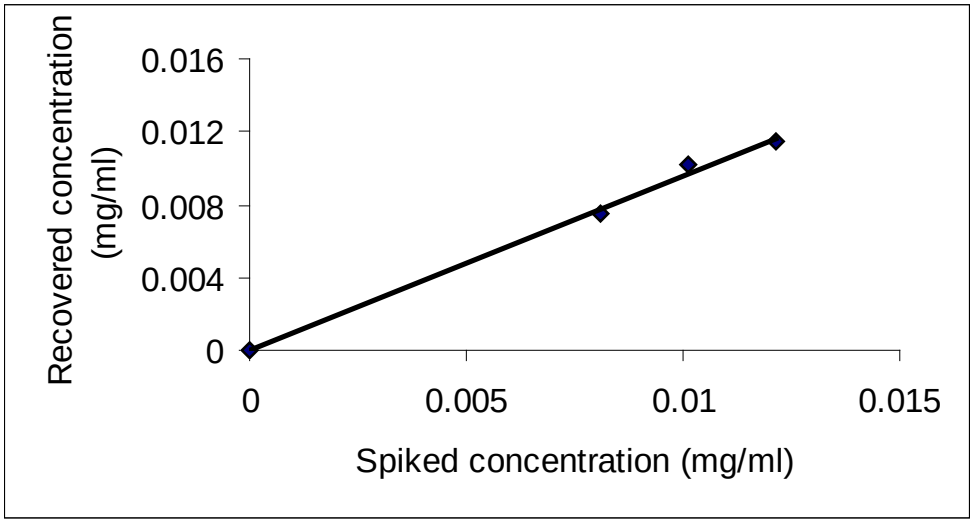

Figure A1. Recovered concentration of TPH plotted against spiked concentration.

Table A1. Accuracy of the HPLC method for the analysis of TPH.

Recovery level	Spiked concentration /mg ml^{-1}	Recovered concentration /mg ml^{-1}	% Recovery
80 %	0.00800 0.00808 0.00824	0.00739 0.00746 0.00767	93.0 92.3 93.1 Average = 93
100 %	0.0100 0.0101 0.0103	0.0100 0.0101 0.0103	100.0 100.0 100.0 Average = 100
120 %	0.01200 0.01212 0.01236	0.0113 0.0115 0.01165	94.2 95.0 94.3 Average = 95

A5. Linearity

The linearity of an analytical procedure is a test of the direct proportionality of the analytical response to the concentration (amount) of analyte in the sample within a given range [60]. It is expressed in terms of the variance of the slope of the regression line. It is recommended [66] that linearity should be assessed using at least six concentration levels and that the regression coefficient should be > 0.985 [66]. Linearity is often determined [67] over the range of 50 – 150 % of the expected level. The stock solution of TPH was diluted with ethanol/water to give a range of concentrations from 0.02 to 0.014 mg ml^{-1}. Each solution was injected 3 times and the peak heights of the TPH response were then measured. The results are given in Table

A2. A calibration curve for TPH was then constructed by plotting the mean peak height of the three injections versus the concentration in mg ml^{-1} (Figure A2). The correlation coefficient was found to be 0.998, showing that the method is linear and that Beer's law is obeyed [68]. The slope, needed for the calculation of the LOQ (see below) was 1.29×10^4 mm ml/mg).

Table A2. Calibration of the HPLC method

TPH concentration mg/ml	Measured peak height /mm
0	0
0.002	28
0.004	48
0.006	77
0.008	99
0.010	134
0.012	154

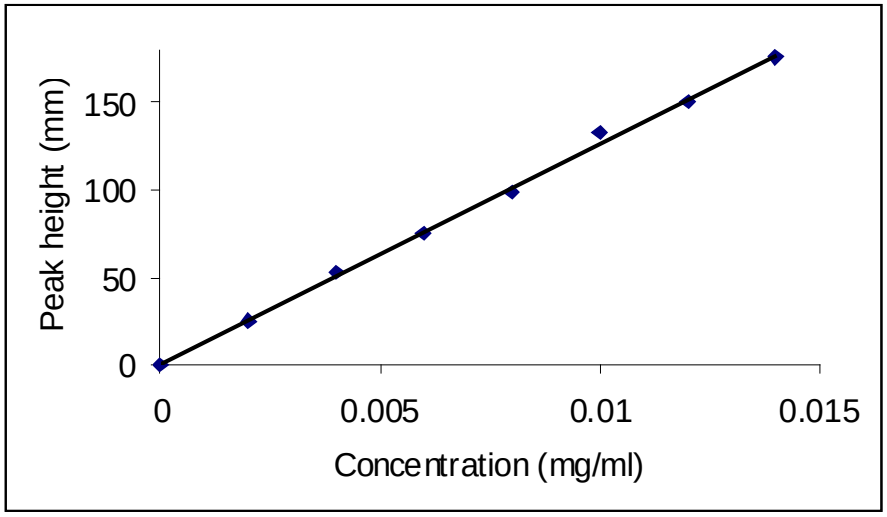

Figure A2. Calibration curve for testing the linearity of the HPLC method (the slope is 1.29 x 10^4 mm ml/mg).

A.6. Precision

The precision of an analytical procedure expresses the closeness of agreement amongst a series of measurements obtained from multiple sampling of the sample under the prescribed conditions [60]. There are various levels at which precision can be assessed, for example, under the same operating conditions over a short period of time (repeatability); and comparison of results obtained on different days by different analysts and/or different equipment (reproducibility) [69]. The repeatability and reproducibility of TPH analyses using the HPLC method are shown in Tables A3 and A4.

Table A3. The repeatability of the HPLC method for the determination of TPH.

No of injection	Peak height /mm at concentration 0.012 mg ml^{-1}	Peak height /mm at concentration 0.006 mg ml^{-1}
1	152.0	77.0
2	151.8	76.8
3	151.6	76.6
4	151.4	76.3
5	151.2	76.1
6	151.0	75.8
Mean / mm	152.3	77.3
Standard deviation (SD)	0.22	0.28
%RSD	0.14	0.36

Methods for stability studies should have an RSD of # 1 % for at least 5 measurements (n ∃ 5) of the active drug in a drug substance or a drug product [65].

Table A4. The reproducibility of the HPLC analysis of TPH over an extended period.

Day	Peak height /mm		Peak height /mm	
	Concentration 0.012 mg ml^{-1}	mean deviation	Concentration 0.008 mg ml^{-1}	Mean deviation
1	152.2	1.3	99.9	1.9
2	151.8	0.9	98.7	0.7
3	151.2	0.3	98.1	0.1
4	150.6	0.3	97.7	0.3
5	150.1	0.8	97.3	0.7
6	149.5	1.4	96.5	1.5
Mean (mm)	150.9		98.0	
Standard deviation (SD)	1.028		1.178	
% RSD	0.68		1.2	

The method shows good repeatability with a RSD (Table A3) < 0.5, while reproducibility is confirmed at 0.012 mg ml^{-1} of TPH.

A.7. Range

The range of a method of analysis gives the upper and lower limits of the concentration of the analyte over which the precision, accuracy and linearity of the instrumental response are acceptable [70]. From the results above it can be seen that the method is acceptable at a concentration of 0.0100 mg ml^{-1} of TPH.

A.8. Quantitation limit

The limit of quantitation (LOQ) is the lowest concentration of the analyte at which the precision accuracy and linearity of the instrumental response are acceptable [60]. Three solutions were prepared with concentrations of 0.002 mg ml^{-1} (i.e. 20 % of the reference level of 0.01 mg ml^{-1}. Injection of these solutions gave the results shown in Table A5. The quantitation limit is expressed as:

$LOQ = 10\ \delta / S$

where δ is the standard deviation of the response after six injections at the lowest target concentration, S is the slope which was estimated from the calibration curve obtained in the linearity test. The LOQ was found to be 3.7×10^{-4} mg ml^{-1}.

Table A5. Test of the limit of quantitation for TPH

Injection	Peak height /mm
1	28
2	27.6
3	27.3
4	27
5	26.9
6	26.7
Mean	27.25 mm
δ	0.48 mm
S	1.29×10^4 mm ml/mg
LOQ = $10\ \delta / S = 4.8/1.29 \times 10^4$	= 3.7×10^{-4} mg ml^{-1}

Comment: This result proves that the drug can be accurately quantitated to 4 % of drug remaining, which is below the level required in this study.

A.9. Specificity/selectivity

This is the ability of the method to assess unequivocally the presence of components which may be expected to interfere with the analysis [60]. These might include impurities, degradants etc.

The HPLC-Diode array was used to determine the effect of excipients such as glucose and BCD and to determine whether any photodegradants may interfere with the quantitation of TPH. Results showed that the drug TPH appears after 4.683 min (Figure A3), while for a sample of TPH that had been irradiated for 20 hours in clear glass ampoules a broader peak, also after 4.683 min (Figure A4), was obtained, confirming that the method can be used to quantitate TPH in photostability studies.

The effect of the excipients, glucose and BCD, on the behaviour of TPH was evaluated. HPLC analysis of the aqueous mixture of TPH and BCD (by dissolving 1 mg of TPH and 1 mg of BCD in 100 ml of 50/50 % of 95 % of ethanol and water) shows that the peak for TPH has shifted from 4.683 min (see above) to 4.733 min, while in the mixture of TPH and glucose the peak appears after 5.750 min. Despite the shifts in the TPH peak, the purity of the TPH peak in the presence of BCD and glucose is confirmed as shown in Figures A5 and A6.

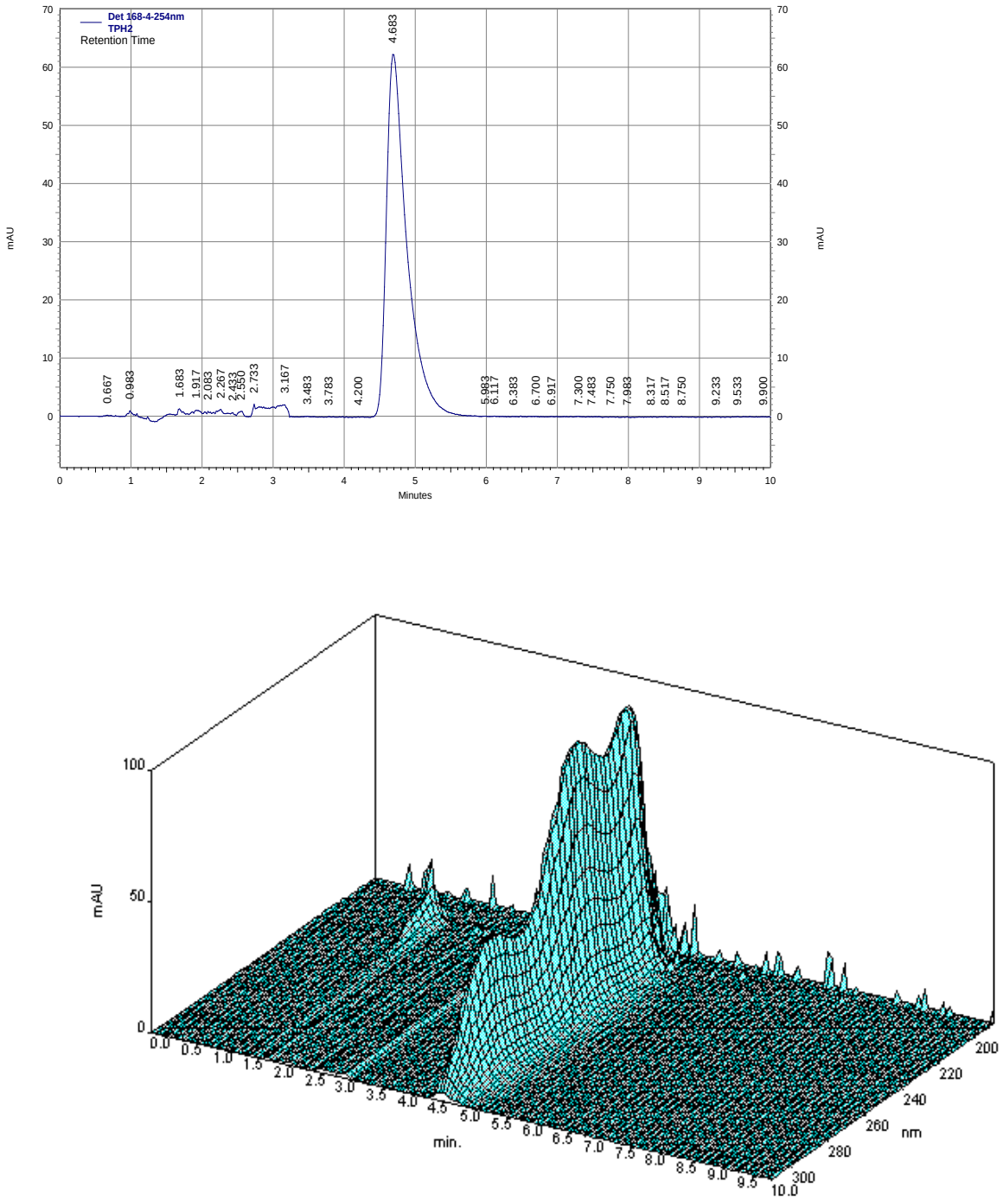

Figure A3. HPLC-photodiode array analysis for TPH. Two-dimensional plot of absorbance (mAU) against retention time (min) and three-dimensional plot of absorbance against wavelength (nm) and retention time.

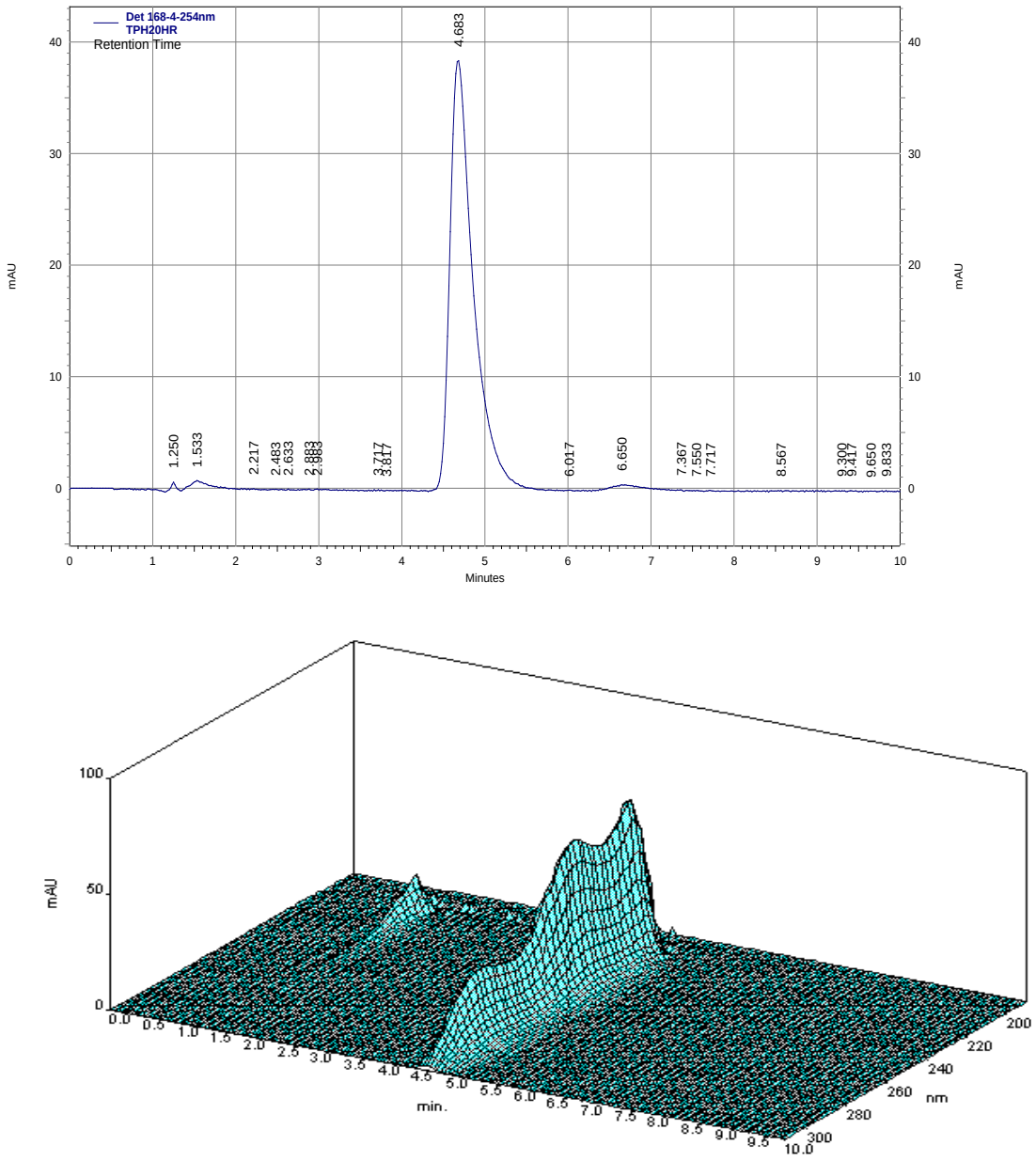

Figure A4. HPLC-Diode array analysis for a TPH solution (0.01 mg/ml) that had been irradiated for 20 hours in a clear ampoule. Two-dimensional plot of absorbance (mAU) against retention time (min) and three-dimensional plot of absorbance against wavelength (nm) and retention time.

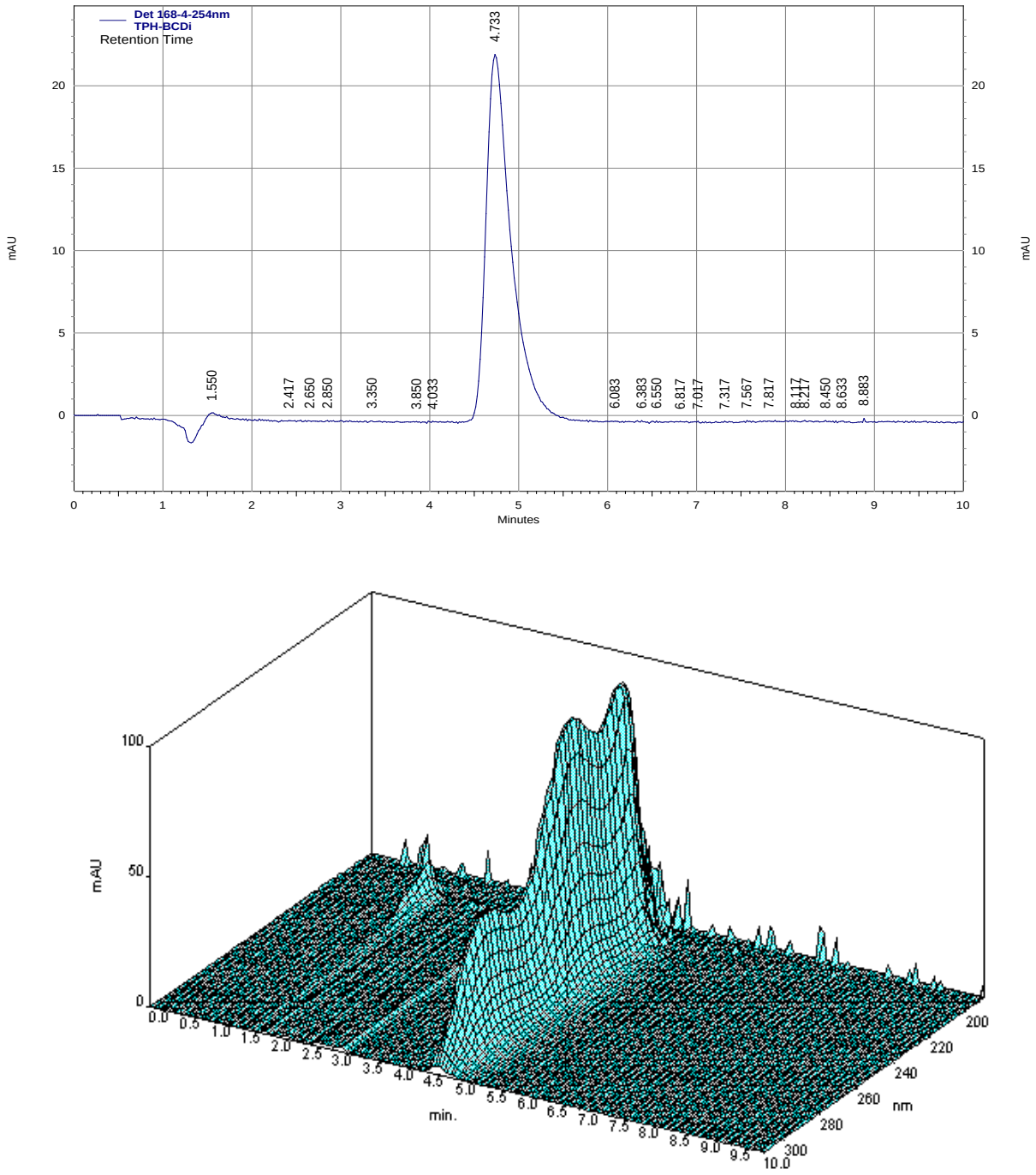

Figure A5. HPLC-photodiode array analysis of an aqueous mixture of TPH and BCD (0.02 mg/ml) that had been irradiated for 20 hours in a clear ampoule. Two-dimensional plot of absorbance (mAU) against retention time (min) and three-dimensional plot of absorbance against wavelength (nm) and retention time.

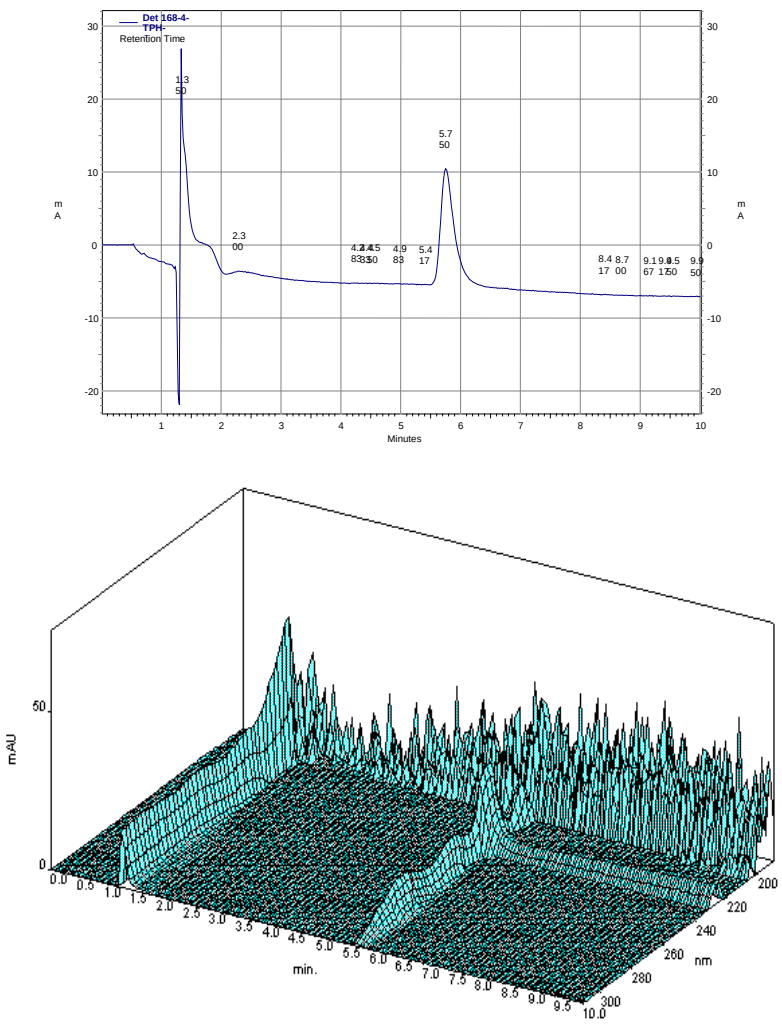

Figure A6. HPLC-photodiode array analysis of an aqueous mixture of TPH and glucose (0.02 mg/ml) that had been irradiated for 20 hours in a clear ampoule. Two-dimensional plot of absorbance (mAU) against retention time (min) and three-dimensional plot of absorbance (mAU) against wavelength (nm) and retention time (min).

A10. Robustness

Robustness is a measure of the capacity of the assay to remain unaffected by small but deliberate changes and provides an indication of the reliability of the method during normal usage [60]. An indication of robustness can be obtained by studying the influence of the pH of the mobile phase, the use of different columns, and variation of the mobile phase, etc. The shifts in the retention times for TPH found on changing the

solvent ratios in the mobile phase were: (A) 4.683 min (B) 4.681 min and (C) 4.686 min.

A11. The stability of the sample solution

The stability of the solution (analyte) which is being investigated needs to be determined under various conditions [62]. About 100 mg of TPH was dissolved in 50/50 volume % of ethanol and water. 1 ml samples of this solution were diluted to 100 ml. Some of these diluted solutions were stored in a dark cupboard and others in diffuse fluorescent light. The solutions were analyzed after various times, 0, 3, 6, 12, 15, 18, 21 and 24 hours.

Table A6. Stability of solutions on storing.

Time (hours)	Mean peak height			
	Dark cupboard	Fluorescent light	% deviation after storage in the dark	% deviation after exposure to fluorescent light
0	13.4	13.4	0	0
3	13.3	13.2	0.78	1.49
6	13.3	13.0	0.78	2.98
9	13.2	12.7	1.50	5.22
12	13.1	12.6	2.23	5.9
15	13.0	12.4	2.98	7.4
18	12.9	12.0	3.7	10.4
21	12.8	11.9	4.47	11.2
24	12.8	11.9	4.47	11.2

The results in Table A6 show that storage for 24 hours in the dark produces less than 5 % deviation as compared with 11.2 % under fluorescent light. Solutions of TPH should thus be protected from light during storage and analyses should be carried out within 9 hours of preparation.

A12. Conclusion

The HPLC method has been successfully developed for the analysis of TPH in the presence of its photodegradation products, glucose and BCD. The method has been validated according to international guidelines for accuracy, linearity and precision. The photodiode array analysis proved to be reliable in evaluating the specificity of the assay in the presence of potential photodegradants, glucose and BCD.